

**ANALYSIS OF BEDROCK EROSIONAL FEATURES IN
ONTARIO AND OHIO: IMPROVING UNDERSTANDING
OF SUBGLACIAL EROSIONAL PROCESSES**

ANALYSIS OF BEDROCK EROSIONAL FEATURES IN ONTARIO AND OHIO:
IMPROVING UNDERSTANDING OF SUBGLACIAL EROSIONAL PROCESSES

By

STACEY LEIGH PUCKERING. B.Sc. (Hons)

A Thesis

Submitted to the School of Graduate Studies

in Partial Fulfilment of the Requirements

for the Degree

Master of Science

McMaster University

© Copyright by Stacey Leigh Puckering, August 2011

Master of Science (2011)
(Geography and Earth Sciences)
Canada

McMaster University
Hamilton, Ontario,

**TITLE: ANALYSIS OF BEDROCK EROSINAL FEATURES
IN ONTARIO AND OHIO: IMPROVING UNDERSTANDING OF
SUBGLACIAL EROSIONAL PROCESSES**

AUTHOR: Stacey Leigh Puckering

B.Sc. (Hons)

(McMaster University, Hamilton,
2009)

SUPERVISOR:

Professor Carolyn H. Eyles

NUMBER OF PAGES:

xv, 167

ABSTRACT

Extensive assemblages of glacial erosional features are commonly observed on bedrock outcrops in deglaciated landscapes. There is considerable debate regarding the origins of many subglacial erosional landforms, due to a relative paucity of detailed data concerning these features and a need for improved understanding of the subglacial processes that may form them. This study presents detailed documentation and maps of assemblages of glacial erosional features from select field sites throughout the Great Lakes basins. The characteristics and spatial distribution of p-forms exposed on variable substrates at the Whitefish Falls, Vineland, Pelee Island and Kelleys Island field sites were investigated in order to determine the mode of p-form origin to identify significant spatial and temporal variability in subglacial processes operating at these locations. Observations from this work suggest that p-forms evolve through multiple phases of erosion, whereby glacial ice initially abrades the bedrock surface, leaving behind streamlined bedrock highs, striations and glacial grooves. Subsequent erosion by vortices in turbulent subglacial meltwater sculpts the flanks of bedrock highs and grooves into p-forms. These forms are subjected to a second phase of subglacial abrasion that ornaments the sinuous, sharp rimmed features with linear striae. The presence of multi-directional ('chaotic') striae at some sites suggests erosion by saturated till may contribute to, but is not essential for p-form development. Investigation in the Halton Hills region of Ontario focused on modeling bedrock topography in order to delineate the extent and geometry of buried bedrock valleys thought to host potential municipal significant aquifer units.

Various approaches to subsurface modeling were investigated in the Halton Hills region using a combination of primary data (collected from boreholes and outcrop), intermediate data collected through aerial photography and consultant reports, and extensively screened low quality data from the Ontario Waterwell Database. A new, ‘quality weighted’ approach to modeling variable quality data was explored but proved ineffective for the purposes of this study, as differential weighting of high and low quality data either over-smoothed the model or significantly altered data values. A series of models were interpolated and compared using calculated RMSE values derived from model cross-validation. The preferred bedrock topography model of the Halton Hills region had the lowest RMSE score, and allowed identification of three major buried bedrock valleys systems (the Georgetown, Acton and 16 Mile Creek buried valleys) which contain up to 40 – 50 m of Quaternary infill. These valleys were likely carved through a combination of fluvial and glacial erosion during the late Quaternary period, and their orientation may be influenced by pre-existing structural weaknesses in the bedrock. Future work on subglacial erosional landforms should focus on the temporal scale in which subglacial processes, through association with other subglacial landforms and dating methods.

ACKNOWLEDGEMENTS

First and foremost, I would like to thank my supervisor, Dr. Carolyn Eyles for providing me with countless opportunities, including (but not limited to) the work presented in this thesis. Her ongoing encouragement, support (and incredible patience) are greatly appreciated, and will never be forgotten. Thank you sincerely to all of the members of the Glacial Sedimentology Lab for all of your help, and more importantly, your friendship over the past few years. Thank you to Kelsey MacCormack and John MacLachlan for offering me advice and always answering my questions. Thank you to Jess Slomka, Paul Durkin, Riley Mulligan and Prateek Gupta for your incredible help in the field, and for your helpful discussions regarding this research. Thanks also to Rodrigo Narro and Nora Labbanz who dedicated many hours to the finishing touches of this thesis. I would also like to thank additional members of the School of Geography and Earth Science, including Bill Spicer, for his continuous help with my equipment and software issues and to Jason Brodeur for coming to my rescue several times when computers or hard-drives crashed. I would also like to extend thanks to the members of my thesis committee Dr. Joe Boyce, and Tim Lotimer, whose input during presentations, workshops or other check points have greatly contributed to the quality of the work presented here. Finally, thank you to my friends, my family, and Dave for their constant support and understanding, and for dealing with me while I completed this thesis.

TABLE OF CONTENTS

ABSTRACT	iii
ACKNOWLEDGEMENTS	v
LIST OF FIGURES	ix
LIST OF TABLES	xv
CHAPTER 1 INTRODUCTION	1
Organization of this thesis	7
References	7
CHAPTER 2 COMPARATIVE ANALYSIS OF P-FORM ASSEMBLAGES ON BEDROCK SURFACES IN ONTARIO AND OHIO: IMPLICATIONS FOR UNDERSTANDING SUBGLACIAL PROCESSES	10
Abstract	10
2.1 Introduction	12
2.1.1 Glacial History of Southern Ontario	19
2.1.2 P-Form Assemblages	20
2.2 Field Observations	22
2.2.1 Whitefish Falls, Ontario	24
2.2.2 P-form Morphologies	31
2.2.3 Kelleys Island, Ohio	37
2.2.3.1 P-form Characteristics	42
2.2.4 Vineland, Ontario	51
2.2.4.1 P-form Characteristics	54
2.2.5 Pelee Island, Ontario	60
2.2.5.1 P-form Characteristics	61
2.3 Comparison of the P-form Assemblages	64
2.3.1 Similarities between p-form assemblages	64
2.3.2 Differences between p-form assemblages	68
2.3.3 Substrate type	69

2.3.4 Topography	70
2.3.5 Bedrock Structures	71
2.4 Inferred Subglacial Processes	71
2.4.1 Subglacial meltwater erosion	72
2.4.2 Glacial Abrasion	74
2.4.3 Saturated Till Erosion	75
2.5 Discussion.....	77
2.6 Conclusions	79
Reference List.....	81
CHAPTER 3 MODELING BEDROCK TOPOGRAPHY IN THE HALTON HILLS REGION OF SOUTHERN ONTARIO	85
Abstract.....	85
3.1 Introduction	87
3.2 Geologic background.....	95
3.3 Data sources.....	98
3.3.1 Identifying & Defining Variable Quality Data	102
3.3.2 The Modeling Process.....	104
3.3.3 Model Validation	104
3.4 Modeling Bedrock Topography in the Halton Hills Region	105
3.4.1 Modeling Exclusively with High Quality Data	105
3.4.2 Modeling All Data with Minimal Screening.....	109
3.4.3 Modeling with Extensive Screening of Low Quality Data.....	113
3.4.4 Modeling with “Push Down” Points.....	117
3.4.5 Summary and Comparison of Model Results	123
3.5 Modeling using a Quality Weighted Approach.....	126
3.5.1 Results of Quality Weighting within the Georgetown Study Area.....	129
3.6 Bedrock Topography in the Halton Hills Region.....	132
3.6.1 Defining Buried Bedrock Valleys.....	133
3.6.2 Drift Thickness.....	139

3.6.3 Buried Bedrock Valleys in Halton Hills, Ontario	142
3.6.3.1 Georgetown Bedrock Valley	145
3.6.3.2 Acton (Re-Entrant) Bedrock Valley.....	147
3.6.3.3 16 Mile Creek Bedrock Valley.....	147
3.6.4 Origin of Buried Bedrock Valleys in Halton Hills	148
3.7 Conclusions	150
References	154
CHAPTER 4 CONCLUSION.....	159
4.1 Future Directions	162
References	163
APPENDIX A	164
Screening Stage 2-Georeferencing Errors	164
Screening Stage 3-Geologic Inaccuracies	165
References	167

LIST OF FIGURES

Figure 1.1: Map showing the locations of study sites (Halton Hills, Whitefish Falls, Vineland, Pelee Island and Kelleys Island) investigated as a part of this thesis.....	5
Figure 2.1: Map showing location of study sites, the Niagara Escarpment and the position of the Laurentide Ice Sheet (LIS) in the modern Great Lakes region during the last glacial maximum ~ 18 000 BP (Barnett, 1993) and the locations of the Whitefish Falls, Vineland Quarry, Kelleys Island and Pelee Island field sites.....	13
Figure 2.2: Common p-form morphologies according to the Kor et al. (1991) classifications system. These p-forms were all observed on argillite at the Whitefish Falls field site. A) Longitudinal furrow form B) longitudinal spindle flute form C) transverse muschelbruche form D) two transverse comma forms E) transverse sichelwannen form F) non-directional pot hole feature.	16
Figure 2.3: A) Satellite photograph (courtesy of IKONOS) of the Whitefish Falls field site overlain with colours representing bedrock types (see map elements key). B) Location map of Whitefish Falls. C) Idealized N-S geological cross section of the study area modified from Young & Nesbitt (1985).....	25
Figure 2.4: Satellite photograph (courtesy of IKONOS) of the Whitefish Falls study area overlain with a digital elevation model (courtesy of Dr. Ugalde, McMaster University) and the location of glacial erosional landforms.	27
Figure 2.5: Detailed map of a complex p-form assemblage at Whitefish Falls (see inset on upper left for location). Surface topography mapped with a Magellan ProMark3 differential GPS. Note the strong spatial relationship between the location of areas ornamented with chaotic striae (shaded red).....	29
Figure 2.6: Longitudinal furrow forms at Whitefish Falls located on the sides of (argillite) bedrock highs ornamented with striae. A) A linear longitudinal furrow form containing parallel linear striae. B) A sinuous longitudinal furrow, where striae conform to the curved course of the p-form as opposed to the regional ice flow direction (indicated by striae above the p-form). Note how the striae appear to move up out of a poorly developed pothole feature. C) Chaotic striae ornamenting the wall of a longitudinal furrow form.	33
Figure 2.7: A) Topographic map of the Kelleys Island region with location of the Glacial Grooves State Memorial (GGSM), and locations where quarrying practices have removed other reported grooves (modified from Goldthwait, 1979). B) Inset map showing the location of Kelleys Island.....	38

Figure 2.8: Examples of where the location and morphology of p-forms is influenced by the presence of fossil material. A) The comma form is incised into limestone containing few fossils, and undercuts the highly fossiliferous horizon above it. B) Sinuosity initiated by a coral fossil in a narrow cavetto form on the GGSM furrow wall. C) A large sichelwannen feature eroded around a bedrock high containing a large coral fossil. 40

Figure 2.9: A) View to the west (down-ice flow) along eroded bedrock surface exposed at the Glacial Grooves State Memorial (GGSM) on Kelleys Island, Ohio, showing locations of longitudinal furrows (f) on the flanks of bedrock rises and glacial grooves (g) ornamenting bedrock rises and furrows. The entire GGSM site is classified as a longitudinal furrow with several other p-forms superimposed on its floor and walls. B) Schematic cross section through part of the GGSM furrow. 43

Figure 2.10: Common transverse erosional forms at Kelleys Island, Ohio (sw: sichelwannen, cf: comma form, g: glacial groove, f: furrow). A) An assemblage of sichelwannen and comma forms ornamenting the stoss sides of streamlined bedrock highs. B) A series of sichelwannen as ‘multiple trough forms’ (Munro-Stasiuk et al., 2005) ornamenting the stoss sides of streamlined bedrock highs. Note the truncation of the central portion of these features by a deep glacial groove. C) A series of ‘multiple trough forms’ extending over 2 m from the stoss end of a streamlined bedrock high, with their central portions truncated by glacial grooves. Note the improved definition of these multiple trough forms closer to the streamlined bedrock high. D) Sinuous, parallel multiple trough forms around a streamlined bedrock high. 45

Figure 2.11: Large ‘plunging’ form observed on the uppermost portion of the northern furrow wall at the Kelleys Island GGSM. A) The upper portion of the plunging form has an almost vertical orientation B) the plunging form then turns almost 180°, redirecting itself to conform with the regional ice flow direction. Person for scale is standing at the same position in both photographs. Note the extensive grooves and striations conforming to the curved course of this plunging form. 47

Figure 2.12: P-forms observed at Vineland Quarry, Vineland, Ontario. A) A digital elevation model of the relatively small bedrock high exposing longitudinal furrows, sichelwannen and comma forms. Forms that are not labelled are undefined morphologies. B) View of the site (looking south-west) showing p-forms within a 2 m thick bed of dolostone. C) Sketch of the features shown in photograph B, where thicker lines represent bedding planes, and thinner lines represent p-form boundaries. 52

Figure 2.13: P-form morphologies identified at the Vineland Quarry field site. A) Shallow, sinuous longitudinal furrows (lf) following the course of a bedding plane in dolostone. B) Examples of comma forms (cf) as multiple trough forms adorning the stoss

flanks of a bedrock rise. C) Small muschelbruche (mb) feature containing chaotic striae (below compass). Note how this feature truncates the linear striae that lie in the up ice direction..... 55

Figure 2.14: Aerial photograph of the Pelee Island field site (south-eastern shoreline), with p-forms and glacial grooves ornamenting Columbus Limestone pavement. Several linear features are visible from the aerial photograph. Aerial photograph courtesy of South-Western Ontario Orthophotography Project (SWOOP) 2006. 58

Figure 2.15: Glacial erosional features observed on exposed limestone pavement on the south-eastern shore of Pelee Island, Ontario. A) Shallow, linear glacial grooves. B) Longitudinal furrow infilled with lake sediment and algae. Most longitudinal furrows were submerged, this feature is about 0.5 m deep, and displays striae on the sculpted walls. C) One longitudinal furrow form (lf) and two superimposed comma forms (cf; ~ 2 m in total length), or ‘multiple trough forms’ on the north west facing side of a small bedrock high. D) Extensively striated pavement displaying a range of orientations. 62

Figure 2.16: Rose diagrams showing striae orientations of linear p-forms, glacial striae and joints from Whitefish Falls, Vineland and Pelee Island. Detailed measurements were not taken at Kelleys Island as striae and p-form orientations were extremely similar, and very few fractures were observed. Arrows on rose diagrams for p-forms represent the ice-flow direction at each site based on observations and glacial striae. 65

Figure 3.1: A) Location of study area and Paleozoic stratigraphy (Armstrong & Dodge, 2007) of the southern Ontario region overlain on bedrock topography (modified from Gao et al., 2006). B) The Halton Hills study area showing Paleozoic stratigraphy overlain on surface topography (Armstrong & Dodge, 2007). The contact between the Amabel/Clinton-Cataract and Queenston Formations is expressed at surface as the Niagara Escarpment. The dashed black box represents the Acton re-entrant valley. C) Cross-section of the southern Ontario region displaying the Niagara Escarpment and gently dipping Paleozoic strata (modified from Meyer & Eyles, 2007). 88

Figure 3.2: Tertiary fluvial network in the southern Ontario region directing drainage eastward toward the Atlantic Ocean. Note the locations of re-entrant valleys along the Niagara Escarpment and the position of the Laurentian Channel, a large buried bedrock valley. 90

Figure 3.3: Glacial history of the southern Ontario region. A) Nissouri Stadial (25 - 18 Ka). Glacial ice completely covered the region at this time. B) Early Port Huron Stadial (13.2-12 Ka). Note changed direction of ice flow with the Ontario Lobe ice moving northwestward across the Halton Hills study area. Modified from Straw, 1968; Barnett, 1992; Karrow, 2005; Meyer & Eyles, 2007). 92

Figure 3.4: Outputs from modeling exclusively with high quality data. A) The relatively sparse and clustered distribution of high quality data points results in unrealistic interpolation of the bedrock topography and creates sharp ridges and boundaries in some areas. B) Manual removal of data points (declustering) in areas of significant clustering create a more smoothed interpolation, particularly within the areas around. Inset figure at lower right shows the points removed (blue) and points remaining (red) after declustering of data points along Silver Creek. 100

Figure 3.5: Flow diagram of the various approaches to subsurface modeling explored in this study, associated RMSE values, and commentary on the decision-making process. Numerical validation results of modeling using each of these approaches are summarized in Tables 2 and 3. Note that for the Quality Weighting approach, the study area was reduced and the RMSE values reflect validation with high quality data points..... 106

Figure 3.6: 'All-Original' grid: Bedrock topography grid interpolated from OWD data (grey) and primary data (red) using a 'Minimal Screening' approach. Data were extracted from the OWD, combined with primary data and modeled using the Ordinary Kriging algorithm in ArcGIS with no screening of data points..... 110

Figure 3.7: Bedrock topography models created at different stages of screening of the low quality (OWD) dataset. For each stage of screening the remaining points after screening are displayed in grey. A) Model created from the 'Low Quality- Original' dataset extracted from the OWD prior to screening. Note the white areas where no interpolation could be made. B) Screen 1: model created after removal of obvious erroneous data points (0 or null values, duplicates resulting in "white gaps"). Data points removed from the dataset are displayed in pink. Note the change in minimum bedrock elevation from 118 m asl to 169 m asl due to the removal of a zero value. C) Screen 2: model created after removal of points outside 300 m location confidence, displayed in pink. Many of these correspond to locations in between major roads where water wells are unlikely to be located (see the area outlined in red). Note the change in valley continuity between interpolations at Screen1 and Screen2 within the red square. D) Screen3: removal of points with inaccurate geologic descriptions. Points coloured red (shale), blue (dolostone) and yellow (sandstone) were removed at this stage of screening as they have incorrect geologic descriptions based on their locations. Refer for Fig. 1 for the bedrock geology of the Halton Hills region). Generally, shale underlies the lower, eastern portion of the study area, while dolostone underlies the western, upland region. Sandstone outcrops minimally along the Niagara Escarpment boundary. 114

Figure 3.8: "All Data-Screened" bedrock topography model of the Halton Hills region, including high quality primary data (borehole and outcrop) and low quality data from consultant reports and from aerial photography and a DEM of the study area..... 118

Figure 3.9: Residual map to show the difference between the bedrock topography model created from the ‘Push Down’ and the ‘All - Screened’ grid. ‘Push down’ points could only be directly compared to the ‘All – Screened’ grid at the exact location of the ‘push down’ to determine if they terminated below the modeled bedrock surface. Negative values (shown in red) represent areas where ‘push down’ points have actually increased the bedrock elevation value, despite selecting only data points which terminated below the previously interpolated bedrock surface. The elevation of bedrock has been changed by more than 10 m due to the push down process at very few locations. 121

Figure 3.10: Quality weighting approach to subsurface modeling. Data were separated into the ‘High Quality – Declustered’ and the ‘Low Quality – Screened’ subsets, which were each allocated a particular ‘weighting’ or degree of influence on the final model. Four model outputs are shown with weightings of 80:20 (high quality: low quality; top right) to 50:50 (bottom right). The weighted data (adding to 100%) were recombined using the Raster Calculator in ArcGIS. High quality data points (orange) and low quality data points (grey) used for these grids are displayed. Note the relatively low amount of topographic detail associated with greater weighting of higher quality data. Numerical results of this procedure are summarized in Table 3.2. 127

Figure 3.11: Predicted thalwegs of bedrock valleys in the Halton Hills area based on the ‘All – Screened’ grid. Predicted and ‘potential’ valley thalwegs are identified through visual analysis of the bedrock topography model created from the ‘All – Data Screened’ dataset. Note the appearance of the Acton reentrant valley as well as several, potentially interconnected valleys around the town of Georgetown. The continuity of these bedrock valleys is uncertain in some areas due to lack of high and low quality data. 134

Figure 3.12: Bedrock topography model (All – Screened, unweighted) comparing buried valley thalwegs and modern fluvial systems using ArcGIS hydrology tools (Flow Accumulation and Stream Order). Progressively darker shades (higher values) of stream order represent the direction down gradient. A) Buried valley thalwegs determined mathematically by determining direction of drainage based on the direction of maximum slope in each grid cell. B) Modern fluvial network (showing major systems; Credit River, Silver and Black Creeks) as well as relevant tributaries and stream reaches coincident with the buried valleys. 136

Figure 3.13: “All – Screened’ bedrock topography model displaying three major bedrock valley systems: A) Georgetown buried bedrock valley B) Acton buried bedrock (re-entrant) valley C) 16 Mile Creek buried bedrock valley. Predicted thalwegs of these valleys are shown in red, and problematic areas where valley continuity is uncertain are highlighted in blue dashed boxes that correspond to areas where data (high or low quality) is relatively sparse. 140

Figure 3.14: Drift thickness of the Halton Hills area and location of interpreted buried bedrock valley boundaries and thalwegs. Drift thickness map is created from subtraction of the “All-Screened” bedrock topography model from the regional digital elevation model. Note the thickness of sediments within the identified buried valleys (1: Georgetown Buried Valley; 2: Sixteen Mile Creek Buried Valley; 3: Limehouse Buried Valley. 143

LIST OF TABLES

Table 2.1: Landforms and scales (after Kor et al., 1991; Glasser & Bennett, 2004)	18
Table 2.2: P-form classifications (after Kor et al., 1991).....	23
Table 3.1: Summary of RMSE values of cross-validation and validation with high quality data points for grids created at various stages of screening, and incorporation of push-down points	112
Table 3.2: Summary of statistics for various combinations of weighted grids (high quality, low quality) and an unweighted version ('All – Screened'). compared to an unweighted version. Note that grids more heavily weighted towards high quality data are better able to predict high quality observations. However, weighting grids no longer honours the high quality data points, as the unweighted grid does.....	131
Table 3.3: Summary of buried bedrock valley characteristics from the Halton Hills region determined from the 'All – Screened' bedrock topography model. Valley depth was determined solely from the change in elevation of the highest observed bedrock point to the lowest observed bedrock point within a valley system. Some valleys contain substantial thicknesses of sediment above bedrock valley walls. *Note that there is some surface expression of the Acton (re-entrant) valley (0 m drift thickness), but large portions of this valley are buried, allowing it to be classified as a partially "buried bedrock valley."	146
Table A-1: Table of location confidence codes associated with data from the Ontario Waterwell Database (OWD). For the purposes of this study, data points outside of 300 m location confidence (code > 5), were removed from the interpolation.	166

CHAPTER 1

INTRODUCTION

Many types of erosional features can be observed on bedrock outcrops in deglaciated landscapes and provide valuable information about the nature of former subglacial processes. Glacial erosional landforms and features occur on a wide range of scales ranging from small superficial marks on bedrock such as striae, to larger landforms such as roches moutonnee and whalebacks, and extensive terrains of areal abrasion that record long term regional patterns of glacial erosion (Kor et al., 1991; Glasser & Bennett, 2004; Benn & Evans, 2010). Erosional features of different scales are often found superimposed on one another as small features such as striae commonly ornament intermediate scale features such as roches moutonnee or p-forms, which in turn form part of a larger scale erosional landscape or assemblage of landforms (Kor et al., 1991; Glasser & Bennett, 2004; Benn & Evans, 2010).

Glaciers are capable of eroding bedrock through a variety of processes including direct glacial abrasion and streaming of basal ice (Boulton, 1974, Rea et al., 2000), erosion by deforming beds/saturated till (Gjessing, 1965; Boulton & Hindmarsh, 1987; Hart, 2006) and erosion by subglacial meltwater (Dahl, 1965; Eyles, 2006). The nature and rate of glacial abrasion on substrates of different lithologies has been documented in the field (Boulton, 1979) and some small scale erosional features (e.g., rat tails, sichelwannen; Kor et al., 1991) have been recreated in laboratory flume experiments under unidirectional turbulent flows (Allen, 1971; Sharpe & Shaw, 1989). The analogy of

these smaller scale forms to larger forms such as p-forms and erosional ‘tunnel’ or bedrock channels has been used to support formation of these larger features by catastrophic subglacial meltwater flood events (Shaw, 1988; Sharpe & Shaw, 1989; Kor et al., 1991; Brennand & Shaw, 1994; Munro-Stasiuk et al., 2005).

The origin of many glacial erosional features, particularly p-forms and bedrock channels/valleys, is widely debated in the literature (Kor et al., 1991; Munro-Stasiuk et al., 2005; Clarke et al., 2005; O’Cofaigh et al., 2010) add references). Controversy surrounding the origin of many of these landforms is often due to a lack of detailed information about their form, characteristics and spatial distribution, problems associated with determining their time of origin (Glasser & Bennett, 2004), and the possibility that many morphologically similar features can be created by more than one erosional process (Straw, 1968; Allen, 1971; Kor et al., 1991; Tinkler & Stenson, 1994; Glasser & Bennett, 2004; Benn & Evans, 2010; Gao, 2011).

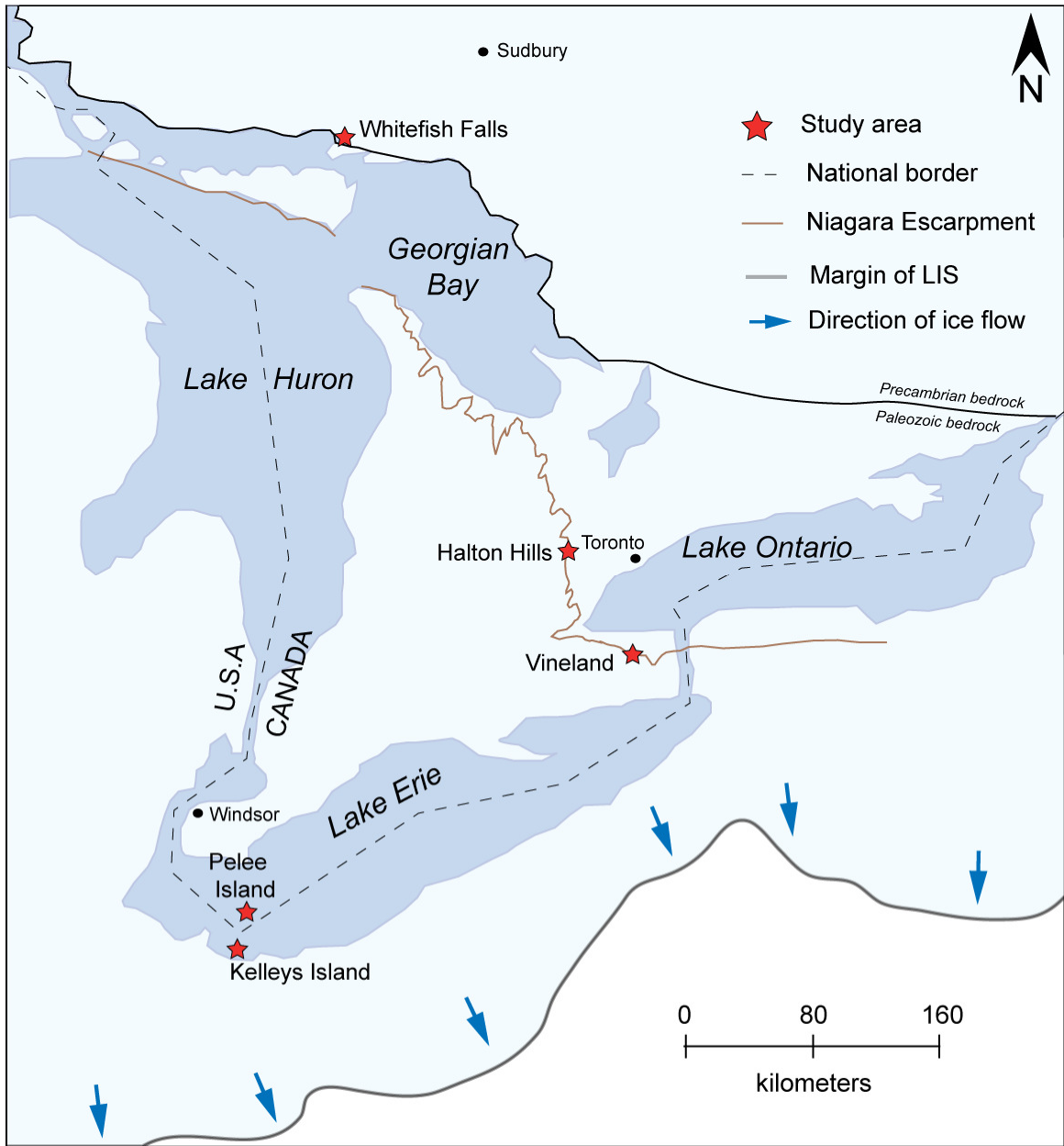
Relatively few studies present detailed maps of former glaciated surfaces and landforms that can be used to determine the spatial variability and/or organization of erosional processes or the controls on landform development. Landforms provide the most spatially continuous record of former sub-ice sheet conditions available to us, and should serve as the basis for interpretation of former glacier dynamics (Kleman, 1994). Detailed mapping of former subglacial surfaces therefore provides an important contribution to the understanding of subglacial processes and to past, present and possible future ice sheet behaviour (Glasser & Bennett, 2004).

The work in this thesis focuses on small and large scale bedrock erosional features (p-forms and buried bedrock valleys, respectively) and the investigation of the characteristics of these features to infer controls on their development. To improve upon the current understanding of subglacial erosional processes and ice sheet dynamics, a series of former glaciated surfaces exposed at field sites in Ontario and Ohio and ornamented with p-forms were investigated (Chapter 2). The field sites are located at Whitefish Falls, Pelee Island and Vineland in Ontario, and Kelleys Island in Ohio (Fig. 1.1). P-forms are erosional landforms that can display significant variability in terms of their morphology, scale and orientation with respect to ice flow. These features rarely occur in isolation, and are commonly observed in assemblages consisting of a variety of erosional landform types. P-forms have been attributed to subglacial erosional processes including glacial abrasion, erosion by saturated till, erosion by subglacial meltwater, and erosion by catastrophic outburst flooding (Dahl, 1965; Gjessing; 1965; Kor et al., 1991; Rea et al, 2000; Munro-Stasiuk et al., 2005; Hart, 2006; Benn & Evans, 2010). Assemblages of p-forms from each of the four field sites investigated were documented in detail and compared in an attempt to understand the various factors responsible for p-form development and distribution on different bedrock surfaces.

While Chapter 2 of this thesis focuses on smaller scale erosional features such as p-forms in various sites across Ontario and Ohio, Chapter 3 focuses on larger scale erosional features incised into the Paleozoic bedrock surface in the Halton Hills region. Enhancing understanding of larger scale erosional bedrock features such as bedrock valleys has applications in groundwater exploration in southern Ontario, as well as other regions of

North America, where productive aquifers are hosted within Quaternary sediments infilling buried bedrock valley networks (Kempton et al., 1991; Meyer & Eyles, 2007). The Halton Hills region of southern Ontario (a part of the rapidly growing Greater Toronto Area), is currently entering a ‘water crisis’ in which it is unable to meet the potable water demand for projected urban growth under the province of Ontario’s “Places to Grow” growth plan (RMH, 2009). A part of this issue is the relatively poor understanding of the complex groundwater system, which is hosted within Quaternary sand and gravel aquifers that infill an inferred network of buried bedrock valleys (Meyer & Eyles, 2007). Groundwater exploration and protection plans require a detailed understanding of the buried bedrock surface in order to efficiently locate and characterize such systems (Easton, 1988; Meyer & Eyles, 2011). In order to better understand the nature and form of buried bedrock valleys in the Halton Hills region, the bedrock surface must be modeled as accurately as possible using all available sources of subsurface information. Unfortunately many subsurface models are created using data from large digital databases in which the quality of the records can be highly variable and may include erroneous information that can severely compromise the reliability of the final model (Thorliefson & Berg, 2002; Bajc et al., 2004; Logan et al., 2006; Gao et al., 2006; Kaufmann & Martin, 2008; MacCormack & Eyles, 2010; Gao, 2011). This study investigates the bedrock topography of the Halton Hills region using a combination of primary data collected from boreholes and outcrop, as well as carefully screened data from the Ontario Waterwell Database (OWD) to delineate the bedrock valley systems in the region.

Figure 1.1: Map showing the locations of study sites (Halton Hills, Whitefish Falls, Vineland, Pelee Island and Kelleys Island) investigated as a part of this thesis.



Organization of this thesis

The research conducted for this thesis is reported in two chapters which are intended for eventual submission and publication in international scientific journals. Chapter 2 reports the results of comparative p-form analysis at four sites in Ontario and Ohio. Chapter 3 reports on the investigation and modeling of the bedrock surface in the Halton Hills region of southern Ontario. The main conclusions reached as a result of this research are presented in Chapter 4.

References

- Allen, J.R.L. 1971. Transverse erosional marks of mud and rock: Their physical basis and geological significance in *Sedimentary Geology* 5, 167-185.
- Bacj, A.F., Endres, A.L., Hunter, J.A., Pullen, S.E. & Shiota, J. 2004. Three-Dimensional Mapping of Quaternary Deposits in the Waterloo Region, Southwestern Ontario in *Illinois State Geological Survey (IGSG) Open File Series 2004-2008* 12-15.
- Benn, D.I., & Evans, D.J.A. 2010. *Glaciers and Glaciation*. Hodder Education, London.
- Boulton, 1974. G.S. Boulton, Processes and patterns of glacial erosion. In: D.R. Coates, Editor, *Glacial Geomorphology*, State University of New York, Binghamton, NY (1974).
- Boulton, G.S. & Hindmarsh, R.C.A. 1987. Sediment deformation beneath glaciers: rheology and geological consequences in *Journal of Geophysical Research* 92, 9059-9082.

- Brennand, T. & Shaw, J. 1994. Tunnel channels and associated landforms, south-central Ontario: their implications for ice sheet hydrology. *Canadian Journal of Earth Sciences* 31, 505-522.
- Dahl, R. 1965. Plastically sculptured detail forms on rock surfaces in Northern Nordland, Norway in *Geografiska Annaler Series A: Physical Geography* 47, 83-140.
- Easton, J.A. 1988. Buried valleys near Limehouse, Ontario. Unpublished M.Sc. thesis, University of Waterloo, Waterloo, Ontario.
- Eyles, N. 2006. The role of meltwater in glacial processes in *Sedimentary Geology* 190, 1-4, 257-268.
- Gao, C. 2011. Buried bedrock valleys and glacial and subglacial meltwater erosion in southern Ontario, Canada in *Canadian Journal of Earth Sciences* 48, 801-818.
- Gao, C., Shiota, J., Kelly, R.I., Brunton, F.R. & van Haaften, J.S. 2006. Bedrock topography and overburden thickness mapping, southern Ontario, in *Ontario Geological Survey, Miscellaneous Release – Data 207*.
- Gjessing, J. 1965. On ‘plastic scouring’ and subglacial erosion in *Norsk Geologisk Tidsskrift* 20, 1-37.
- Glasser, F. N. & Bennett, M.R. 2004. Glacial erosional landforms: origins and significance for paleoglaciology in *Progress in Physical Geography* 28, 1, 43-75.
- Hart, J.K. 2006. Athabasca Glacier, Canada- a field example of subglacial ice and till erosion? in *Earth Surface Processes and Landforms* 31, 1, 65-80.
- Kauffman, O. & Martin, T. 2008. 3D geological modeling from boreholes, cross-sections and geological maps, application over former natural gas storage in coal mines in *Computers & Geosciences* 34, 278-290.
- Kempton, J.P., Johnson, W.H., Heigold, P.C. & Cartwright, K. 1991. Mahomet Bedrock Valley in east-central Illinois; topography, glacial drift stratigraphy, and hydrogeology. In: W.N. Melhorn & J.P. Kempton (Eds.) *Geology and hydrogeology of the Teays-Mahomet Bedrock Valley System*. Geological Society of America, Special Paper 258.
- Kleman, J. 1994. Preservation of landforms under ice sheets and ice caps in *Geomorphology* 9, 1, 19-32.
- Kor, P.S.G., Shaw, J. & Sharpe, D.R. 1991. Erosion of bedrock by subglacial meltwater, Georgian Bay, Ontario: a regional view in *Canadian Journal for Earth Sciences* 28, 623-642.

- Logan, C., Russel, H.A.J., Sharpe, D.R. & Kenny, F.M. 2006. The role of GIS and expert knowledge in 3-D modeling, Oak Ridges Moraine, southern Ontario. In J.R.Harris (Ed.), *GAC Special Paper 44: GIS for the Earth Science* (pp. 519-542). St. John's: Geological Association of Canada.
- Meyer, P.A & Eyles, C.H. 2007. Nature and origin of sediments infilling poorly defined buried bedrock valleys adjacent to the Niagara Escarpment, southern Ontario, Canada in *Canadian Journal of Earth Sciences* 4, 1, 89-105.
- Munro-Stasiuk, M.J., Fisher, T.G., & Nitzche, C.R. 2005. The origin of the western lake Erie grooves, Ohio: implications for reconstructing the subglacial hydrology of the great Lakes sector of the Laurentide Ice Sheet in *Quaternary Science Review* 24, 2392-2409.
- Rea, B.R., Evans, D.J.A., Dixon, T.S. & Whalley, W.B. 2000. Contemporaneous, localized, basal ice-flow variations: implications for bedrock erosion and the origin of p-forms in *Journal of Glaciology* 46, 154, 470-47.
- Sharpe, D.R. & Shaw, J. 1989. Erosion of bedrock by subglacial meltwater in *Geological Society of America Bulletin* 101, 1011-1020.
- Shaw, J. 1988. Subglacial erosional marks, Wilton Creek, Ontario in *Canadian Journal of Earth Science* 25, 1256-1267.
- Straw, A. 1968. Late Pleistocene glacial erosion along the Niagara Escarpment of southern Ontario in *Geological Society of America Bulletin* 79,7, 889-910.
- Thorleifson, L.H. & Berg, R.C. 2002. Introduction-The need for high-quality three-dimensional geological information for groundwater and other environmental application in *Geological Survey of Canada, Open File 1449*.
- Tinkler, K.J. & Stenson, R.E. 1992. Sculpted bedrock forms along the Niagara Escarpment, Niagara Peninsula, Ontario in *Geographie physique et Quaternaire* 46, 197-207.

CHAPTER 2

COMPARATIVE ANALYSIS OF P-FORM ASSEMBLAGES ON BEDROCK SURFACES IN ONTARIO AND OHIO: IMPLICATIONS FOR UNDERSTANDING SUBGLACIAL PROCESSES

Abstract

Reconstructing the characteristics and behaviour of large ice sheets (such as the Laurentide Ice Sheet), is particularly challenging to geoscientists due to the relative paucity of information regarding the nature of subglacial processes and the landforms they create. Glacial erosional features have the potential to provide a substantial amount of information about former subglacial conditions but their origin is often poorly understood. Erosional features known as p-forms are particularly interesting as they are commonly observed on glaciated bedrock surfaces but their mode of origin is uncertain. P-forms have been variably reported to form as a result of abrasion by glacial ice, abrasion by saturated till, erosion by subglacial meltwater, and erosion by catastrophic outburst flood events.

This study presents detailed documentation and analysis of p-form assemblages exposed on four former glaciated surfaces within the Great Lakes basins. The characteristics and spatial distribution of p-forms exposed on Paleoproterozoic metasedimentary rocks at Whitefish Falls, and on Paleozoic sedimentary rocks at Vineland, Pelee Island and Kelleys Island are investigated in order to determine their

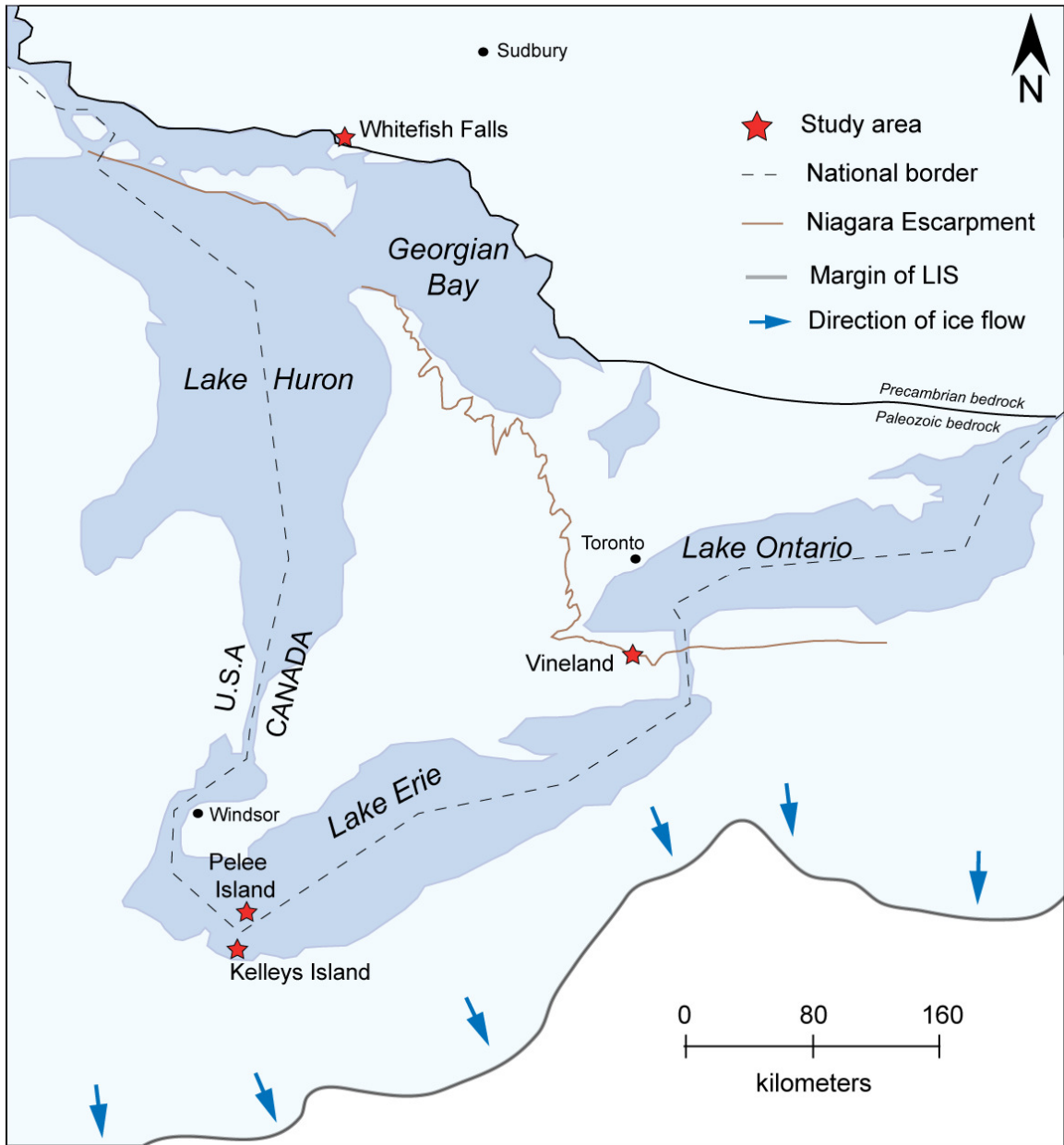
mode of origin and to identify significant spatial and temporal variability in the subglacial processes. A multi-phase evolution of p-form development is proposed here whereby glacial ice initially abrades the bedrock surface, leaving behind streamlined bedrock highs, striations and glacial grooves. The flanks of bedrock highs and grooves are subsequently sculpted into p-forms through erosion by vortices in turbulent subglacial meltwater. These forms are subjected to a second phase of subglacial abrasion that ornaments the sinuous, sharp rimmed features with linear striae. The presence of multi-directional ('chaotic') striae at some sites suggests erosion by saturated till may contribute to, but is not essential for p-form development.

2.1 Introduction

Reconstructing the characteristics and behaviour of the Laurentide Ice Sheet that covered large areas of northern North America during the Wisconsin glaciation between 25,000 and 12,000 years ago is a particular challenge to geoscientists due to the relative paucity of information regarding the nature of subglacial processes and resulting landforms that develop beneath such large and extensive ice bodies (Glasser & Bennett, 2004; Benn & Evans, 2010). There is considerable debate about the relative importance of ‘glacial’ and ‘fluvial’ processes operating at the base of large ice sheets (Boulton and Hindmarsh, 1987; Sharpe and Shaw, 1989) and their role in the creation of subglacial landforms, particularly erosional forms. Few studies present detailed maps of former glaciated surfaces that can be used to determine the spatial variability and/or organization of subglacial processes or the controls on erosional landform development.

In the Great Lakes Basin, glacially eroded landscapes have developed on both resistant Precambrian rocks of the Canadian Shield and on younger and less resistant Paleozoic cover rocks (Fig. 2.1; Sharpe & Shaw, 1989; Kor et al., 1991; Tinkler & Stenson; 1992). Subglacial erosion involves a range of processes including glacial quarrying, abrasion and meltwater erosion, which together can create a collection of landforms that are commonly observed in deglaciated areas (Glasser & Bennett, 2004). These landforms, such as striae, roches moutonnee, whalebacks, and p-forms are often found in close proximity to one another and can occur at a variety of scales extending from centimetres to thousands of metres (Table 2.1; Kor et al., 1991; Glasser & Bennett,

Figure 2.1: Map showing location of study sites, the Niagara Escarpment and the position of the Laurentide Ice Sheet (LIS) in the modern Great Lakes region during the last glacial maximum ~ 18 000 BP (Barnett, 1993) and the locations of the Whitefish Falls, Vineland Quarry, Kelleys Island and Pelee Island field sites.



2004; Benn & Evans, 2010). P-forms are erosional landforms that show considerable variability in terms of their morphology, scale, and orientation with respect to ice flow, and include features such as longitudinal furrows, grooves, crescentic troughs, sichelwannen and muschelbrusche (Fig. 2.2; Table 2.1; Kor et al., 1991; Glasser & Bennett, 2004; Benn & Evans, 2010). P-forms rarely occur in isolation but most commonly form spatially-related assemblages of a variety of erosional landform types. The p-form assemblage has been attributed to a range of subglacial erosional processes including glacial abrasion, meltwater erosion and erosion by saturated till (Dahl, 1965; Gjessing, 1965, Kor et al., 1991; Rea et al., 2000; Munro-Stasiuk, 2005; Hart, 2006). There is much controversy regarding the origin of p-forms and their significance as indicators of specific subglacial conditions such as deforming sediment beds (Gjessing, 1965), or megafloods (Shaw, 1988; Sharpe & Shaw, 1989; Kor et al., 1991; Munro-Stasiuk et al., 2005), has been challenged by some researchers (Clark et al., 2010). Unfortunately, few descriptive data are available to evaluate the constituent landforms within p-form assemblages, their spatial distribution, and their relationship to bedrock type and other erosional landforms. These data have the potential to identify key processes involved in the development of p-form assemblages and to enhance understanding of the spatial variability of these processes beneath large ice masses.

This paper provides comparative data on p-form assemblages exposed at four sites in the Great Lakes Basins (Fig. 2.1). These four sites were selected for study due to the excellent exposures of variable p-form types as well as other glacial erosional features

Figure 2.2: Common p-form morphologies according to the Kor et al. (1991) classifications system. These p-forms were all observed on argillite at the Whitefish Falls field site. A) Longitudinal furrow form B) longitudinal spindle flute form C) transverse muschelbruche form D) two transverse comma forms E) transverse sichelwannen form F) non-directional pot hole feature.



Table 2.1: Landforms and scales (after Kor et al., 1991; Glasser & Bennett, 2004)

		Scale						Inferred subglacial process
		0.01 m	0.1 m	1 m	10 m	100 m	1 km	
Feature/Landform		streamlined bedrock features (whalebacks)						glacial abrasion
		stoss and lee forms (roches moutonnee)						glacial abrasion, likely with abundant meltwater
		striae						glacial abrasion
		bedrock gouges						glacial abrasion
		p-forms' or 's-forms'						glacial abrasion, meltwater erosion, saturated till erosion
			rock grooves and small rock basins					glacial abrasion
		tunnel channels/valleys						meltwater erosion

such as striae, roches moutonnee, and whalebacks. The characteristics of p-forms exposed at Whitefish Falls, Vineland, Pelee Island (Ontario) and Kelleys Island (Ohio) are compared in an attempt to understand the various factors responsible for the formation and spatial distribution of p-forms on former glaciated surfaces. Of particular interest in this investigation is the influence of bedrock type and structure on the development and morphology of p-forms.

2.1.1 Glacial History of Southern Ontario

Quaternary glaciations have played a major role in creating the Ontario landscape, including the scoured and ornamented bedrock surfaces exposed at the Whitefish Falls, Vineland, Pelee Island, and Kelleys Island study areas (Fig. 2.1). During the Last Glacial Maximum (LGM), twenty thousand years ago, 80% of Canada was covered by the Laurentide Ice Sheet and Ontario was completely covered by ice up to two kilometres thick (Fig. 2.1; Barnett, 1992; Benn & Evans, 2010; Eyles, 2002). The Southern Ontario (and Northern Ohio) landscape has been subjected to many re-advances and retreats of the Laurentide Ice Sheet (LIS) during the Pleistocene, the most recent of which evacuated the area between 14,000 and 10,000 ybp (Barnett, 1992). Observations of glacial erosional and depositional features (e.g., striae, moraines) in the Western Lake Erie region indicate that the flow pattern of the Laurentide Ice Sheet (and particularly the Erie Lobe of the LIS) was relatively complex as it moved west-south-west along the Lake Erie basin, terminating in a series of sublobes (Versteeg & Yunck, 1935; Snow et al., 1991; Munro-Stasiuk et al., 2005). Four distinct directions of glacial ice movement are identified in the Lake Erie basin by Yunck & Versteeg (1935), passing from an early

south-western flow direction to a more southern direction during late glacial maximum conditions. During deglaciation, ice returned to a south-western flow direction, and in final stages a north-south flow direction is reported (Yunck & Versteeg, 1935; Snow et al., 1991; Munro-Stasiuk et al., 2005). Most of the Western Lake Erie region was free of glacial ice by ~ 14 000 years ago (Barnett, 1992; Munro-Stasiuk et al., 2005). Ice flow direction at the Vineland and Whitefish Falls field sites is reported to have been from the north-east to the south-west (Young & Nesbitt, 1985; Tinkler & Stenson, 1992), and that ice overrode the prominent Niagara Escarpment at Vineland (Tinkler & Stenson, 1992). Ice had retreated from the Vineland area vicinity by 11 800 years ago, and from the Whitefish Falls area by 10 000 years ago (Barnett, 1992).

2.1.2 P-Form Assemblages

The term ‘p-form’ was introduced by Dahl (1965) to describe bedrock erosional features identified in deglaciated terrain that he called ‘plastically sculpted detail forms’ and suggested they were formed by a plastic medium. P-forms of a variety of scales are commonly observed incised into bedrock in deglaciated terrain and can be shaped like troughs, pots or channels, often displaying strongly marked relief, a curved course, and sharp edges (Fig. 2.2; Dahl, 1965). P-forms are typically found at scales of centimetres to several metres (Glasser & Bennett, 2004) but have been reported to have some morphologies (e.g., furrows or troughs) that reach lengths of 1000s of metres (Kor et al., 1991). P-forms are often found ornamenting larger subglacial erosion features such as roches moutonnee or whalebacks, and commonly contain smaller features such as glacial striae or glacial grooves/gouges (Table 2.1; Dahl, 1965; Glasser & Bennett, 2004; Benn &

Evans, 2010). The term ‘groove’ or ‘glacial groove’ has been used in the literature to represent both a p-form morphology (e.g., Dahl, 1965; Goldthwait, 1979; Munro-Stasiuk et al., 2005) as well as an extremely linear feature of glacial abrasion, similar to a striation, but wider and deeper (e.g., Glasser & Bennett, 2004; James, 2005; Benn & Evans, 2010). For the purposes of this paper, the term ‘groove’ will be used in the manner of Glasser & Bennett (2004), James (2005) and Benn & Evans (2010) to refer to long, linear glacial abrasion features which are not considered here as p-forms.

Three main types of p-forms exist; longitudinal p-forms which are oriented parallel to ice flow direction; transverse forms which are oriented transverse to ice flow direction, and non-directional forms, which show no relationship to ice flow direction (Fig. 2.2; Table 2.2; Kor et al., 1991; Glasser & Bennett, 2004; Benn & Evans, 2010). There is considerable inconsistency in the terminology used to describe specific p-form types, in particular longitudinal forms. Terms such as longitudinal furrow (Kor et al., 1991), stoss-side furrow (Kor et al., 1991), fluted surface/furrow (Tinkler & Stenson, 1992), linear erosion form (Munro-Stasiuk et al., 2005), and sine groove (Goldthwait, 1979) have all been used to describe similar features. Given the wide range of landform types described as p-forms in the literature (Dahl, 1965; Kor et al., 1991; Glasser & Bennett, 2004; Benn & Evans, 2010), and their close spatial proximity on glaciated surfaces, the term ‘p-form assemblage’ is used here to include all medium scale (centimetres to several metres) glacial erosional landforms with the exclusion of glacial grooves. Specific p-form morphologies are defined using the classification scheme established by Kor et al. (1991; Table 2.2).

While there is general consensus that p-forms are created under subglacial conditions, the specific subglacial process responsible for their formation is highly debated in the literature. Three main hypotheses have been proposed to explain the genesis of p-forms and include; formation under debris rich basal ice (Boulton, 1974), formation by subglacial meltwater erosion (Dahl, 1965; Shaw, 1988; Kor et al., 1991), and through abrasion by saturated till (Gjessing, 1965). Some recent studies have indicated that p-forms may be 'polygenetic' forms created by a combination of different subglacial processes (Rea et al., 2000). Given uncertainties regarding the origin of p-forms, several authors have suggested that the term p-form too strongly infers an origin by plastically deforming ice or till, and have introduced the term 'sculpted form' or 's-form' (Shaw, 1988; Kor et al., 1991) in its place. However, the term 's-form' has itself come to infer a meltwater origin for these features (Rea et al., 2000). The original term 'p-form' is used in this paper as a general descriptor but does not imply any particular genetic origin for the erosional landforms.

2.2 Field Observations

This study is based on qualitative field observations that focus on the identification and description of p-forms as per the classification system developed by Kor et al. (1991). P-form assemblages were mapped at each of the four study sites on

Table 2.2: P-form classifications (after Kor et al., 1991)

P-form Class	Morphology	Description
Longitudinal forms	Furrows	long, linear troughs often containing other p-forms
	Stoss-side furrows	shallow depressions on the stoss side of bedrock rises, often linear, with rounded rims and open at both ends
	Spindle flutes	Long, narrow, spindle shaped marks which broaden down flow
	Cavettos	Often sinuous, undercut channels eroded into steep rock faces
Transverse forms	Sichelwannen	sickle shaped marks with sharp rims that are convex upflow, with two arms extending around a medial ridge
	Comma forms	Similar to sichelwannen, but with only well developed arm
	Muschelbrusche	mussel-shaped, shallow depressions, with sharp rims which are convex up flow, and indistinct downflow boundaries
	Transverse troughs	typically linear, narrow troughs oriented perpendicular to flow
Non-directional forms	Potholes	deep, circular depressions
	Undulating surfaces	smooth, low-amplitude surfaces found on the gentle slopes in the lee of bedrock obstacles

regional and localized scales (where applicable) in attempt to identify patterns of p-form distribution and their spatial association with other landforms.

The largest scale mapping of p-forms was conducted over a 1 km² area in Whitefish Falls, Ontario (Figs. 2.3, 2.4), where the location coordinates of observed landforms were recorded with a Garmin handheld GPS unit. Attributes such as orientation, morphology, scale (dimensions) of the observed p-forms, and the substrate type on which they were developed, were added to a database for use in a GIS (ESRI ArcMap 9.3 and 10). At Whitefish Falls and Vineland, Ontario (Fig. 2.1) a Magellan ProMark3 differential GPS was used to conduct detailed kinematic surveys of the bedrock surface containing complex p-form assemblages, creating high resolution, small scale digital terrain models (Fig. 2.5). The data collected from these kinematic surveys were used to create small scale digital terrain models which were able to capture the scale, morphology and positions of p-forms ornamenting bedrock. At all four sites, erosional features on the bedrock surface were photographed and mapped in detail, noting substrate, scale, morphology, and most importantly the spatial relationships between p-forms and topography, striae and other glacial erosional landforms.

2.2.1 Whitefish Falls, Ontario

The 1 km² Whitefish Falls field site (Figs. 2.3, 2.4) exhibits a variety of well exposed glacial erosional landforms including p-forms, roches moutonnee, whalebacks and glacial striae. These features indicate that paleo-ice flow direction in the area is from north-east to south-west (Young & Nesbitt, 1985). However, striae indicate two distinct

Figure 2.3: A) Satellite photograph (courtesy of IKONOS) of the Whitefish Falls field site overlain with colours representing bedrock types (see map elements key). B) Location map of Whitefish Falls. C) Idealized N-S geological cross section of the study area modified from Young & Nesbitt (1985).

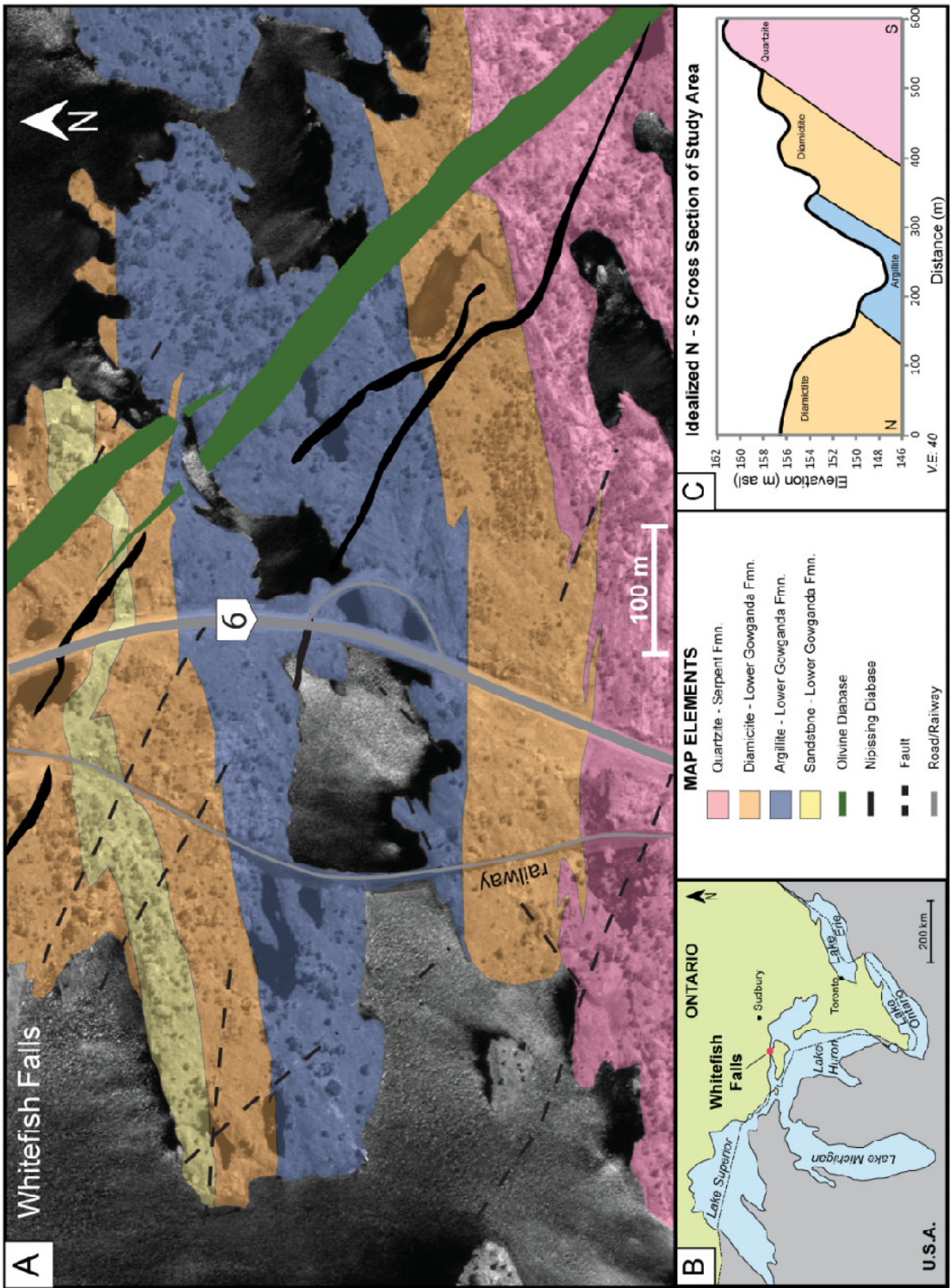


Figure 2.4: Satellite photograph (courtesy of IKONOS) of the Whitefish Falls study area overlain with a digital elevation model (courtesy of Dr. Ugalde, McMaster University) and the location of glacial erosional landforms.

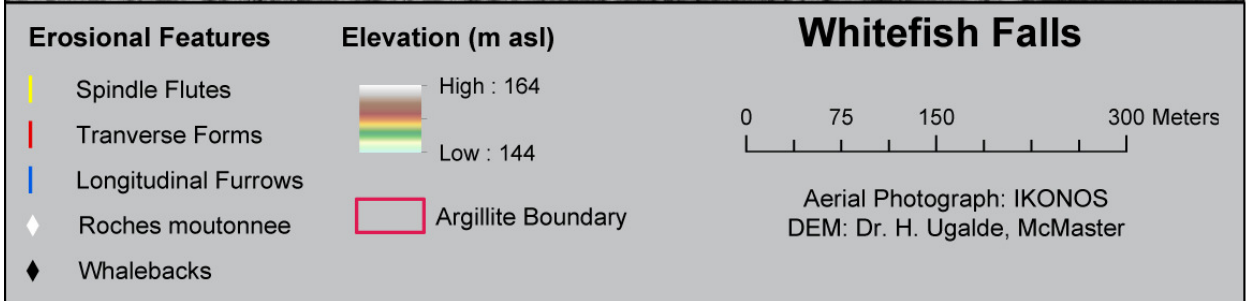
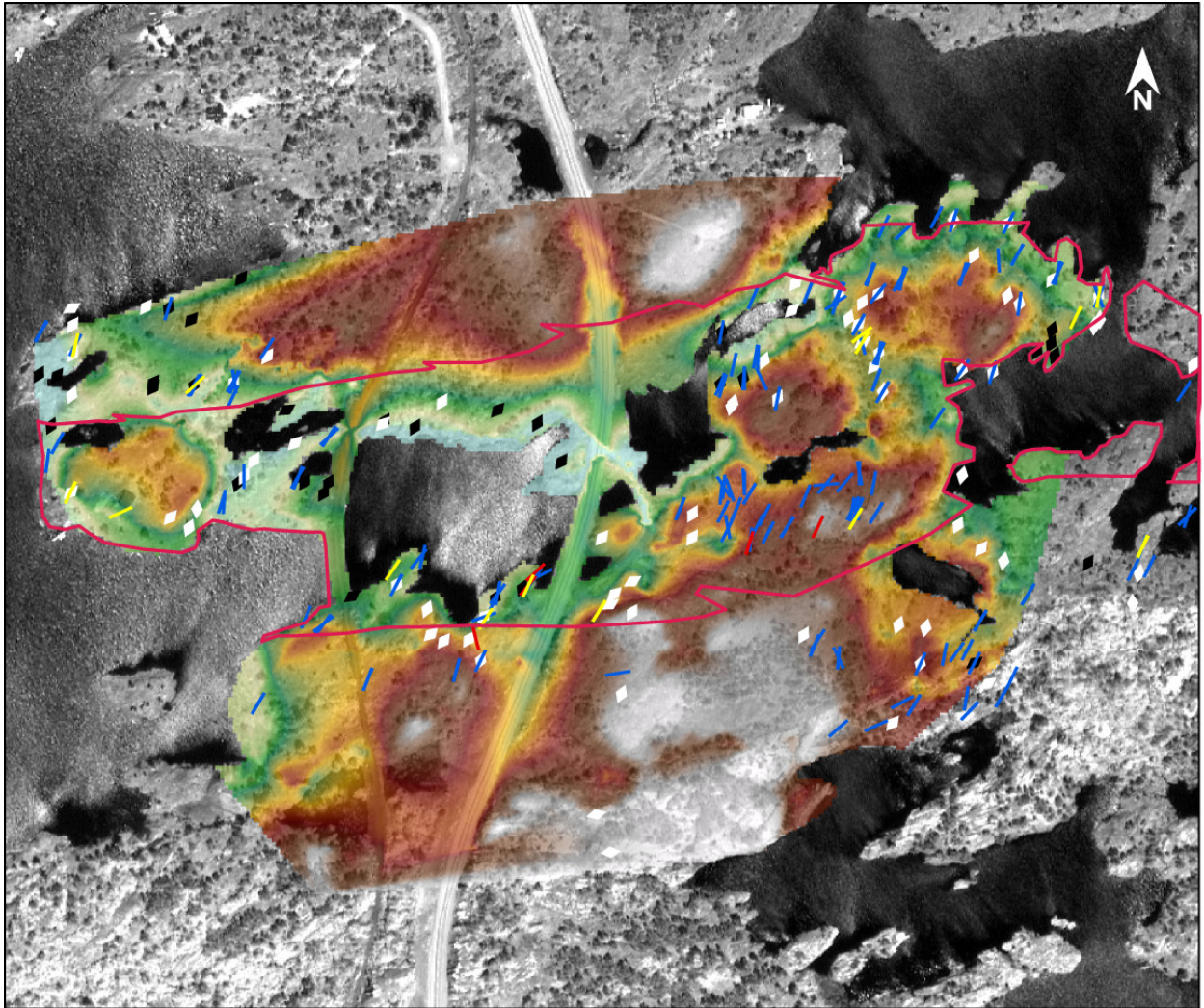
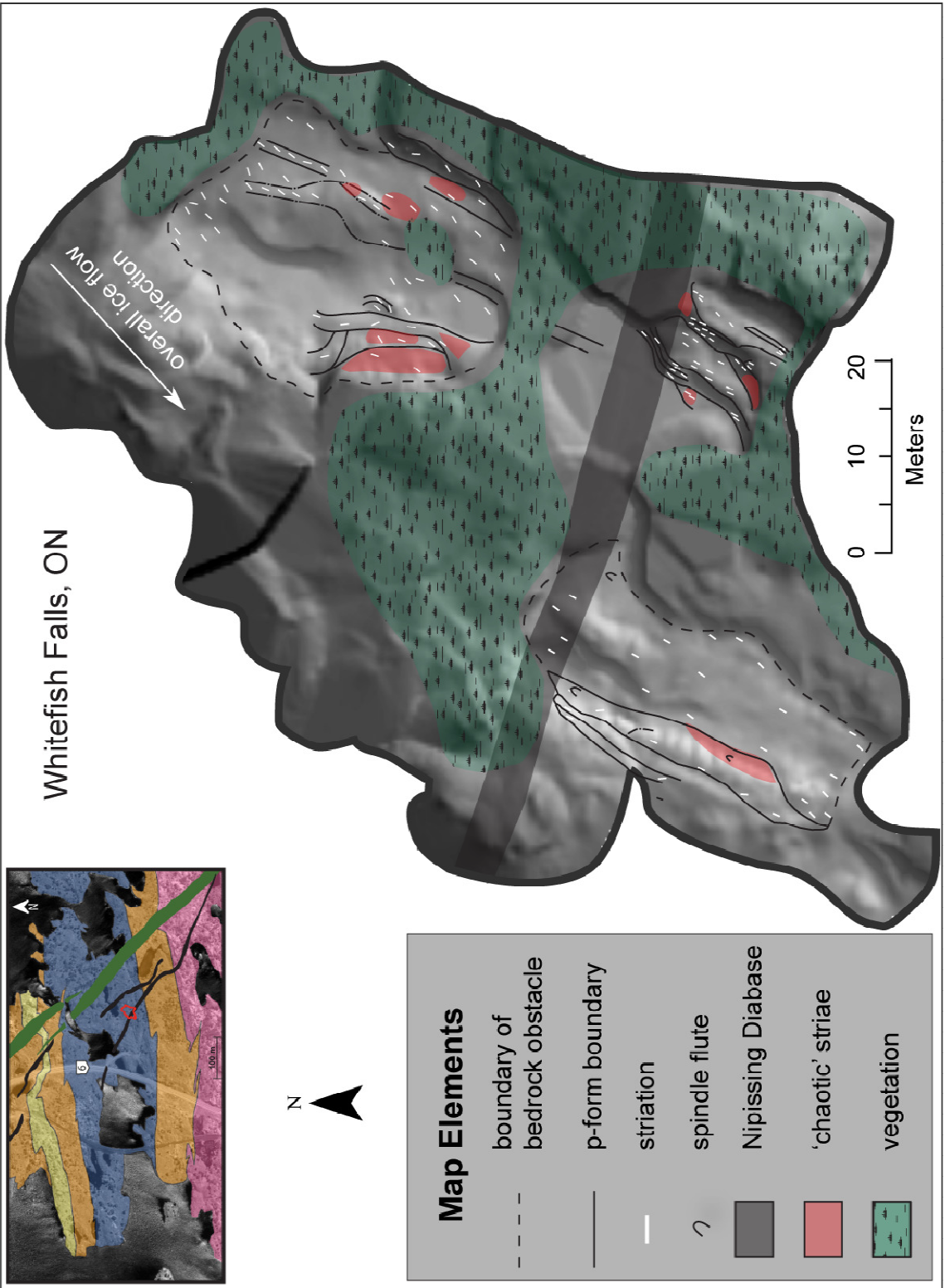


Figure 2.5: Detailed map of a complex p-form assemblage at Whitefish Falls (see inset on upper left for location). Surface topography mapped with a Magellan ProMark3 differential GPS. Note the strong spatial relationship between the location of areas ornamented with chaotic striae (shaded red)



ice flow directions at 210-225° and 195-210°, where the former represents the dominant and most recent ice flow direction, which likely represents ice flow during the Late Wisconsinan prior to complete deglaciation (ca. 10 000 ybp; Barnett, 1992).

At Whitefish Falls, glacial erosional landforms are developed on Paleoproterozoic metasedimentary rocks of the Huronian Supergroup, specifically the Serpent and Lower Gowganda formations, both of which are penetrated by igneous intrusions of olivine diabase (Fig. 2.3 Bennett et al., 1991; Young & Nesbitt, 1985). The Serpent Formation is a feldspathic quartzite, which is extremely resistant to erosion and forms a relative topographic high in the area (Fig. 2.3; Bennett et al., 1991; Young and Nesbitt, 1985). The overlying Lower Gowganda Formation contains three distinct lithologic units, the first of which is a weathered diamictite which is overlain by a metamorphosed mudstone (argillite) that occupies a relative topographic low within the study area, likely due to its relatively high susceptibility to erosion (Fig. 2.3). The argillite unit has two distinct joint sets oriented at 320° and 230° (Young and Nesbitt, 1985). The uppermost unit of the Lower Gowganda Formation is a diamictite complex consisting of interbedded diamictites, argillites and sandstones (Bennett et al., 1991).

2.2.2 P-form Morphologies

The p-form assemblage at Whitefish Falls contains p-forms with four distinct morphologies that can be listed in order of abundance as longitudinal furrow forms (Fig. 2.2A), longitudinal spindle flute forms (Fig. 2.2B), transverse forms (including muschelbruche, comma forms and sichelwannen; Fig. 2CDE), and non-directional forms or 'pot-holes' (Fig. 2.2F). Longitudinal furrow forms at Whitefish Falls are linear to

highly sinuous and range from centimetres to several meters in length and width, and centimetres to 2 m in depth (Figs. 2.2A, 2.6A). These features occur predominantly on the argillite unit of the Lower Gowganda Formation (Fig. 2.4). Longitudinal furrow forms often form stoss-side furrows (Kor et al., 1991), adorning the up-glacier flanks of bedrock obstacles, such as roches moutonnee, with which they share a strong spatial association (Puckering, 2009). In many cases, stoss-side furrows appear to be superimposed on one another. Longitudinal furrows and stoss side furrows typically trend parallel or sub-parallel to reconstructed ice flow direction (approximately NE-SW: Fig. 2.6A), except in cases where furrows are located within localized topographic lows and are oriented parallel to the strike of the topographic low.

Longitudinal spindle flute forms, transverse forms (including sichelwannen), comma-forms, muschelbruche, and potholes (Fig. 2.2; Kor et al., 1991) are also identified at Whitefish Falls, although these morphologies are relatively rare in comparison to longitudinal furrow forms. These forms range between 10 cm to 1 m in scale, and were observed predominantly on the Lower Gowganda argillite (Fig. 2.4). Spindle flutes occur exclusively in the lowest topographic regions of the study area, commonly on the flanks of bedrock obstacles or the extensively striated walls of longitudinal/stoss side furrows (Fig. 2.4). Spindle flute features often contain linear glacial striae. Sichelwannen and comma forms are identified on argillite and diamictite substrates in the southern portion of the study area, adjacent to the higher relief quartzite 'uplands'. Muschelbruche

Figure 2.6: Longitudinal furrow forms at Whitefish Falls located on the sides of (argillite) bedrock highs ornamented with striae. A) A linear longitudinal furrow form containing parallel linear striae. B) A sinuous longitudinal furrow, where striae conform to the curved course of the p-form as opposed to the regional ice flow direction (indicated by striae above the p-form). Note how the striae appear to move up out of a poorly developed pothole feature. C) Chaotic striae ornamenting the wall of a longitudinal furrow form.



(scalloped type surfaces) occur most commonly on the lee side of bedrock obstacles. Only two well developed potholes (Fig. 2.2F) were identified in the Whitefish Falls region, approximately 2 km north-west of the 1 km² study area. These potholes are eroded into argillite and occur on the lee side of a rather large (10 m high, 50 m long) roches moutonnee. An interesting erosional form observed at the Whitefish Falls field site was a series of parallel, symmetrical p-forms surrounding the stoss end of a streamlined bedrock high. These features may be examples of ‘multiple trough forms’ as described by Munro-Stasiuk et al. (2005).

Striae

All of the p-forms observed at the Whitefish Falls site are extensively striated, with long linear striae (Fig. 2.6A). These striae typically conform to the curved course of sinuous p-forms and/or approximate regional ice flow direction (Fig. 2.6B). P-forms align most strongly with the secondary ice flow direction (195-210°) observed in the study area. In many cases, p-forms are ornamented by what are described here as ‘chaotic striae.’ Regions of chaotic striae are characterized by numerous, relatively short, deep striae and gouges showing a wide range of orientations (up to 90° in some cases; Fig. 2.6C); some of these striae are curved and/or sinuous. Areas of randomly oriented striae have not been described extensively in the literature, but may be similar to areas of long-sinuuous striae described by Gjessing (1965) or the ‘v-shaped’ striae documented by Hart (2006). The chaotic striae observed at Whitefish Falls are only found in association with p-forms, often occurring on the stoss and lee sides of furrow floors, and steep furrow

walls (Figs. 2.5, 2.6C,). Regions of chaotic striae are also common on muschelbruche-type “scalped” surfaces on the lee side of streamlined bedrock obstacles.

Bedrock controls

Glacial erosional features occur on all bedrock types at Whitefish Falls but p-forms are most abundant on the least resistant bedrock substrates, which are the argillite and diamictite units of the Lower Gowganda Formation (Figs. 2.2, 2.4). P-forms are rarely seen on more resistant lithologies such as sandstone and quartzite, and those that do occur on those substrates are small and poorly developed.

The p-forms at Whitefish Falls form assemblages or ‘systems’ comprising several longitudinal furrow forms (and occasionally other morphologies) adorning the flanks of streamlined bedrock obstacles, such as whalebacks or roches moutonnee. Detailed mapping of p-form assemblages indicated that longitudinal furrows are located on all regions of bedrock highs, including the stoss and lee sides, eastern and western flanks, and occasionally the flat central portions (Fig 2.5). However, longitudinal furrows reach their maximum size and are most pronounced on the north-west facing flanks of bedrock obstacles. Bedrock (particularly argillite) at Whitefish Falls is heavily fractured and jointed but the location and orientation of p-forms are typically not consistent with fracture or joint orientations, suggesting that their development was not influenced by these features.

2.2.3 Kelleys Island, Ohio

Kelleys Island, Ohio is one of many small islands composed of the locally resistant Paleozoic bedrock in the Western Lake Erie Basin (Fig. 2.7). At Kelleys Island, nine large scale longitudinal furrows (Kor et al., 1991) or ‘mega-grooves’ (Goldthwait, 1979) have been identified (Versteeg & Yunck, 1935; Goldthwait, 1979, Snow et al., 1991). Unfortunately, most of these features have been removed due to extensive quarrying practices, leaving behind remnants of only one ‘glacial groove,’ at the Glacial Grooves State Memorial (GGSM; Figs. 2.7, 2.8). The GGSM itself is a large scale groove system which contains a number of smaller scale p-form assemblages that generally trend east to west (Yunck & Versteeg, 1935; Goldthwait, 1979). Smaller glacial gouges/grooves and striated pavements are also documented on the shorelines of Kelleys Island.

Kelleys Island is underlain by the Paleozoic Columbus Limestone, a highly fossiliferous carbonate that contains abundant gastropods, corals, cephalopods and trilobites (Feldman & Bjerstadt, 1987; Munro-Stasiuk et al., 2005). The Columbus Limestone is relatively flat-lying with a regional dip of 6° (Ver Steeg & Yunck, 1935). The uppermost portion of the exposed limestone at the GGSM is relatively thinly bedded (beds averaging 5 – 10 cm) compared to the lower portion which is more massive. The limestone at the GGSM is cut by several fractures/joints oriented north-east to south-west (~225°) and north-west to south-east (~120°).

Figure 2.7: A) Topographic map of the Kelleys Island region with location of the Glacial Grooves State Memorial (GGSM), and locations where quarrying practices have removed other reported grooves (modified from Goldthwait, 1979). B) Inset map showing the location of Kelleys Island.

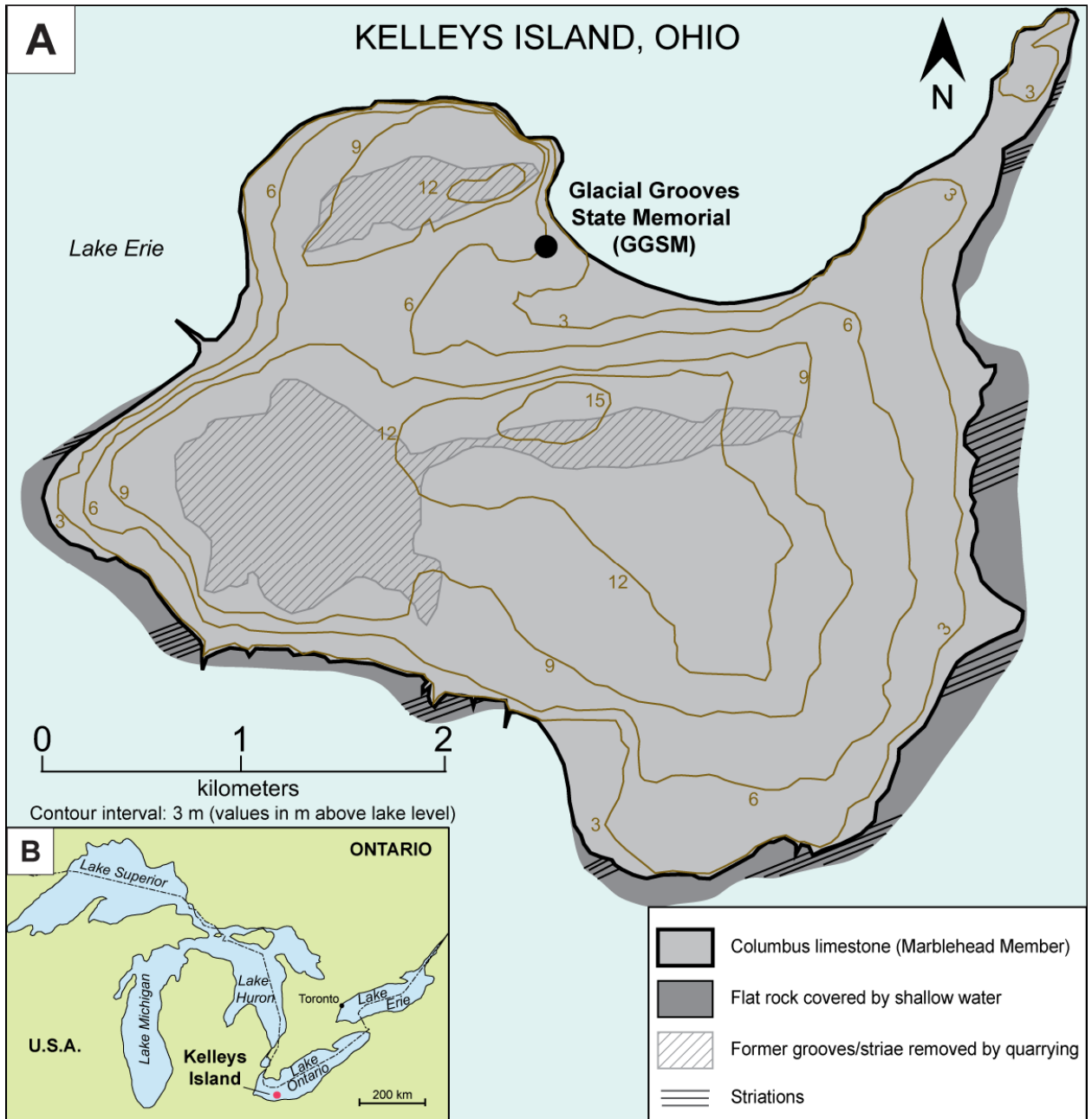


Figure 2.8: Examples of where the location and morphology of p-forms is influenced by the presence of fossil material. A) The comma form is incised into limestone containing few fossils, and undercuts the highly fossiliferous horizon above it. B) Sinuosity initiated by a coral fossil in a narrow cavetto form on the GGSM furrow wall. C) A large sichelwannen feature eroded around a bedrock high containing a large coral fossil.



2.2.3.1 P-form Characteristics

The entire Glacial Grooves State Memorial Site (GGSM) consists of a deeply incised longitudinal furrow form, over 100 m long, up to 10 m wide, and up to 3 m deep, which is oriented east-west consistent with the regional paleo-ice flow direction (Fig. 2.9; Versteeg & Yunck, 1935). Several smaller scale longitudinal furrow forms, sichelwannen, grooves, and streamlined bedrock ridges are eroded into the larger scale furrow (Figs. 2.9, 2.10). All parts of the large scale GGSM furrow have been ornamented with p-forms, including the steep furrow walls, and the furrow floor (Figs. 2.8-2.11). Several smaller scale longitudinal furrow forms are incised into the overall GGSM furrow (Fig. 2.9). At the GGSM longitudinal furrows are linear, up to 1 m wide and deep, are continuous for several metres, and often display deep undercutting along their margins (Figs. 2.9, 2.10). Some furrow forms are sinuous, particularly in the western section of the GGSM. Goldthwait (1979) reported extremely sinuous (meandering) furrows to the immediate north-west of the GGSM, at a site which has subsequently been removed by quarrying. The Kelleys Island site also contains extremely linear, smaller scale (centimetres wide and deep) grooves created by relatively large ($> 0.01\text{m}$) abrasive tools (Glasser & Bennett, 2004; James, 2005; Benn & Evans, 2010). These glacial grooves (along with linear glacial striae) are common on the floors and walls of p-forms as well as on streamlined bedrock rises at the site. The extremely linear longitudinal furrows and glacial grooves are observed predominantly in the eastern (up-ice) portion of the GGSM site (Fig. 2.9) and are generally continuous for several metres before they are truncated by

Figure 2.9: A) View to the west (down-ice flow) along eroded bedrock surface exposed at the Glacial Grooves State Memorial (GGSM) on Kelleys Island, Ohio, showing locations of longitudinal furrows (f) on the flanks of bedrock rises and glacial grooves (g) ornamenting bedrock rises and furrows. The entire GGSM site is classified as a longitudinal furrow with several other p-forms superimposed on its floor and walls. B) Schematic cross section through part of the GGSM furrow.

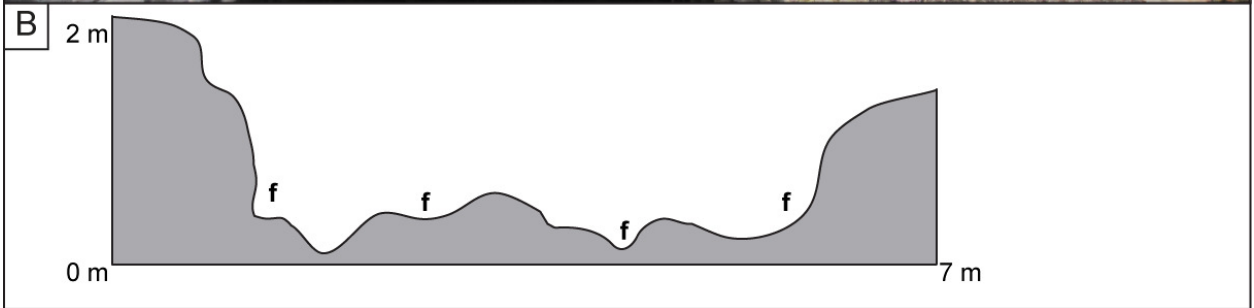


Figure 2.10: Common transverse erosional forms at Kelleys Island, Ohio (sw: sichelwannen, cf: comma form, g: glacial groove, f: furrow). A) An assemblage of sichelwannen and comma forms ornamenting the stoss sides of streamlined bedrock highs. B) A series of sichelwannen as ‘multiple trough forms’ (Munro-Stasiuk et al., 2005) ornamenting the stoss sides of streamlined bedrock highs. Note the truncation of the central portion of these features by a deep glacial groove. C) A series of ‘multiple trough forms’ extending over 2 m from the stoss end of a streamlined bedrock high, with their central portions truncated by glacial grooves. Note the improved definition of these multiple trough forms closer to the streamlined bedrock high. D) Sinuous, parallel multiple trough forms around a streamlined bedrock high.

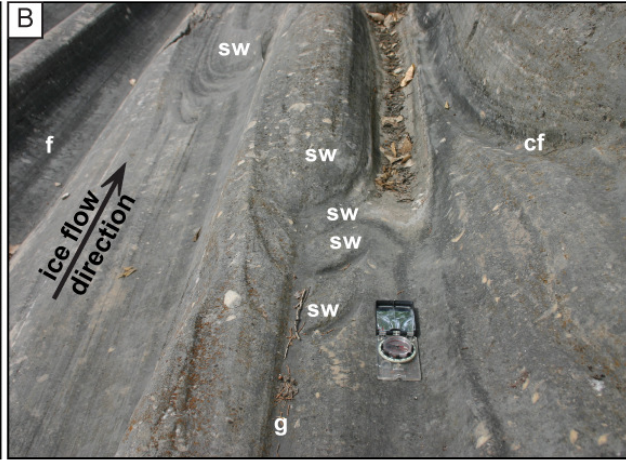
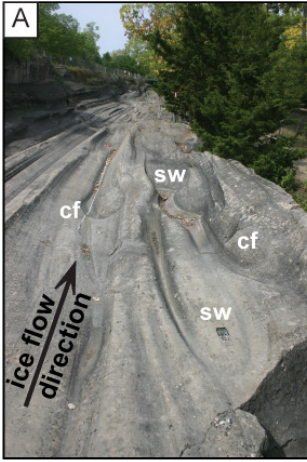


Figure 2.11: Large ‘plunging’ form observed on the uppermost portion of the northern furrow wall at the Kelleys Island GGSM. A) The upper portion of the plunging form has an almost vertical orientation B) the plunging form then turns almost 180°, redirecting itself to conform with the regional ice flow direction. Person for scale is standing at the same position in both photographs. Note the extensive grooves and striations conforming to the curved course of this plunging form.



longitudinal furrow forms or sichelwannen forms that adorn the stoss sides of bedrock highs in the western (down-ice) portion of the GGSM.

Sichelwannen are abundant at the GGSM, commonly eroded into the stoss-side flanks of streamlined bedrock obstacles (Fig. 2.10). An interesting feature at Kelleys Island is a series of several (up to 10), symmetrical and parallel sichelwannen, or comma-forms, with the appearance of ribs, which emanate from a streamlined bedrock obstacle (Figs. 2.10B, C). In some cases these parallel sichelwannen features are sinuous (Fig. 2.10D). These features were referred to as ‘scoop marks’ by Goldthwait (1979) and as ‘multiple trough forms’ by Munro-Stasiuk et al (2005). The scale of these multiple trough forms is proportional to the scale of the streamlined bedrock obstacles that make up the remnant ridge between the ‘arms’ of the sichelwannen (Kor et al., 1991). For instance, small scale multiple trough forms (few centimetres wide and extending less than 1 meter up-ice of the obstacle) occur around smaller bedrock obstacles, whereas the largest series of multiple trough forms are 10 – 15 cm wide and extend over 2 metres from the nose of a large streamlined bedrock obstacle (Fig. 2.10C). Sichelwannen or comma form features formed closest to the streamlined obstacle are typically the most pronounced and well preserved (Fig. 2.10C). Some multiple trough forms were missing their central portions, which were incised by deep glacial grooves.

Another interesting feature of the Kelleys Island field site is the presence of several irregular erosional features, typically between a few centimetres to half a meter in scale, which incise longitudinal furrows and remnant erosional ridges and are commonly oriented transverse to ice flow direction. These features were described as ‘plunging

forms/scours' by Munro-Stasiuk et al. (2005) and are similar to those identified at the Whitefish Falls field site. The most notable plunging form is located on the upper part of the northern wall of the GGSM, and appears to 'enter' the furrow from the north-west, turning sharply to orient parallel (east to west) to other streamlined forms within the furrow (Fig. 2.11). This plunging form is approximately 0.5 m wide and deep, and two metres long with very well defined, sharp edges, and is ornamented with several smaller scale furrows and abundant striations whose orientation conforms to the sinuous nature of the overall form.

Striae

The entire bedrock surface of the Kelleys Island GGSM is extensively striated, with long, linear, grooves and striae (Figs. 2.9, 2.10). Glacial striae are found on all surfaces of the various p-form types, and where p-forms are sinuous, the striae conform to the sinuosity of the p-form as opposed to the regional ice flow direction. Percussion marks, such as chatter marks or crescentic gouges, as well as chaotic striae are notably absent from this field site.

Bedrock Controls

Heterogeneities within the fossiliferous Columbus Limestone at Kelleys Island appear to have exerted some control on p-form development. P-forms within the GGSM furrow are most abundant, and largest, on the floor of the furrow, which is coincident with a thickly bedded limestone unit. Some p-forms are located on the walls of the GGSM furrow, but they are least common toward the top of the furrow walls, an area characterized by thinly bedded (5 – 10 cm) limestone. Several p-forms observed at

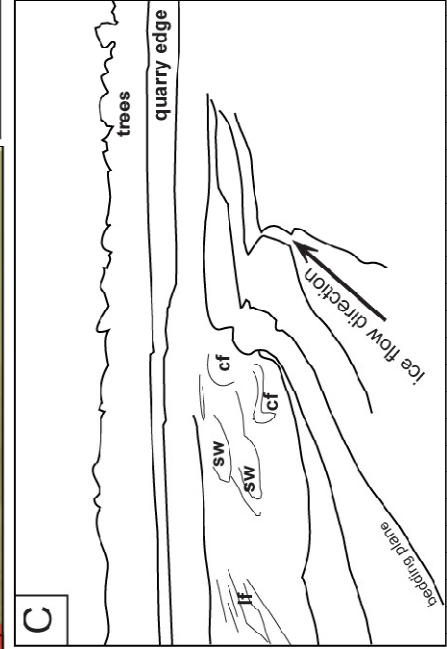
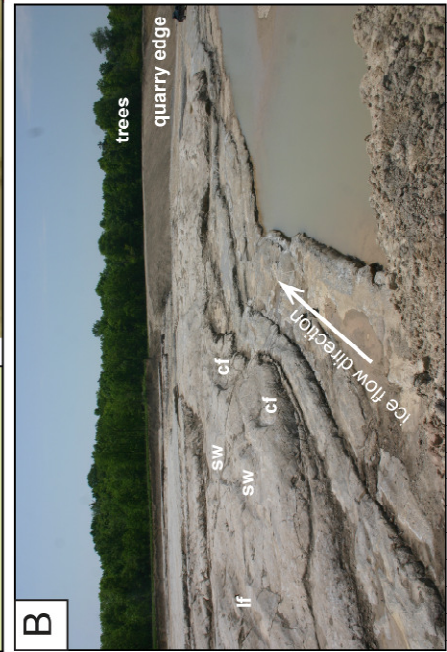
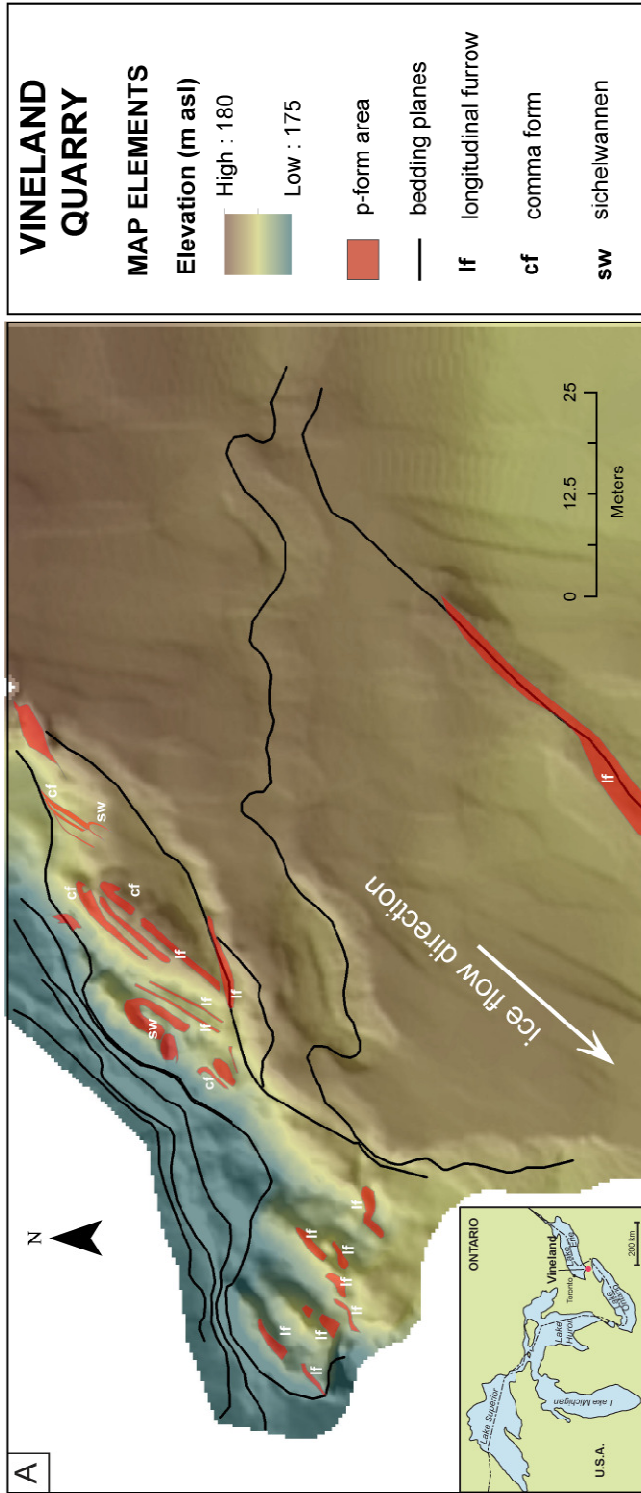
Kelleys Island appear to preferentially undercut into less resistant limestone immediately underlying highly fossiliferous horizons and the deeply incised portions of most furrows and sichelwannen are eroded into limestone relatively devoid of fossil material (Fig. 2.8).

Two joints sets (oriented north-east to south-west and south-east to north-west) are observed within the GGSM; however, these joints do not conform to the regional jointing pattern of Paleozoic strata in the area (Holcombe et al., 1997). The joints do not appear to have been preferentially exploited by glacial erosion processes and probably formed during or after deglaciation of the region.

2.2.4 Vineland, Ontario

An assemblage of p-forms was identified on a recently exposed, 100 m by 80 m bedrock rise of Middle Silurian Lockport dolostone at Vineland Quarry, in Vineland, Ontario (Fig. 2.12). Vineland Quarry is located 10 km south of Lake Ontario, on the brow of the Niagara Escarpment. Variable thicknesses (3 – 8 m) of overburden sediments, including fine grained clays and silts, as well as glaciotectonized diamicts cover the bedrock in most areas of the quarry (MacLachlan & Eyles, 2011). The p-form assemblage observed at this site was uncovered by removal of overburden material prior to quarrying. Two distinct sets of glacial striae were observed on the bedrock surface

Figure 2.12: P-forms observed at Vineland Quarry, Vineland, Ontario. A) A digital elevation model of the relatively small bedrock high exposing longitudinal furrows, sichelwannen and comma forms. Forms that are not labelled are undefined morphologies. B) View of the site (looking south-west) showing p-forms within a 2 m thick bed of dolostone. C) Sketch of the features shown in photograph B, where thicker lines represent bedding planes, and thinner lines represent p-form boundaries.



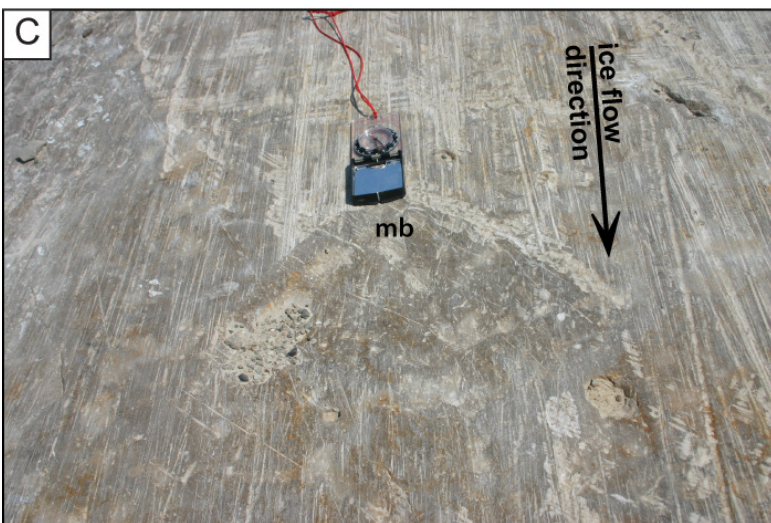
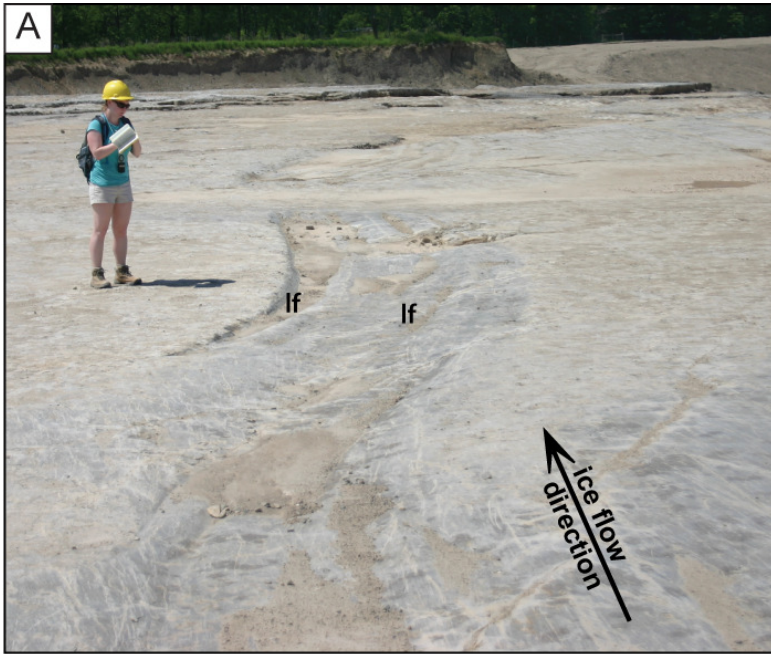
with orientations of 216° and 228°, indicating a general paleo-ice flow direction of north-east to south-west.

The p-form assemblage exposed at Vineland Quarry is eroded into dolostones of the Lockport Formation (Armstrong & Dodge, 2007). In the Niagara region, the Gasport Member of the Lockport Formation is characterized by relatively thick beds (observed in this study to be between 20 and 50 cm thick) of blue-grey dolostone containing abundant crinoids (Armstrong & Dodge, 2007). The uppermost bedrock unit in the study area, interpreted to be the Ancaster Member of the Lockport Formation, is extremely flat lying, and is composed of relatively thinly bedded (5 – 10 cm) dolostone containing abundant chert nodules (Armstrong & Dodge, 2007; Brunton, 2009). The bedrock at Vineland Quarry is fractured with joint orientations ranging between 285° and 300°, directions which are inconsistent with the regional north-east to south-west jointing patterns recorded in Paleozoic dolostones elsewhere in the region (Eyles & Scheidegger, 1995).

2.2.4.1 P-form Characteristics

In general, the p-forms at Vineland Quarry are not well developed and have shallow relief (centimeters to tens of centimetres), and relatively poorly defined edges (Figs. 2.12, 2.13). The majority of p-forms are oriented in a similar direction to paleo-ice flow (aligned north-east to south-west).

Figure 2.13: P-form morphologies identified at the Vineland Quarry field site. A) Shallow, sinuous longitudinal furrows (lf) following the course of a bedding plane in dolostone. B) Examples of comma forms (cf) as multiple trough forms adorning the stoss flanks of a bedrock rise. C) Small muschelbruche (mb) feature containing chaotic striae (below compass). Note how this feature truncates the linear striae that lie in the up ice direction.



The longitudinal furrow form is the dominant p-form morphology identified at Vineland Quarry. Longitudinal furrows are relatively linear in the north-eastern (stoss) portion of the study site and are continuous for several metres (Fig. 2.13A). Comma forms and sichelwannen are also common in this area, together with several narrow (a few centimetres wide) and poorly defined multiple trough forms (Fig. 2.13B; Munro-Stasiuk et al., 2005) centred on streamlined bedrock obstacles. Muschelbruche-type features were also identified throughout the Vineland field site, particularly on the lee side of bedrock highs (Fig. 2.13C). In the down-ice portion of the study area (to the south-west), erosional forms ornament the stoss and lee sides of relatively small bedrock rises (< 1 meter high, metres long; Fig. 2.12A) but they are poorly developed and difficult to assign a specific morphology according to the Kor et al. (1991) classification.

Striae

P-forms observed at Vineland Quarry are extensively striated, with long linear striae ornamenting the floors of furrows, sichelwannen and comma forms (Fig. 2.13A). Chaotic striae (see section 2.1.1.), are also abundant and are found everywhere except on the uppermost portions of the streamlined bedrock obstacles, where linear striae are commonly observed. Chaotic striae are particularly common on the walls and margins of p-forms and within muschelbruche-type scalloped surface (Fig. 2.13C).

Bedrock Controls

At the Vineland Quarry, p-forms are most abundant and well developed on massive dolostones of the Gasport Member but are rare and poorly developed on

Figure 2.14: Aerial photograph of the Pelee Island field site (south-eastern shoreline), with p-forms and glacial grooves ornamenting Columbus Limestone pavement. Several linear features are visible from the aerial photograph. Aerial photograph courtesy of South-Western Ontario Orthophotography Project (SWOOP) 2006.



exposures of thinly bedded dolostone of the Ancaster (Goat Island) Member. While other studies have observed strong a relationship between p-form orientations and fracture and jointing patterns (Rea et al., 2000), the development and orientation of p-forms at Vineland Quarry does not seem to have been influenced by the few fractures observed at this site, as fractures are rare, irregular and inconsistent with the overall directional trend of the p-forms.

2.2.5 Pelee Island, Ontario

Pelee Island, Ontario is the most southerly point in Canada, located in western Lake Erie, and is one of many small islands composed of the locally resistant Paleozoic bedrock in the Western Lake Erie Basin (Fig. 2.14). Similar to Kelleys Island, Pelee Island is underlain by the highly fossiliferous Middle Devonian Columbus Limestone (Feldman & Bjerstadt, 1987; Snow et al., 1991; Holcombe et al., 1997). While most of the island is covered by overburden sediment, the Columbus limestone outcrops on the south-eastern shore of the island and displays an assemblage of striations, grooves and p-forms. Striae orientations range from 204° to 280° and suggest paleo- ice flow directions from north-east to south-west, which is typical of all of the Western Lake Erie islands (Holcombe et al., 1997; Munro-Stasiuk et al., 2005).

The Columbus Limestone at Pelee Island is thinly bedded (beds range between 5 and 10 cm thick) and, although it is typically fossil-rich, (Feldman & Bjerstadt, 1987; Munro-Stasiuk et al., 2005), the bedrock exposures containing p-forms do not contain

abundant fossil material. Bedrock is well jointed with joint orientations primarily between 204° and 209°, with a secondary orientation of 240°, (the latter more closely represents the prevailing east-west joint direction reported by Holcombe et al., 1997).

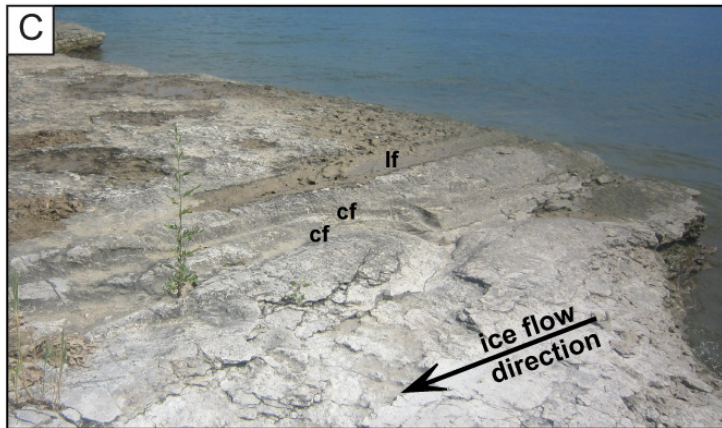
Similar to most of the islands in the Western Lake Erie basin, the topography of Pelee Island is extremely flat, with underlying bedrock strata displaying only a slight north-eastern dip (6°; Holcombe et al., 1997).

2.2.5.1 P-form Characteristics

The south-eastern shoreline of Pelee Island exposes an extensive set of linear, shallow glacial grooves (Fig. 2.15A), with some features that can be classified as p-forms, eroded into the Columbus limestone pavement (Fig. 2.15B). Extremely linear longitudinal furrow forms (oriented between 240° and 250°) can be observed across the study area, most commonly in topographic lows between streamlined bedrock highs. The largest longitudinal furrow observed was continuous for several metres, up to 4 m wide, and displayed minor undercutting of the limestone on the flanks of the surrounding bedrock highs.

The only other p-form morphology identified at Pelee Island is the comma form. Two small comma-form features, lying parallel to one another and eroded into a streamlined bedrock rise were observed (Fig. 2.15C). These may be considered as multiple trough forms similar to those described from Kelleys Island (Fig. 2.10C; Munro-Stasiuk et al., 2005).

Figure 2.15: Glacial erosional features observed on exposed limestone pavement on the south-eastern shore of Pelee Island, Ontario. A) Shallow, linear glacial grooves. B) Longitudinal furrow infilled with lake sediment and algae. Most longitudinal furrows were submerged, this feature is about 0.5 m deep, and displays striae on the sculpted walls. C) One longitudinal furrow form (lf) and two superimposed comma forms (cf; ~ 2 m in total length), or ‘multiple trough forms’ on the north west facing side of a small bedrock high. D) Extensively striated pavement displaying a range of orientations.



Striae

The bedrock at Pelee Island was extensively striated, with a wide range of striae oriented between 204° and 280°, which probably record different phases within an overall episode of glacial abrasion. However, it was not possible to determine the temporal relationships between these phases due to difficulties in determining consistent cross-cutting patterns (Fig. 2.15D). While there are a wide range of striae orientations, these striae did not classify as ‘chaotic’ striae as documented in the Whitefish Falls and Vineland Quarry field sites. Many p-forms are ornamented with continuous, linear glacial striae oriented parallel to the long axis of the p-form.

2.3 Comparison of the P-form Assemblages

The p-form assemblages observed at the four field sites share many similar characteristics but also display significant differences in the morphology of the p-forms, relationships to bedrock lithology and structure, relationships to topography, as well as their association with other features such as grooves and striae. Table 2.3 summarizes the dominant characteristics of the p-form assemblages examined at each of the four sites.

2.3.1 Similarities between p-form assemblages

At each of the field sites the orientation of linear p-forms is parallel or sub-parallel to regional paleo-ice flow direction (north-east to south-west; Fig. 2.16) and all p-form morphologies are heavily striated with long, linear, glacial striae or chaotic striae

Figure 2.16: Rose diagrams showing striae orientations of linear p-forms, glacial striae and joints from Whitefish Falls, Vineland and Pelee Island. Detailed measurements were not taken at Kelleys Island as striae and p-form orientations were extremely similar, and very few fractures were observed. Arrows on rose diagrams for p-forms represent the ice-flow direction at each site based on observations and glacial striae.

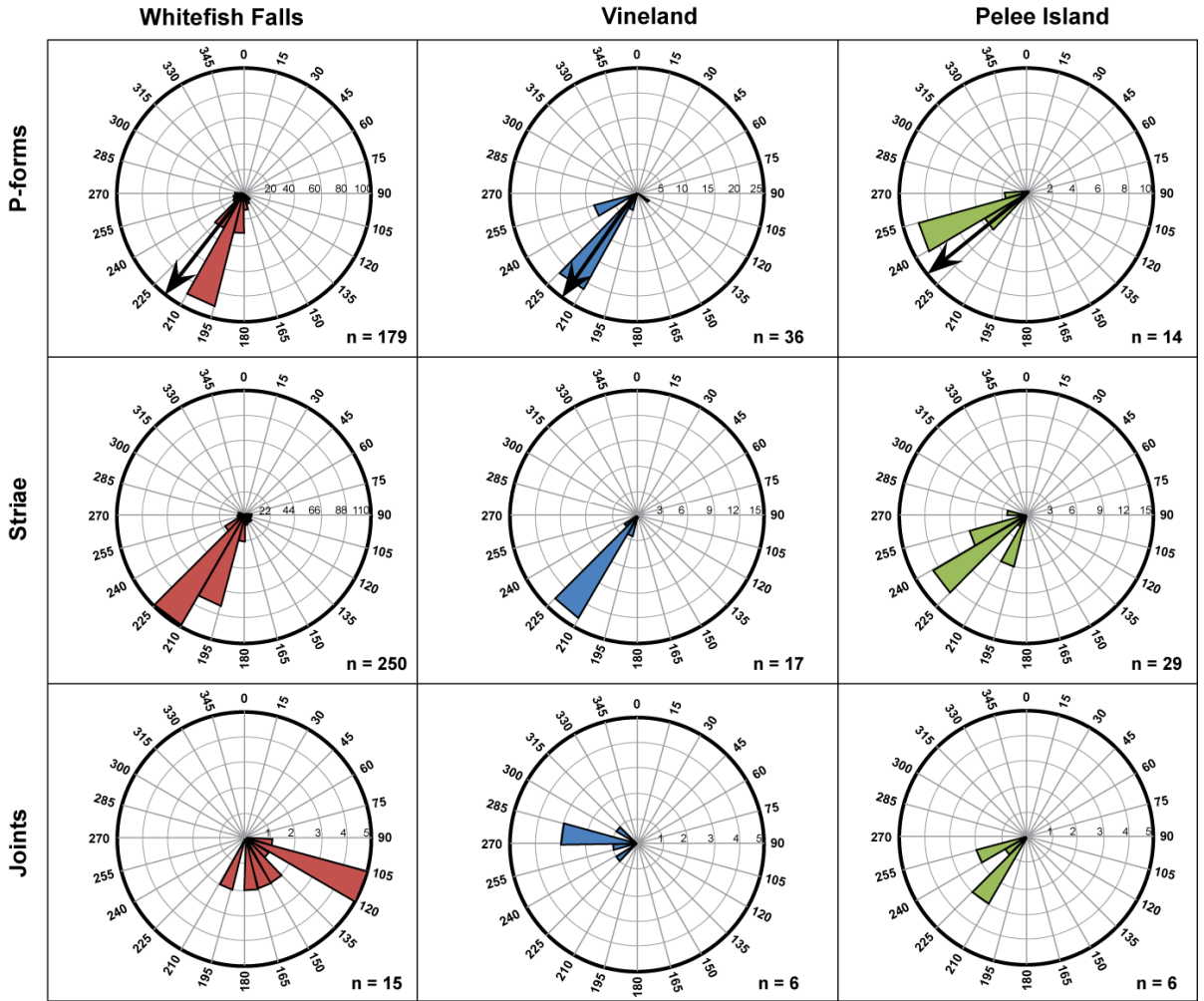


Table 2.3 Comparisons of p-form characteristics and controls on erosion from the four study sites.

	Whitefish Falls	Vineland	Kelley's Island	Pelee Island
Bedrock Substrate	Metasedimentary	Dolostone	Limestone	Limestone
Dominant Form	Longitudinal furrow	Longitudinal Furrow	Longitudinal Furrow	Longitudinal Furrow
Secondary Forms	Spindle flutes	Sichelwannen / comma forms Muschelbruche	Multiple trough forms Plunging forms	Comma form
Rare Forms	sichelwannen	multiple trough forms	cavettos	
	potholes			
	cavettos			
	plunging forms			
multiple trough forms				
Forms contain glacial striae	Yes	yes	yes	yes
Sinuuous Forms	abundant	occasional	occasional	rare
Chaotic Striae	abundant	abundant	absent	absent
Topographic Influence	Yes	Undetermined	Yes	n/a
Lithological Influence	affinity for argillite substrate	n/a	fossils & fossiliferous horizons	n/a
Structural Influence	Minimal	bedding	bedding	p-forms coincident with joints
Average P-form Orientation (° N)	195-210	225-240	245	240-250
PF deviation from Striae	15	n/a	n/a	15

(Figs. 2.3, 2.6AB, 2.9, 2.13A, 2.15B). The presence of linear, glacial striae within p-forms suggests that glacial ice had contact with the bedrock surface, and played some role in developing or ornamenting the p-forms observed at each field site. The longitudinal furrow form is the most common form observed at each field site, and is often found on the lateral flanks of streamlined bedrock highs. The only other p-form morphologies that are observed at all four field sites are comma forms, which are often observed on the stoss flanks of bedrock highs. Comma forms occur as a series of ‘multiple trough forms’ around the stoss sides of resistant bedrock rises at all four field sites, and are particularly abundant and well developed at Kelleys Island. The occurrence of multiple trough forms at all four sites is an important observation as it records multi-stage incision of comma form and/or sichelwannen features around bedrock obstacles, where a remnant ridge is progressively eroded down flow (Munro-Stasiuk et al., 2005). This suggests that these features develop over an extended time period and may not result from a single ‘geologically instantaneous’ event as has been suggested by some workers (Sharpe & Shaw, 1989; Kor et al., 1991; Munro-Stasiuk et al., 2005).

2.3.2 Differences between p-form assemblages

The p-forms observed at Whitefish Falls and Kelleys Island are the largest, and best developed of all those observed as they show deep incision into bedrock, often with significant undercutting, and have well defined rims and sharp edges (Figs. 2.3A, 2.8A, 2.11, ; Table 2.3). P-forms at the Pelee Island and Vineland Quarry sites are generally much shallower (centimetres to tens of centimetres) with much less well defined (or

sharp) boundaries. While the p-forms at all of the sites investigated in this study were extensively striated with glacial striae, only two sites (Whitefish Falls and Vineland Quarry) displayed abundant chaotic striae. This difference in the scale and development of the p-forms at each site may be related to substrate type, topography and structure as well as the length of exposure to, and erosive capability of the scouring mechanism responsible for p-form development.

2.3.3 Substrate type

The p-forms investigated in this study were observed on several different substrates, including the metasedimentary rocks of the Gowganda and Serpent Formations at Whitefish Falls, and Paleozoic limestones and dolostones at the Kelleys Island, Pelee Island and Vineland Quarry field sites. The Whitefish Falls study site displays the full suite of p-form morphologies and was the only site studied in which longitudinal spindle flute forms and potholes (as described by Kor et al., 1991; Benn & Evans, 2010) were observed. The other three sites show significantly fewer p-form morphologies (Table 2.3) which may be due in part to the limited exposure of bedrock at these sites and the shorter duration of subglacial conditions and the period of erosion. Sichelwannen and comma forms are abundant at Kelleys Island and Vineland (Table 2.3), most commonly eroded into the stoss end of a streamlined bedrock obstacle, but are relatively rare at Whitefish Falls, and Pelee Island. Sichelwannen and comma forms documented at Whitefish Falls are comparatively small, and are rarely observed on the stoss-sides of streamlined bedrock obstacles, despite the abundance of streamlined bedrock obstacles at the site. This difference in p-form development may again be related to the nature of the

Paleoproterozoic metasedimentary bedrock which is much more resistant to erosion than the limestones and dolostones found at the other sites.

Whitefish Falls and Kelleys Island were the only two sites studied in which significant on site lithological differences were identified, and at these locations p-forms occurred predominantly on the substrate which was most susceptible to erosion. This suggests that where major lithologic changes can be identified, the erosive agent responsible for p-form development will preferentially erode areas with higher susceptibility to erosion. The bedding of the of the substrate appeared to be quite influential on p-form development at the Kelleys Island and Vineland Quarry sites, as p-forms identified at these sites were more common in massive beds, while p-forms were relatively rare in more thinly bedded substrates, where plucking may have been a more influential process (Benn & Evans, 2010).

2.3.4 Topography

Observations at the Whitefish Falls and Kelleys Island field sites indicate that bedrock topography appears to exert at least some control on the development of p-forms. At these sites, p-form assemblages were most commonly observed ornamenting the sides of streamlined bedrock highs within regional topographic lows. At Whitefish Falls and Vineland, p-forms were most abundant, and most well developed on the north-west facing slopes of bedrock obstacles. A regional topographic control on p-form development could not be clearly identified at Vineland Quarry or Pelee Island due to the thick overburden cover and limited exposure of eroded bedrock surfaces.

2.3.5 Bedrock Structures

Although the presence of fractures and joints did not appear to significantly influence p-form development at Vineland and Kelleys Island, some p-forms at Whitefish Falls closely conformed to fracture orientations within argillite, diamictite, and quartzite bedrock. There is also a coincident relationship between p-form orientation and joint orientation at the Pelee Island field site. However, this may be related to the conformity of the jointing pattern with the observed paleo-ice-flow direction in the area (both about 240°).

2.4 Inferred Subglacial Processes

The variability of p-form characteristics observed at the four sites examined in this study (Whitefish Falls, Kelleys Island, Vineland Quarry and Pelee Island; Table 2.2) can be used to make some inferences about the nature of subglacial erosional processes and controls on the development of p-forms. Several theories have been presented in the literature which assign the formation of p-forms to specific subglacial processes, including sediment charged meltwater (Dahl, 1965; Allen, 1971), glacial abrasion (Boulton, 1974), and erosion by saturated till (Gjessing, 1965). Different subglacial processes have the potential to produce morphologically similar features (e.g., longitudinal furrows, sichelwannen; Allen, 1971, Boulton, 1974; Kor et al., 1991; Rea et al., 2000), and it is therefore important to consider all factors that may have influenced

their development as well as the possibility that they may result from the operation of multiple processes (Rea et al., 2000).

2.4.1 Subglacial meltwater erosion

P-forms were initially hypothesized to have developed as a result of erosion by sediment charged meltwater (Dahl, 1965), specifically by vortices in turbulent meltwater created by bed irregularities or flow instability (Dahl, 1965; Allen, 1971; Shaw, 1988; Kor et al., 1991). Spindle flutes, potholes and sichelwannen have been attributed to meltwater erosion due to the development of similar forms in fluvially dominated environments (Tinkler & Stenson, 1992; Whipple et al., 2000). Features resembling p-forms have also been recreated in flume experiments under unidirectional turbulent flow conditions (Allen, 1971; Shaw & Sharpe, 1989). The sinuosity of many p-forms is viewed a strong indicator of erosion by turbulent meltwater as glacial ice moves in a laminar fashion and is unlikely to produce highly tortuous features (Shaw, 1994; Benn & Evans, 2010). Substrate erosion by sediment charged meltwater is considered to be a significant contributor to p-form development in areas where subglacial meltwater was likely to have been focused (Shaw, 1988; Kor et al., 1991; Rea et al., 2000).

Observations of p-form assemblages occurring over wide spatial areas of the Canadian Shield (tens to hundreds of kilometres) have been used to support the hypothesis of catastrophic subglacial meltwater flooding, particularly in areas where there is an abundance of spindle flutes, sichelwannen, comma forms and potholes (Shaw, 1988; Sharpe and Shaw, 1989; Kor et al., 1991). This hypothesis requires that all p-forms found in a small geographic area are formed by one simultaneous event, with extensive ice-bed

separation and sufficient current velocity and suspended load to erode bedrock extremely quickly (Shaw, 1988; Sharpe & Shaw, 1989; Kor et al., 1991). However, the catastrophic subglacial meltwater flood hypothesis is extremely controversial and has been widely criticized in the literature (e.g., Clarke et al., 2005; Eyles, 2007; O’Cofaigh et al., 2010).

The exceptionally sharp rims and occasional sinuosity (Fig.2.10) of comma forms, sichelwannen and multiple trough forms (particularly at the Kelleys Island, Whitefish Falls and Pelee Island sites) around streamlined bedrock highs suggests that these forms were eroded by vortices in turbulent meltwater propagated by bedrock ‘obstacles’ (Shaw, 1988; Kor et al., 1991; Shaw, 1994; Munro-Stasiuk et al., 2005). The presence of spindle flute forms and potholes at Whitefish Falls also suggests that subglacial meltwater erosion was an active process (Shaw, 1988; Kor et al., 1991; Rea et al., 2000; Glasser & Bennett, 2004). The development of multiple trough forms may indicate progressive erosion of comma forms or sichelwannen as the streamlined bedrock obstacle was continually eroded down-flow by vortices in turbulent meltwater (Munro-Stasiuk et al., 2005). This may explain why the nested features more proximal to the streamlined bedrock obstacle are more pronounced, as they are likely the most recent of the series and developed progressively over time rather than as the product of a single ‘instantaneous’ event. The longitudinal furrows observed at each of the field sites often have sharp, undercut rims and display some sinuosity, suggesting that these features may also have been influenced by turbulent meltwater erosion (Shaw, 1988; Kor et al., 1991; Shaw, 1994; Munro-Stasiuk et al., 2005).

The concentration of p-forms types attributed to erosion by subglacial meltwater (e.g., potholes, spindle flutes, sichelwannen, comma forms; Shaw, 1988; Kor et al., 1991; Glasser & Bennett, 2004; Munro-Stasiuk et al., 2005), in regional topographic lows in the Whitefish Falls and Kelleys Island study areas suggests that subglacial meltwater was likely focussed in these areas.

2.4.2 Glacial Abrasion

P-forms have also been attributed to development by glacial abrasion under debris rich basal ice, specifically where basal ice streams around bedrock obstacles such as lodged boulders, or knobs of relatively resistant bedrock (Boulton, 1979). As basal ice tends to move more rapidly around an object than over it, debris-rich ice can become concentrated in troughs between bedrock obstacles, creating optimal conditions for p-forms to develop on the flanks of features such as roches moutonnee (Goldthwait, 1979; Benn and Evans, 2010). Glacial abrasion occurs as a result of debris entrained in basal ice being dragged over the substrate and the intensity of abrasion is dependent upon the hardness of the bedrock substrate relative to abrading clasts. Rates of glacial abrasion are inversely proportional to the hardness of bedrock (Glasser & Bennett, 2004; Benn & Evans, 2010) and are also dependent upon the grain size of the debris held in basal ice (Boulton, 1974, 1979; Benn & Evans, 2010).

Striae and grooves produced by glacial abrasion are present at each of the four field sites examined in this study and can be continuous for several metres, indicating persistent contact between debris rich basal ice and the bedrock surface (Glasser & Bennett, 2004). These features are often used to determine paleo-ice flow directions as

their orientations are consistent with the local ice movement (Glasser & Bennett, 2004; Benn & Evans, 2010). The p-forms observed at each site are most often oriented parallel or sub-parallel to ice flow direction and contain linear striae. The presence of striae indicates that glacial ice played at least some role in their formation, either creating them through glacial abrasion or at the very least, modifying them after development by other processes. At Pelee Island, p-forms are extremely linear and consistent with the observed paleo-ice flow direction determined from striae, suggesting that p-form development was strongly influenced by glacial abrasion processes. Some linear striae fully conform to the curvature of sinuous p-forms and provide evidence for intense glacial abrasion and local variations in flow direction as ice deformed and moved around bedrock obstacles (Boulton, 1974). Alternately, these linear striae may have been abraded after the creation of the initial sinuous form (e.g., Rea et al., 2000).

At Whitefish Falls, the orientation of several p-forms located on the topographically highest reaches of the study area (the quartzite uplands) conforms to fracture orientations in the bedrock, which suggests that glacial abrasion exploited these pre-existing structures.

2.4.3 Saturated Till Erosion

Not all p-forms have been attributed to an origin by sediment charged meltwater or glacial abrasion. Gjessing (1967) observed long sinuous striae ornamenting the lee sides of bedrock obstacles as well as vertically oriented striae within potholes. The close

association of these striae with p-forms lead him to propose that these features were forming simultaneously by a 'plastic scouring substance', thought to be a saturated till, lying between basal ice and the bedrock surface. This notion is supported by recent observations at Athabasca Glacier where a saturated, mobile till sheet was observed beneath the rapidly flowing ice (Hart, 2006). Both the till matrix and large mobile clasts within this deforming sediment layer were capable of eroding the underlying limestone bedrock.

The chaotic striae observed at Whitefish Falls and Vineland Quarry may be similar to the long sinuous striae observed by Gjessing (1965) or the 'v-shaped' striae ornamenting recently deglaciated limestone at Athabasca Glacier, Alberta (Hart, 2006), both of which are attributed to erosion by a saturated till. The multidirectional nature of these striae argues against an origin by debris held firmly within the ice base but suggests clast movement in the abrading medium. Similar striae have been described on bedrock substrates overridden by drift ice (Dionne, 1985) as well as by debris flows (Atkins, 2003). The presence of zones of chaotic striae at both Whitefish Falls and Vineland Quarry suggests that a saturated till was present in these areas, was capable of eroding the bedrock, and may have played at least a partial role in the development p-forms. No 'chaotic striae' were observed at the Pelee Island and Kelleys Island field sites, suggesting that saturated till erosion was not an active erosional mechanism at the Western Lake Erie sites. The presence of chaotic striae on p-forms at some sites, and their absence at others, may indicate saturated till erosion is not a requirement for p-form

development, but can modify or enhance the development of p-forms after they have been created by some other subglacial erosion process.

2.5 Discussion

Analysis of the p-form assemblages at each of the four sites suggests that multiple subglacial erosional processes are operating concurrently, or at least closely spaced in time. Cross cutting striae are documented extensively at the Whitefish Falls, Pelee Island and Vineland field sites, providing evidence for slight changes in ice flow direction during the period of erosion. The products of glacial abrasion, such as striae, glacial grooves, and streamlined bedrock features (whalebacks and roches moutonnee) are often truncated by various types of p-forms, indicating that regional glacial abrasion was an active process prior to the development of localized p-forms. The spatial association of simple linear features such as striae, grooves, and streamlined bedrock features, formed by glacial abrasion with more complex, often sinuous p-forms created by vortices in turbulent subglacial meltwater may indicate both spatial and temporal changes in subglacial erosional process.

The truncation of glacially abraded features such as grooves and striae by more sinuous, meltwater features including sichelwannen, comma forms, and multiple trough forms at Kelleys Island indicates that the formation of p-forms may be temporally staged. At this site, linear grooves created by glacial erosion may have acted as subglacial meltwater drainage pathways along which sediment charged meltwater was able to flow and further modify these features into sinuous, sharp rimmed p-forms (Benn & Evans, 2010). At Whitefish Falls and Vineland Quarry, saturated till may have also been present

in the later stages of p-form development, as chaotic striae are common on the surfaces of p-forms at both sites. Further evidence for multi-stage development of p-forms is provided through observations of several stages of incision and erosion of the forms themselves that show the progressive development of multiple trough forms around a medial ridge eroding down flow, the presence of spindle flutes within longitudinal furrows, or the superimposition of longitudinal furrows on the flanks of bedrock obstacles.

Local and regional topographic variability may also be important in determining the position and morphology of p-forms (Kor et al., 1991; Rea et al., 2000). P-forms at Whitefish Falls and Kelleys Island are found within a regional topographic low, and occur specifically on localized bedrock highs or streamlined bedrock features such as roches moutonnee within these topographic lows. These areas of variable topography can result in highly variable ice flow pathways, and the development of low pressure cavities into which debris rich basal ice, subglacial meltwater (Rea et al., 2000), and potentially saturated till (Hart, 2006) can become focussed, enhancing bedrock erosion. Areas with high localized topographic variability examined in this study contain abundant glacial striae, p-form features attributed to meltwater erosion (e.g., spindle flutes, sichelwannen, comma forms) and chaotic striae, which suggests that all three erosive agents were operational in these areas. The concentration of p-forms at Whitefish Falls and Vineland particularly on the north-west facing (stoss) walls of bedrock obstacles may be related to focussing of erosion by glacial ice, meltwater and saturated till in areas where ice was impacting bedrock highs as it flowed from the north-east to the south-west.

2.6 Conclusions

A wide variety of p-form morphologies were documented at the Whitefish Falls, Vineland, Kelleys Island and Pelee Island field sites. The longitudinal furrow form is the most common p-form morphology observed at each site, although sichelwannen and/or comma forms (occasionally occurring as ‘multiple trough forms’) were identified within each study area. Differences in the nature of the p-forms and their development at each site allows some inferences to be made about factors influencing their spatial and temporal development. Bedrock controls appear to be highly influential in the development and morphology of p-forms. P-forms develop preferentially and with higher definition on substrates which are most susceptible to erosion. In some instances, the spatial distribution of p-forms appears to be influenced by variations in the erosive susceptibility of the substrate as p-forms commonly adorn the flanks of resistant bedrock highs (e.g. Whitefish Falls). At Kelleys Island, p-forms preferentially erode into limestone horizons that are relatively devoid of more resistant fossil material. The nature of bedding within a bedrock substrate is also important, as p-forms are found in the highest concentrations in thickly bedded or massive lithologies, and their development appears to be inhibited on substrates which display thinner bedding, where plucking may be a more effective erosive process.

Observations from Whitefish Falls, Kelleys Island, Vineland Quarry and Pelee Island provide evidence for the creation of p-forms through erosion by glacial abrasion, subglacial meltwater and saturated till. The highly variable nature of p-form assemblages

documented at each of the four sites in terms of their morphology and spatial distribution suggests that no single process is responsible for their development and that formative processes change both spatially and temporally. A multi-phase evolution of p-form development is proposed here whereby glacial ice initially abrades the bedrock surface, leaving behind streamlined bedrock highs, striations and glacial grooves. The flanks of bedrock highs and grooves are subsequently modified into p-forms through erosion by vortices in turbulent subglacial meltwater (Benn & Evans, 2010). At each site, p-forms are ornamented with linear striae suggesting that glacial abrasion was again an active process, leaving behind striae on the sinuous, sharp rimmed, features (Shaw, 1988; Kor et al., 1991; Shaw, 1994; Rea et al., 2000; Munro-Stasiuk et al., 2005; Benn & Evans, 2010). In areas where saturated till is present and can act as an effective scouring agent, chaotic striae may also ornament p-forms, as is seen at Whitefish Falls and Vineland Quarry. However, the lack of evidence for saturated till erosion at all four sites indicates that this process is not required for p-form development. This study presents detailed documentation of p-form assemblages and maps of former glaciated surfaces which indicate significant spatial and temporal variability in the processes operating beneath the Laurentide Ice Sheet.

Future work should focus on detailed regional mapping of glaciated surfaces in other regions of the Great Lakes basins and elsewhere as this would provide additional data with which to analyse the spatial and temporal scales at which subglacial processes operate, particularly if geochronological data are available.

Reference List

- Allen, J.R.L. 1971. Transverse erosional marks of mud and rock: Their physical basis and geological significance in *Sedimentary Geology* 5, 167-185.
- Armstrong, D.K & Dodge, J.E.P. 2007. Paleozoic geology of southern Ontario in *Ontario Geology Survey Miscellaneous Release Data* 219.
- Atkins, C.B. 2003. Characteristics of striae and clast shape in glacial and non-glacial environment [Ph.D thesis]: Victoria University of Wellington library, 321.
- Barnett, P.J. 1992. Quaternary Geology of Ontario in *Ontario Geology of Ontario Special Volume* 4, 2, 1011-1088.
- Benn, D.I., & Evans, D.J.A. 2010. *Glaciers and Glaciation*. Hodder Education, London. pp734
- Bennett, G., Dressler, B.O. & Robertson, J.A. 1991. The Huronian Supergroup and Associated Intrusive Rocks in *Ontario Geologic Survey Special Volume* 4, 549-591.
- Boulton, G.S. 1974. Processes and patterns of glacial erosion. In: D.R. Coates, Editor, *Glacial Geomorphology*, State University of New York, Binghamton, NY (1974), pp. 41–87.
- Boulton, G.S. 1979. Processes of glacial erosion on different substrata in *Journal of Glaciology* 22, 15-38.
- Boulton, G.S. & Hindmarsh, R.C.A. 1987. Sediment deformation beneath glaciers: rheology and geological consequences in *Journal of Geophysical Research* 92, 9059-9082.
- Brunton, F.R. 2009. Update of Revision to the Early Silurian Stratigraphy of the Niagara Escarpment: Integration of Sequence Stratigraphy, Sedimentology and Hydrogeology to Delineate Hydrogeologic Units in *Summary of Field Work and Other Activities, 2009: Ontario Geological Survey, Open File Report 6240* 25-1 to 25-20.
- Clarke, G.K.C, Leverington, D.W., Teller, J.T. & Dyke, A.S. 2005. Fresh arguments against the Shaw megaflood hypothesis: A Reply to comments by David Sharpe on “Paleohydraulics of the last outburst flood from glacial Lake Agassiz and the 8200 B.P cold event” in *Quaternary Science Reviews* 24, 1533-1541.

- Dahl, R. 1965. Plastically sculptured detail forms on rock surfaces in Northern Nordland, Norway in *Geografiska Annaler Series A: Physical Geography* 47, 83-140.
- Dionne, J.C. 1985. Drift-Ice Abrasion Marks Along Rocky Shores in *Journal of Glaciology* 31, 109, 237-241.
- Eyles, N. 2002. Ontario Rocks: Three Billion Years of Environmental Change. Fitzhenry & Whiteside, Toronto, 339 pp.
- Eyles, N. 2006. The role of meltwater in glacial processes in *Sedimentary Geology* 190, 1-4, 257-268.
- Eyles, N. & Scheidegger, A.E. 1995. Environmental significance of bedrock jointing in southern Ontario, Canada in *Environmental Geology* 26, 269-277.
- Feldman, R.M. & Bjertsedt, T.W. 1987. Kelleys island: giant glacial grooves and Devonian shelf carbonates in north-central Ohio. In: D.L. Biggs, Editor, *North-Central Section of the Geological Society of America: Centennial Field guide*. Geological Society of America, Boulder, CO (1987), p395-398.
- Gjessing, J. 1965. On 'plastic scouring' and subglacial erosion in *Norsk Geologisk Tidsskrift* 20, 1-37.
- Gjessing, J. 1967. Potholes in connection with plastic scouring forms in *Geografiska Annaler. Series A, Physical Geography* 49, 178-187.
- Glasser, F.N. & Bennett, M.R. 2004. Glacial erosional landforms: origins and significance for paleoglaciology in *Progress in Physical Geography* 28, 1, 43-75.
- Goldthwait, R.P. 1979. Giant grooves made by concentrated basal ice stream in *Journal of Glaciology* 23, 297-307.
- Hart, J.K. 2006. Athabasca Glacier, Canada- a field example of subglacial ice and till erosion? in *Earth Surface Processes and Landforms* 31, 1, 65-80.
- Holcombe, T.L., Warren, J.S., Taylor L.A., Reid, D.F. & Herdendorf, C.E. 1997. Lake floor geomorphology of western Lake Erie in *Journal of Great Lakes Research* 23, 2, 190-201.
- James, L.A. 2003. Glacial erosion and geomorphology in the Northwest Sierra Nevada, California in *Geomorphology* 55, 1-4, 283-303.

- Kor, P.S.G., Shaw, J. & Sharpe, D.R. 1991. Erosion of bedrock by subglacial meltwater, Georgian Bay, Ontario: a regional view in *Canadian Journal for Earth Sciences* 28, 623-642.
- Maclachlan, J.C. & Eyles, C.H. 2011. Subglacial deforming bed conditions recorded by late Quaternary sediments exposed in Vineland Quarry, Ontario, Canada in *Sedimentary Geology* 238, 3-4, 277-287.
- Munro-Stasiuk, M.J., Fisher, T.G., & Nitzche, C.R. 2005. The origin of the western lake Erie grooves, Ohio: implications for reconstructing the subglacial hydrology of the great Lakes sector of the Laurentide Ice Sheet in *Quaternary Science Review* 24, 2392-2409.
- Ó Cofaigh, C., Dowdeswell, J.A., King, E., Anderson, J.B., Clark, C.D., Evans, D.J.A., Evans, J., Hindmarsh, R.C.A., Larter, R.D. & Stokes, C.R. 2010. Comment on Shaw J., Pugin, A. and Young, R. (2008): "A meltwater origin for Antarctic shelf bedforms with special attention to megalineations" *Geomorphology* 102, 364-375 in *Geomorphology* 117, 195-198.
- Puckering, S. 2009. Spatial Analysis of Glacial Erosional Landforms at Whitefish Falls, Ontario in *Geological Society of America Abstracts with Programs* 41, 7, 621.
- Rea, B.R., Evans, D.J.A., Dixon, T.S. & Whalley, W.B. 2000. Contemporaneous, localized, basal ice-flow variations: implications for bedrock erosion and the origin of p-forms in *Journal of Glaciology* 46, 154, 470-47.
- Sharpe, D.R. and Shaw, J. 1989. Erosion of bedrock by subglacial meltwater in *Geological Society of America Bulletin* 101, 1011-1020.
- Shaw, J. 1988. Subglacial erosional marks, Wilton Creek, Ontario in *Canadian Journal of Earth Science* 25, 1256-1267.
- Snow, R.S., Lowell, T.V. & Rupp, R.F. 1991. A field guide: the Kelleys Island glacial grooves, subglacial erosion features on the Marblehead Peninsula, carbonate petrology, and associate paleontology in *Ohio Journal of Science* 91, 16-26.
- Tinkler, K.J. & Stenson, R.E. 1992. Sculpted bedrock forms along the Niagara Escarpment, Niagara Peninsula, Ontario in *Geographie physique et Quaternaire* 46, 197-207.
- VerSteeg, K. & Yunck, G. 1935. Geography and geology of Kelley's Island in *Ohio Journal of Science* 35, 6, 421-433.

- Whipple, K.X., Anderson, R.S., Glazner, A.F. & Hancock, G.S., 2000. River incision into bedrock; mechanics and relative efficacy of plucking, abrasion, and cavitation in *Geological Society of America Bulletin* 112, 490–503.
- Young, G.M. & Nesbitt, H.W. 1985. The Gowganda formation in the southern part of the Huronian outcrop belt, Ontario, Canada: Stratigraphy, depositional environments and regional tectonic significance in *Precambrian Research* 29, 265-301.

CHAPTER 3

MODELING BEDROCK TOPOGRAPHY IN THE HALTON HILLS REGION OF SOUTHERN ONTARIO

Abstract

Residents of the Halton Hills region of the Greater Toronto Area rely on groundwater extracted from Quaternary sand and gravel aquifers hosted within a complex system of interconnected buried valleys incised into the Queenston Shale bedrock. Urban growth plans require additional groundwater resources for the Halton Hills region (RMH, 2009) but relatively little is known about the topography of the bedrock surface or the exact location and continuity of bedrock valleys that host productive aquifers. This study explores a number of different approaches that may be used to model the buried bedrock surface in the region using both primary bedrock elevation data obtained from outcrop and cored boreholes and secondary data obtained from consultants reports and the Ontario Waterwell Database (OWD). Large digital databases such as the OWD are known to contain significant georeferencing, elevation and geological errors which can severely compromise the reliability of the final output model and require extensive screening prior to modeling. Three stages of data screening are used in this study. In order to create the bedrock topography model 4236 primary and screened secondary data points were interpolated using the Ordinary Kriging algorithm in ESRI's ArcGIS program. A new approach to modeling data of variable quality was explored (Quality Weighted approach)

but proved ineffective for the purposes of this study, as differential weighting of high and low quality data either over-smoothed the model or significantly altered data values. The accuracy of output models was determined through cross validation tests that compare observed and predicted values and calculate Root Mean Square Errors (RMSEs). After exploration of various modeling approaches the most accurate output model (with lowest RMSE scores) identified three major buried bedrock valley systems, named here as the Georgetown, Acton and Sixteen Mile Creek buried bedrock valley systems. Each buried bedrock valley contains up to 40-50 m of Quaternary sediment infill. These valleys were probably carved by both fluvial and glacial processes during the late Quaternary and their location and orientation may be influenced by structural weaknesses in the bedrock. The bedrock topography maps created here can be used to identify areas of interest for future groundwater exploration programs.

3.1 Introduction

The Halton Hills region of Ontario (Fig. 3.1) is a part of the rapidly growing Greater Toronto Area (GTA), and is currently entering a ‘water crisis’ in which towns such as Georgetown and Acton are unable to meet the potable water needs for projected urban growth. Currently, over 55 000 residents of Halton Hills are supplied with drinking water from a series of municipal wells extracting groundwater from aquifers in Quaternary sediments overlying bedrock. Despite this demand for potable water, the groundwater system of the Halton Hills region is relatively poorly understood and there is an urgent need to characterize known aquifer systems to determine their long term sustainability, and to locate new groundwater supplies (RMH, 2009). The most productive aquifers in the Halton Hills region are hosted in coarse-grained fluvial/glaciofluvial deposits located in bedrock valleys (Meyer and Eyles, 2007, RMH 2009). Future groundwater exploration and protection plans therefore require thorough understanding of the topography of the buried bedrock surface in order to locate and characterize these buried valley systems (Easton, 1988; Meyer & Eyles, 2007).

The Paleozoic bedrock surface of southern Ontario has been subject to intense erosion by both fluvial and glacial processes over the last several million years, creating a complex surface topography incised by several deep valleys (Figs. 3.2., 3.3; Straw, 1968; Eyles et al., 1997; Karrow, 2005; Meyer & Eyles, 2007). Various explanations have been proposed for the development of buried bedrock valleys, including erosion by fluvial, glacial, meltwater or tectonic processes (Straw, 1968; Brennand & Shaw, 1994; Eyles et

Figure 3.1: A) Location of study area and Paleozoic stratigraphy (Armstrong & Dodge, 2007) of the southern Ontario region overlain on bedrock topography (modified from Gao et al., 2006). B) The Halton Hills study area showing Paleozoic stratigraphy overlain on surface topography (Armstrong & Dodge, 2007). The contact between the Amabel/Clinton-Cataract and Queenston Formations is expressed at surface as the Niagara Escarpment. The dashed black box represents the Acton re-entrant valley. C) Cross-section of the southern Ontario region displaying the Niagara Escarpment and gently dipping Paleozoic strata (modified from Meyer & Eyles, 2007).

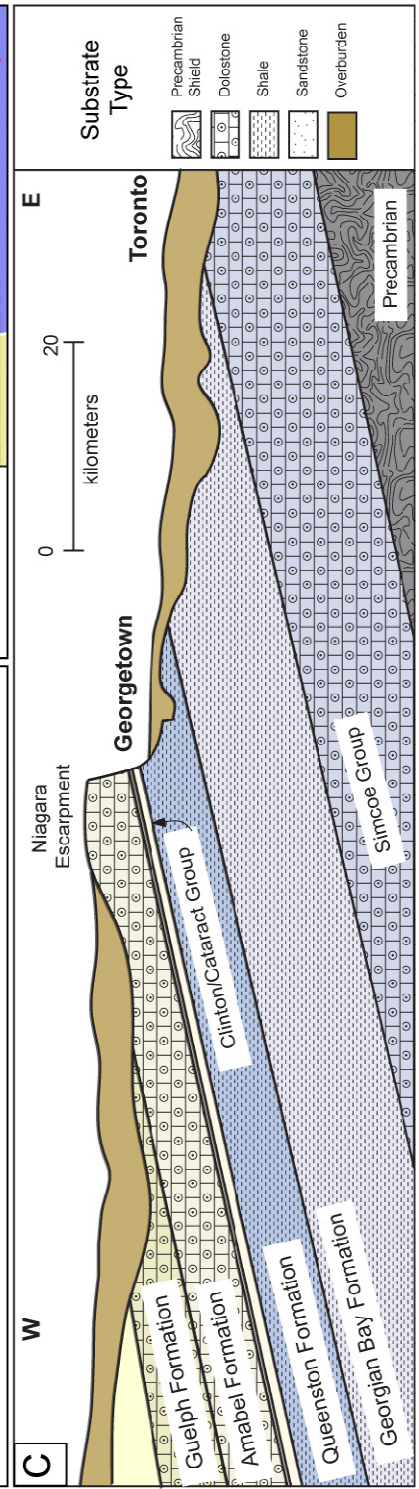
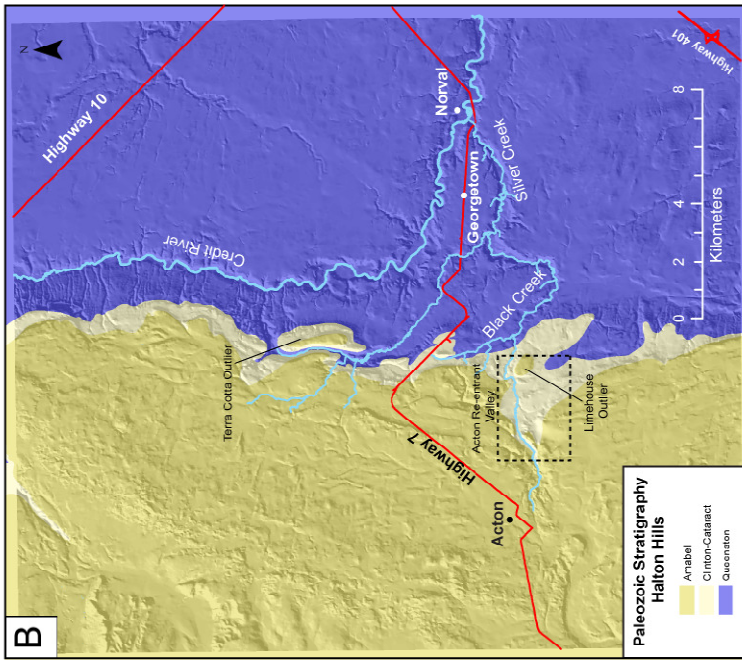
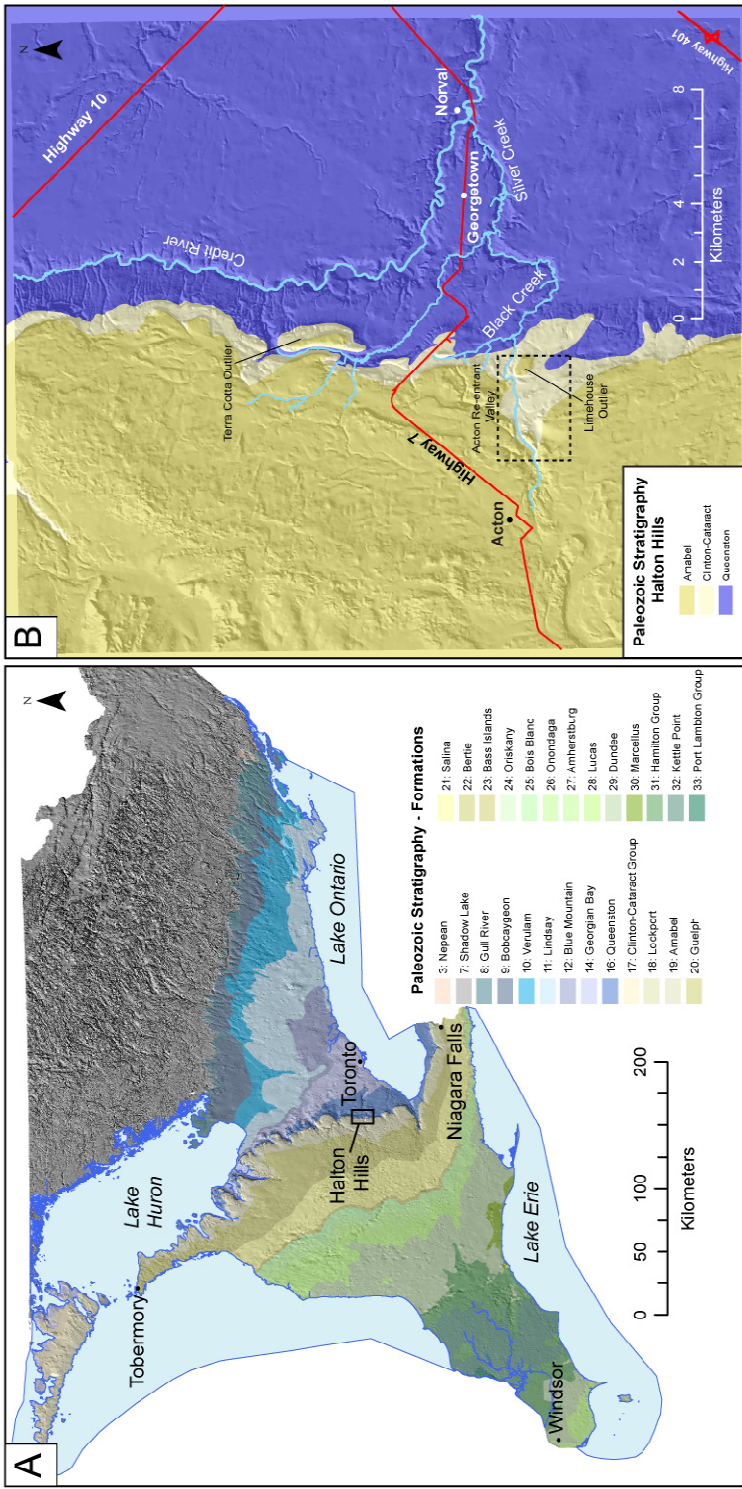


Figure 3.2: Tertiary fluvial network in the southern Ontario region directing drainage eastward toward the Atlantic Ocean. Note the locations of re-entrant valleys along the Niagara Escarpment and the position of the Laurentian Channel, a large buried bedrock valley.

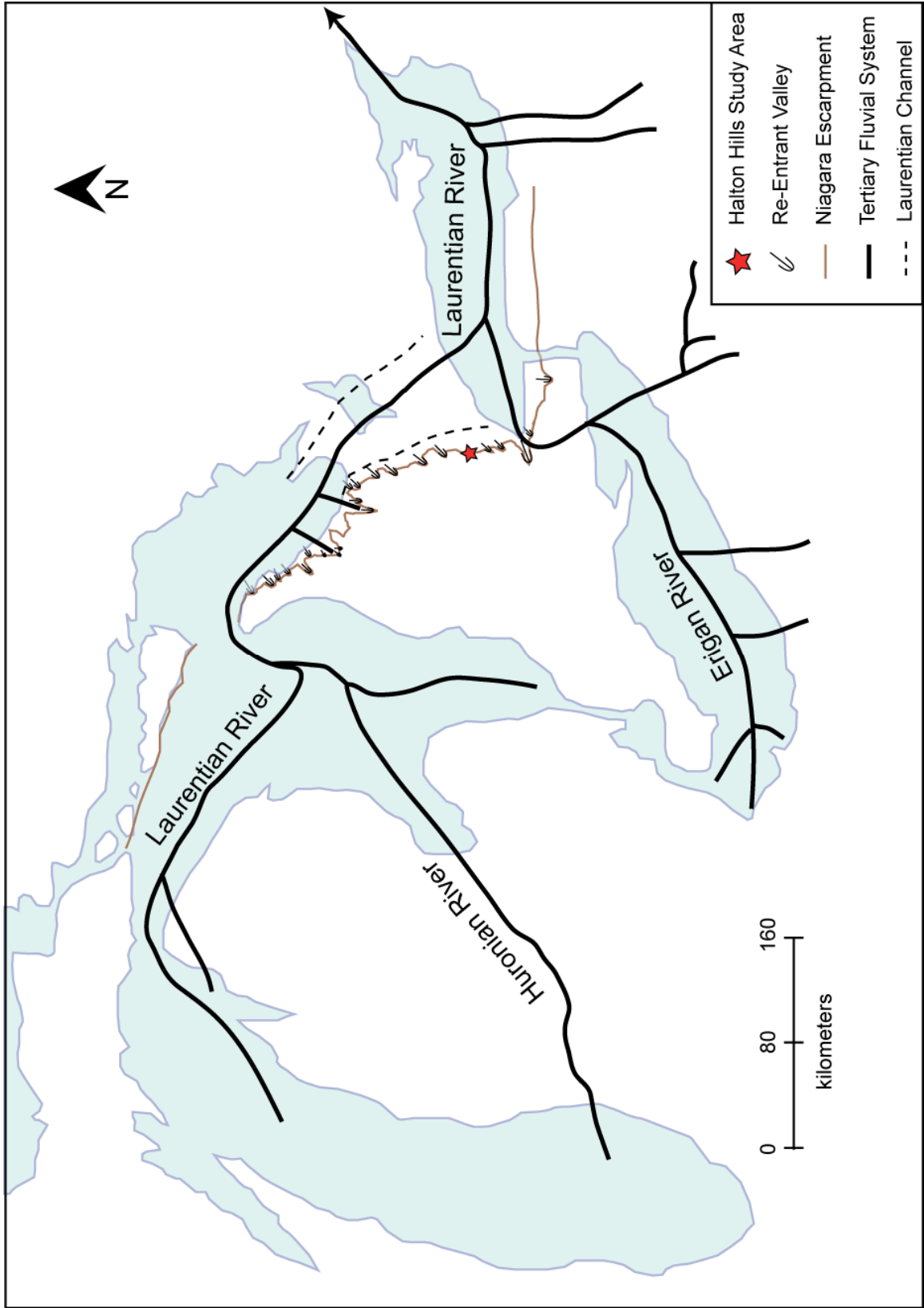
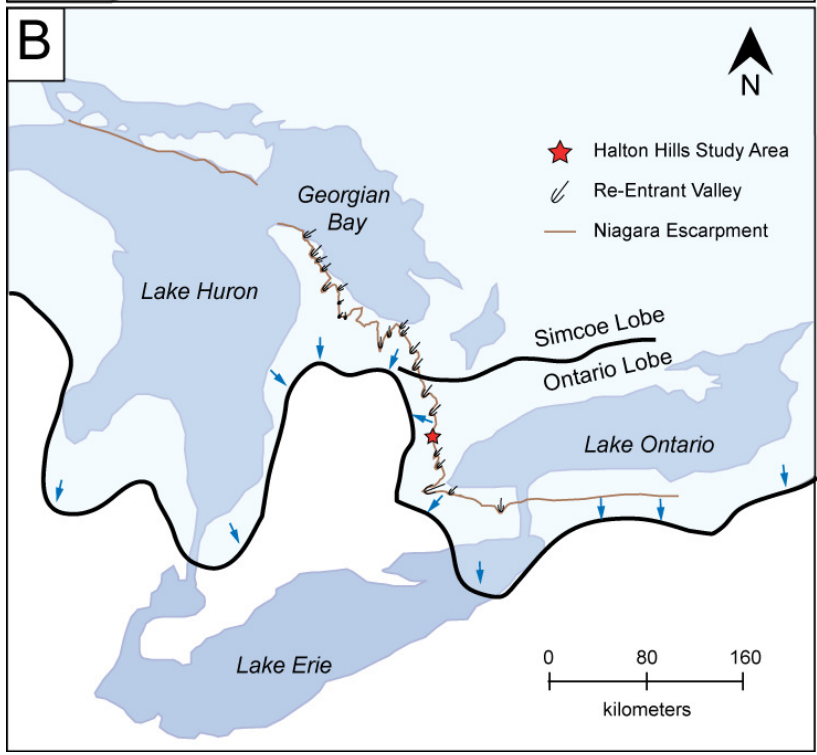
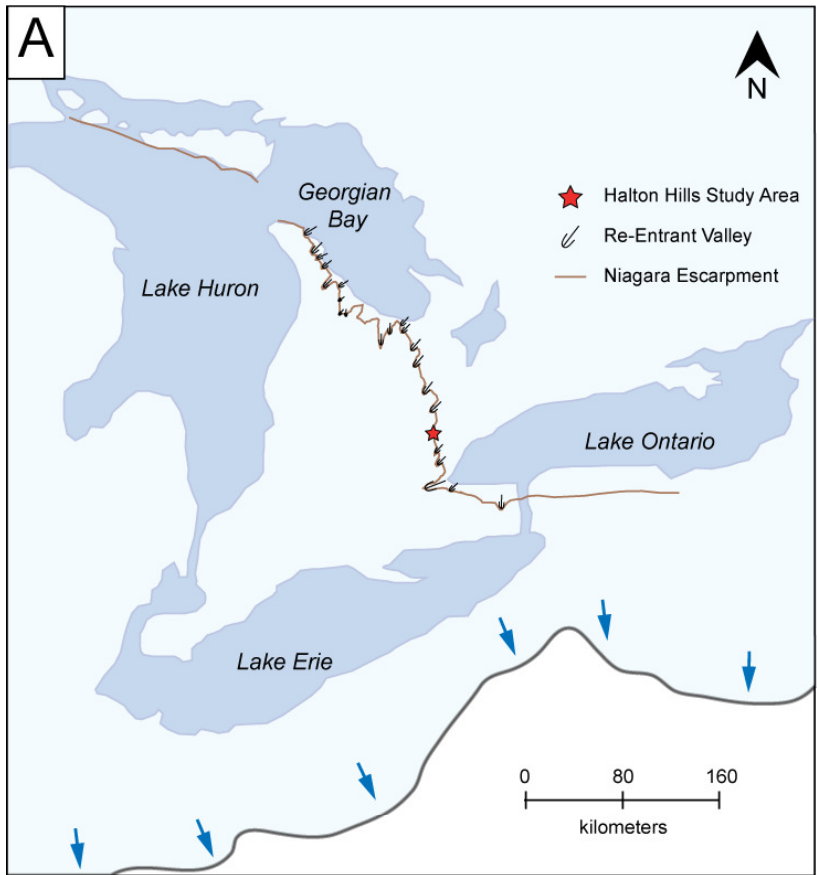


Figure 3.3: Glacial history of the southern Ontario region. A) Nissouri Stadial (25 - 18 Ka). Glacial ice completely covered the region at this time. B) Early Port Huron Stadial (13.2-12 Ka). Note changed direction of ice flow with the Ontario Lobe ice moving northwestward across the Halton Hills study area. Modified from Straw, 1968; Barnett, 1992; Karrow, 2005; Meyer & Eyles, 2007).



al., 1997; Kor & Cowell, 1998; Meyer & Eyles, 2007; Gao, 2011). In the Halton Hills region, buried bedrock valleys are incised into the Queenston Formation shale which acts as a regional basal bedrock aquitard unit (Meyer & Eyles, 2007). These bedrock valleys therefore exert significant control over the depth and spatial extent of aquifer units in overlying Quaternary sediments.

In order to identify and better understand the nature and form of buried bedrock valleys in the Halton Hills region, the bedrock surface must be modeled as accurately as possible using subsurface modeling techniques that are commonly used to guide groundwater exploration programs (Howard, 1997; Howard & Livingstone, 2000; Sharpe et al., 2002). Unfortunately, many subsurface models are created from data within large digital databases in which data quality can be highly variable and may include erroneous information that can severely compromise the reliability of the final model output (Thorliefson & Berg, 2002; Bajc et al., 2004; Logan et al., 2006; Kaufmann & Martin, 2008; MacCormack et al., 2010; Gao, 2011).

This paper describes the results of a study that focuses on modeling the bedrock surface of the Halton Hills area as accurately as possible, using primary data collected from 36 fully cored boreholes, geophysical logs, and bedrock outcrops, as well as data obtained from the digital Ontario Water Well Database (OWD). Several modeling techniques are explored that allow optimization of all available data without compromising model accuracy. The resulting models are compared to allow identification of a bedrock topography model that most accurately reflects the bedrock surface and facilitates the delineation of bedrock valley systems in the Halton Hills area.

3.2 Geologic background

Southern Ontario is underlain by gently southwest dipping Ordovician to Devonian strata (Fig. 3.1: Meyer & Eyles, 2007) which consist of alternating shales, sandstones and dolostones deposited in the Paleozoic Michigan Basin. These strata overlie the Precambrian basement of the North American Craton. In the region of Halton Hills, lowlands to the east of the Niagara Escarpment are underlain by the red and grey, highly fractured Ordovician shales of the Queenston Formation (Fig. 3.1; Brogley et al., 1998; Armstrong & Dodge, 2007). The Queenston shale is highly susceptible to erosion, and has developed incised and interconnected valley systems on its surface (Easton, 1988; Karrow, 2005; Meyer & Eyles, 2007). Regionally, the Queenston Formation is overlain by the Clinton-Cataract Group, a series of interbedded sandstone, dolostone and shale units which outcrops at rare sites in Halton Hills (Fig. 3.1C). The Clinton-Cataract Group is in turn overlain by reefal dolostones of the Lockport Group, (described previously as the unsubdivided Amabel Formation; Brunton, 2009), which forms the cap rock of the Niagara Escarpment in the area. The Lockport Group exhibits variable grain sizes and bedding thickness, as well as substantial jointing (Straw, 1968; Cole et al., 2009).

The most notable bedrock topographic feature in the area is the Niagara Escarpment, which extends from the Niagara region in the south, northwest towards Tobermory on the Bruce Peninsula (Fig. 3.1). In the Halton Hills region, the Niagara Escarpment trends roughly north-south and lies between the towns of Georgetown and Acton (Fig. 3.1B). The Niagara Escarpment is dissected along its length by several

prominent re-entrant valleys (Figs. 3.2, 3.3) that are typically quite deep (100 m to over 670 m), with straight, steep, parallel sides (Straw, 1968). These re-entrant valleys have been studied by numerous authors over the last few decades, and several theories for their formation have been proposed, including erosion by glacial ice (Straw, 1968), subglacial meltwater (Karrow, 2005; Gao, 2011), catastrophic meltwater flood events (Kor & Cowell, 1998) and by fluvial and groundwater ‘sapping’ processes (White & Sharp, 2003; Hoke et al., 2004). Erosion by any one, or combination of these processes, would have been influenced by pre-existing structural weaknesses in the bedrock that would determine valley location and orientation (Straw, 1968; Eyles et al., 1997; Karrow, 2005). A relatively small re-entrant valley, the Acton Re-entrant, is located within the study area, to the west of Georgetown and Limehouse, Ontario (Fig. 3.1; Karrow, 2005).

Prior to the repeated glaciations of the Quaternary period, the bedrock of Ontario was subjected to a lengthy period of subaerial exposure and weathering (Chapman & Putnam, 1966; Barnett, 1992). Extensive fluvial systems developed during this time, with deep channels incised into bedrock types that were most susceptible to erosion, such as the Paleozoic shales underlying carbonate cap rocks (Chapman & Putnam, 1966; Barnett, 1992). The Laurentian Channel, a system of wide, shale-floored bedrock valleys that connect the basins currently occupied by Georgian Bay and Lake Ontario, developed during this period, and served as an outlet from the Upper Great Lakes to the Atlantic Ocean (Fig. 3.2; Spencer, 1890; Straw, 1968; Eyles et al., 1997; Gao et al., 2006; Meyer & Eyles, 2007). To the west of the Laurentian Channel system, the Queenston shale bedrock surface slopes south-eastward from the Niagara Escarpment toward Lake Ontario

and is dissected by a complex system of smaller interconnected bedrock valleys (Karrow, 2005; Meyer & Eyles, 2007). Several buried bedrock valleys have been identified from drill core data and gravity data in the Halton Hills region close to the Acton re-entrant (e.g., the Georgetown, Milton and Meadowvale buried valleys; Fig. 3.1B; Easton, 1988; Meyer & Eyles, 2007); however, the relationship and continuity of these features is poorly understood as they are now buried beneath thick successions of glacial sediment (Barnett, 1992; Karrow, 2005).

Many studies have documented the coincident relationship between bedrock valleys and regional jointing patterns (particularly in the Paleozoic Lockport dolostones), as well as with modern fluvial systems (Straw, 1968; Eyles et al., 1997; Karrow, 2005). In the southern Ontario region, the maximum compressive stress affecting bedrock is oriented northeast to southwest (as indicated by the orientation of surficial bedrock deformation features such as pop ups; Eyles & Scheidegger, 1995; Eyles et al., 1997). The strong correlation between bedrock jointing patterns and the orientation of bedrock and modern river valleys suggests that bedrock joints have been preferentially exploited by erosive agents (fluvial or glacial) and may strongly influence the location and form of bedrock valleys (Straw, 1968; Eyles et al., 1997).

During the past 2 million years large ice sheets have repeatedly advanced and retreated across northern North America but the Quaternary sedimentary record of southern Ontario is largely limited to the most recent (Wisconsinan) glacial event (Barnett, 1992). The onset of the Wisconsinan glaciation began approximately 115 000 years before present, and during the glacial maximum (ca. 20 Ka), the Laurentide Ice

Sheet covered 80% of Canada, and all of Ontario, with ice up to 2 km thick in some areas (Fig. 3.3; Barnett, 1992; Eyles, 2002). This glacial event resulted in erosion of pre-existing sediment and bedrock as well as the deposition of extensive till sheets (e.g., Northern/Newmarket Till; Karrow, 2005). The southern margin of the Laurentide Ice Sheet fluctuated significantly across Ontario during the latest Wisconsin (14 – 12 Ka; Berger & Eyles, 1994) and withdrew from the Halton Hills area during the Mackinaw Interstadial (Fig. 3.3; 14 – 13.2 Ka; Barnett, 1992; Meyer & Eyles, 2007) allowing deposition of fluvial, lacustrine and deltaic sediments in the region. During the Port Huron Stadial (13.2 – 12 Ka), the Ontario Lobe of the Laurentide Ice Sheet readvanced northwestward out of the Lake Ontario basin, overriding the Niagara Escarpment in Milton and Georgetown (Fig. 3.3; Chapman & Putnam, 1966; Costello & Walker, 1972, Barnett, 1992; Karrow, 2005, Meyer & Eyles, 2007).

3.3 Data sources

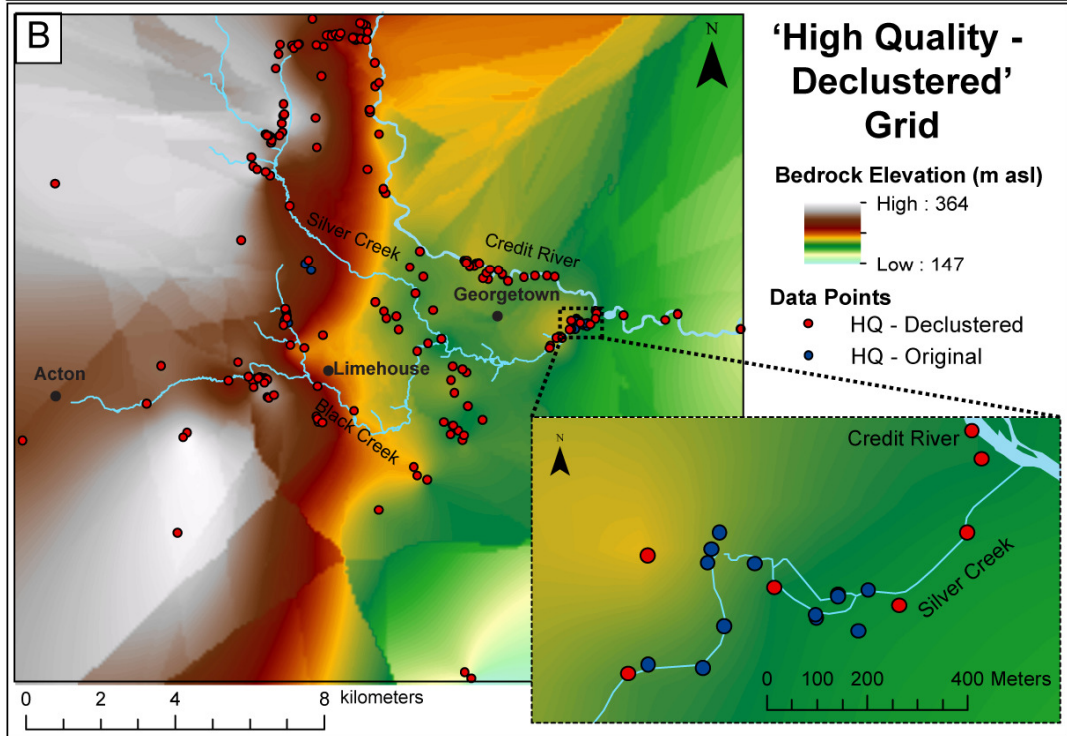
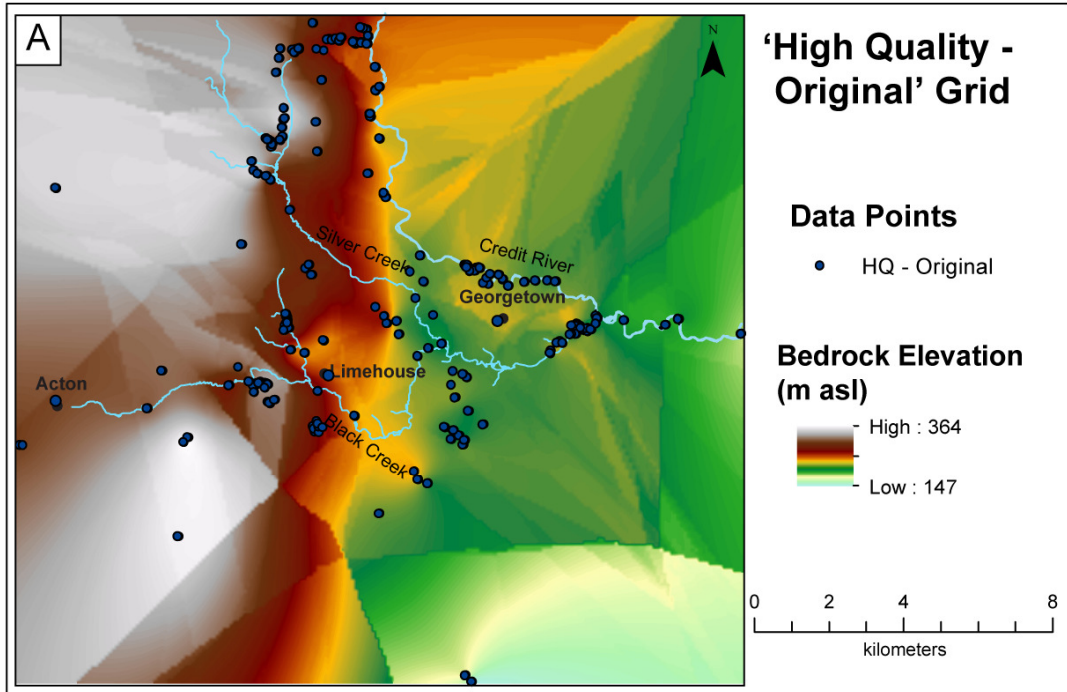
There are a variety of data sources that can be used to create regional geologic subsurface models, the most reliable being primary data collected specifically for the purpose of the study (MacCormack and Eyles, 2010). In this study, primary bedrock elevation data were obtained from 36 continuously cored boreholes drilled between 2006 and 2011, geophysical logs recorded from non-cored boreholes, (Brennan, 2010), and bedrock elevation measurements taken with a differential GPS unit (Magellan ProMark3) at outcrops along creeks, road cuts and in quarries. In some areas, elevation data could not be directly collected with a GPS unit at bedrock outcrops, due to safety concerns or

inaccessibility of the site. In these cases, elevation data were obtained using air photographs and a 10 m digital elevation model (DEM) of the study area.

The primary bedrock elevation data collected from the study area can be classified as ‘highly clustered’ on a regional scale, where several data points are found in close proximity to one another (Galve et al., 2009). Borehole data were collected from wells that were often spaced closely together in areas of interest, and bedrock outcrop data were concentrated only in areas where bedrock was exposed at surface. Across the entire region, primary data are sparsely distributed and there are several sections of the study area which lack primary data (Fig. 3.4). Data distributions are generally considered to be ‘sparse’ when the user feels the distribution of data is insufficient to interpolate a model accurately (MacCormack, 2010).

Because of the clustered and relatively sparse distribution of primary data in the study area, it is necessary to include data from other sources to create an effective model of the bedrock surface (Gao et al., 2006; MacCormack and Eyles, 2010). Additional data used in this study were obtained from consultant reports (some dating back to 1958) and from the Ontario Water Well Database (OWD), a large digital database containing records of sediment and rock types identified during the drilling of water wells across Ontario (Gao et al., 2006; Carter & Castillo, 2006; MacCormack & Eyles, 2010). A total of 4852 records from locations within the study area boundary, and which reached bedrock were extracted from the OWD (Fig. 3.4). The extensive amount of OWD data

Figure 3.4: Outputs from modeling exclusively with high quality data. A) The relatively sparse and clustered distribution of high quality data points results in unrealistic interpolation of the bedrock topography and creates sharp ridges and boundaries in some areas. B) Manual removal of data points (declustering) in areas of significant clustering create a more smoothed interpolation, particularly within the areas around. Inset figure at lower right shows the points removed (blue) and points remaining (red) after declustering of data points along Silver Creek.



available in the study area allows for a much better regional distribution of data points compared to the primary data set alone.

3.3.1 Identifying & Defining Variable Quality Data

A major issue in subsurface modeling is the lack of recognition of the variation in quality and reliability of data that a dataset may contain (MacCormack & Eyles, 2010). Many modellers and modeling programs take data points at face value, without considering that some may be more reliable than others (MacCormack & Eyles, 2010). However, different data sources can be identified as ‘high’ or ‘low’ quality depending on the user's confidence in the accuracy of the data, the user's understanding of the study area, and the purpose for which the data were originally collected (MacCormack & Eyles, 2010). The use of several sources of data to create a subsurface model may require that individual data sources be treated differently both prior to modeling, and during the modeling process. While ‘high quality’ data points, considered by the user to be accurate and reliable, may be directly input and modeled, data from sources considered to be less reliable, such as large digital databases, can contain significant errors and require careful screening prior to modeling (Goodchild & Clark, 2002; Burt, 2004; Dey et al., 2005; Logan et al, 2006; Carter & Castillo, 2006; Venteris, 2007; MacCormack & Eyles, 2010). In this study, ‘high’, ‘intermediate’, and ‘low’ quality data are differentiated on the basis of user confidence in the accuracy of location, elevation and geological information.

The primary data collected specifically for this study (borehole and outcrop data) are considered to be the highest quality data available since there is high confidence in the

location coordinates of data points, geological assessments, and the elevation of the bedrock surface which was measured with a high accuracy differential GPS unit. In the Halton Hills study area, a total of 230 high quality data points were collected, 32 of which were from fully cored boreholes, 14 from interpretations of down-hole geophysical logs (Brennan, 2010), and 184 data points recorded from bedrock outcrops. These primary data are referred to as the ‘High Quality – Original’ dataset (Fig. 3.4). Prior to modeling, elevation values for each of the data points collected were verified by comparison with the regional (10 m) DEM of the Halton Hills area to ensure there were no significant measurement errors associated with GPS data collection.

Bedrock elevation data collected primarily from an aerial photograph and a DEM of the study area are considered to be of lower quality than those collected using a differential GPS which has sub-metre accuracy. Data obtained from legacy consultant reports are also considered to be less reliable than high quality data as the location coordinates and land surface elevations were estimated from hand drawn sketches of borehole locations. Elevation data extracted from aerial photographs and DEM data are therefore considered to be of ‘intermediate quality.’

Data from the OWD are considered to be ‘low quality’ for the purposes of this study because the OWD records are recognized to contain inaccuracies in terms of georeferencing, elevation values, and descriptions of geological materials (Carter & Castillo, 2006; Gao et al., 2006; MacCormack and Eyles, 2010). The ‘Low Quality – Original’ dataset was created from the 4852 data points from the OWD that fell within the study area and reached bedrock (Fig. 3.4).

3.3.2 The Modeling Process

The data used for this study were collected and compiled into a database for use in a GIS (ESRI ArcGIS 10). All of the bedrock topography grids created in this study were interpolated using the Ordinary Kriging algorithm in ArcMap. While several interpolation algorithms are available in the ESRI ArcMap environment, Ordinary Kriging was chosen because it is an exact interpolator, and it is considered to be the most effective algorithm to use when interpolating datasets with irregularly distributed (sparse or clustered) data points (Zimmerman et al., 1999; MacCormack, 2010). The enhanced effectiveness of Ordinary Kriging in modeling irregularly spaced data is due to the use of variograms which incorporate the degree of spatial autocorrelation between nearby data points, and integrate that autocorrelation into a spatial weighting factor during the interpolation process (Isaaks & Srivistava, 1989). Bedrock topography grids were all assigned a grid cell size of 90 m, the default value assigned by ArcGIS based on the spatial extent of the Halton Hills study area, to ensure consistency between grids for comparative purposes.

3.3.3 Model Validation

In order to validate the accuracy of models created from different datasets and using a variety of techniques, a cross validation approach (available within the ArcGIS Geostatistical Analyst Extension) was employed. This method of cross validation compares observed and predicted values in a dataset after each point in the dataset is removed (one at a time) and its values are predicted using the remainder of the dataset (ESRI, 2011). The quantitative results of the cross validation are Root Mean Square Errors (RMSEs), which are calculated to determine how closely a model can predict

observed values, where lower RMSEs indicate more accurate predictions (Johnston et al., 2001; MacCormack & Eyles, 2010).

3.4 Modeling Bedrock Topography in the Halton Hills Region

Several approaches to subsurface modeling are investigated in this study in order to create a bedrock topography model of the Halton Hills region that provides a ‘best estimation’ of the bedrock surface. The approaches addressed in the study include modeling exclusively with high quality data, an approach using all data sources with minimal screening, and an approach using all data sources with extensive screening of low quality data sources (OWD data; Fig. 3.5). As many OWD data points do not reach bedrock, but have been used in some modeling studies to identify a maximum possible elevation for the bedrock surface (called ‘push-down’ points; Gao et al., 2006), modeling with ‘push down’ points was also explored.

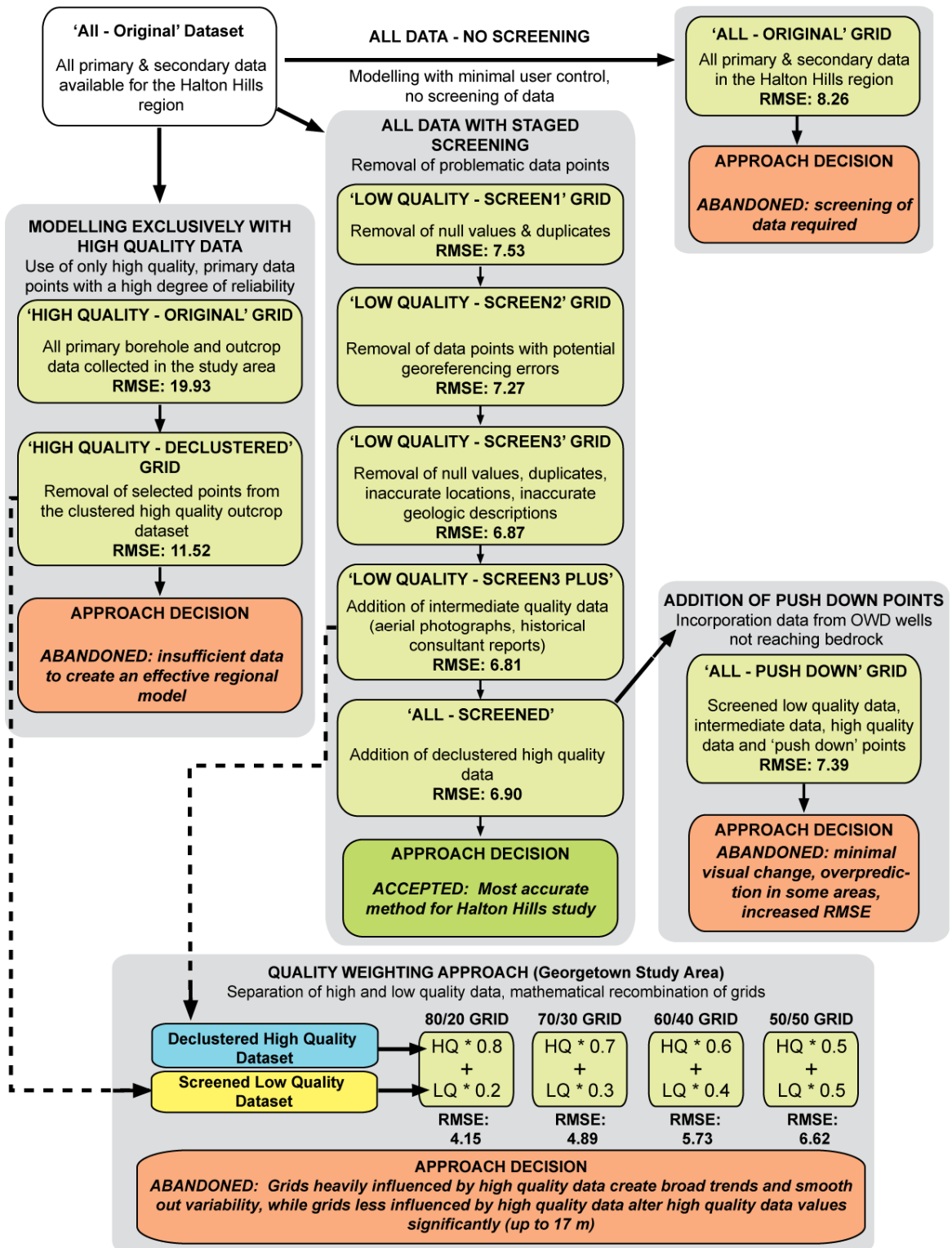
3.4.1 Modeling Exclusively with High Quality Data

When creating subsurface models, it is ideal if the input data are of high quality for the intended purpose of the model, and have a uniform distribution across the study area (Isaaks & Srivastava, 1989; Houlding, 1994; MacCormack & Eyles, 2010).

Unfortunately, high quality data are most often sparse at a regional scale, clustered around localized study areas or areas of interest (MacCormack & Eyles, 2010). In order to analyse the distribution of the high quality data available for the Halton Hills study area, the 230 points that form the ‘High Quality – Original’ dataset were interpolated in

ArcGIS

Figure 3.5: Flow diagram of the various approaches to subsurface modeling explored in this study, associated RMSE values, and commentary on the decision-making process. Numerical validation results of modeling using each of these approaches are summarized in Tables 2 and 3. Note that for the Quality Weighting approach, the study area was reduced and the RMSE values reflect validation with high quality data points.



using the Ordinary Kriging algorithm. The resulting grid (Fig. 3.4A) had an exceptionally high RMSE value of 19.93 (Table 3.1).

The relatively high error values associated with modeling of the ‘High Quality – Original’ dataset may be due to the high degree of clustering of data points in some areas. In order to reduce the error associated with a clustered data distribution (MacCormack & Eyles, 2010), the data were declustered using Kernel Density Estimation (Chang, 2006; Cox, 2007) to identify areas of significant clustering within a 90 m threshold (based on the desired grid cell size of 90 m). 90 m buffers were placed around points in areas of highly clustered data, and points spaced less than 90 m away from each other were manually removed from the dataset in a manner that optimized the area covered by the remaining points (see Fig. 3.4B inset). 80 bedrock outcrop data points were removed from the dataset in this way, leaving 150 data points to form the ‘High Quality – Declustered’ Dataset (Fig. 3.5). The resulting grid (Fig. 3.4B) interpolated from this dataset had an associated RMSE value of 11.52, which although still high, suggests that the declustered data create a slightly more accurate representation of the bedrock surface than the original, clustered dataset (Table 3.1).

The high RSME values obtained from the model produced from the ‘High Quality – Declustered’ dataset may also be explained by the sparse data coverage at a regional scale, and the preferential representation of areas where bedrock outcrop was available. Declustering of the high quality data appears to smooth out some of the sharp, unrealistic changes on the bedrock surface modeled with the ‘High Quality – Original’ dataset particularly around the Georgetown and Limehouse areas (Fig. 3.4), but many areas of the

‘declustered’ grid, particularly in study area boundaries, still appear to be unrealistic (Fig. 3.4B). This degree of uncertainty suggests that high quality data alone are insufficient to model the bedrock topography of the Halton Hills region accurately and that incorporation of additional ‘low quality’ data is necessary.

3.4.2 Modeling All Data with Minimal Screening

All subsurface data available for the Halton Hills region (including high quality primary data, intermediate quality data from aerial photographs and consultant reports, and low quality OWD data) were compiled into the “All – Original” dataset which contains 5132 records (Fig. 3.5). This dataset was interpolated using the Ordinary Kriging algorithm in ArcGIS, and the resulting grid (Fig. 3.6) had an associated RMSE value of 8.26 (Table 3.1). The most noticeable issues with this grid are the presence of several gaps in the interpolation (represented as white spaces in Fig. 3.6) and an anomalous minimum bedrock elevation data point of 117 m asl (the high quality data points identify the minimum bedrock elevation of the region as 147 m asl; Fig. 3.6). The interpolation gaps are likely due to the presence of duplicate data points within the OWD, with identical XY coordinates, but variable elevation values. These variable elevation values appear to prevent the Kriging algorithm interpolating in these areas. Upon review of the regional geological context, the anomalous minimum elevation value appears to be an erroneous data point (outlier) that can be removed from the dataset. Other erroneous data points may also be present in the low quality dataset but cannot be easily identified unless they are radically different from surrounding points. Erroneous data points can introduce

Figure 3.6: 'All-Original' grid: Bedrock topography grid interpolated from OWD data (grey) and primary data (red) using a 'Minimal Screening' approach. Data were extracted from the OWD, combined with primary data and modeled using the Ordinary Kriging algorithm in ArcGIS with no screening of data points.

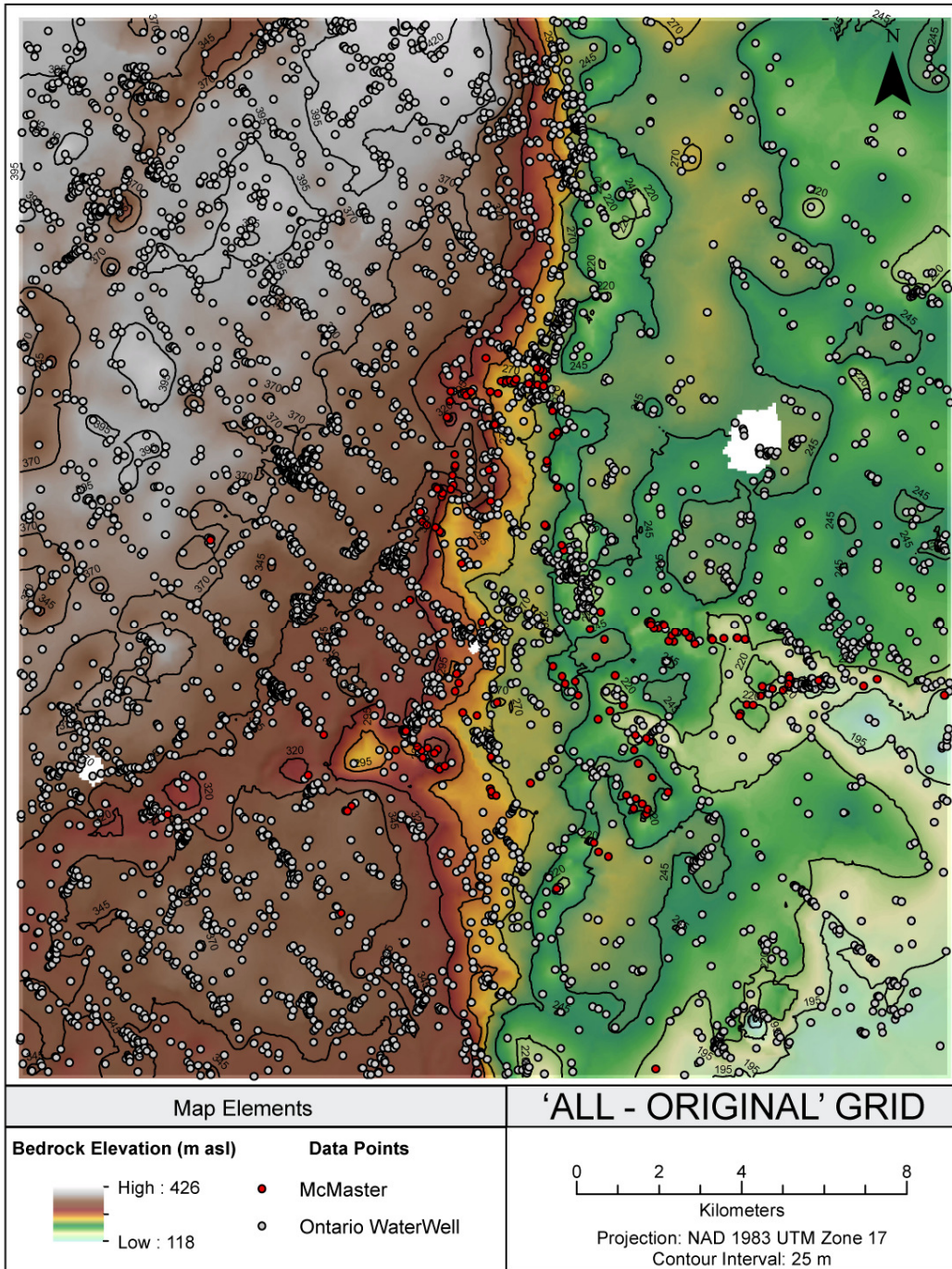


Table 3.1: Summary of RMSE values of cross-validation and validation with high quality data points for grids created at various stages of screening, and incorporation of push-down points

	Grid	# Records	Description	Cross Validation RMSE	HQ Validation RMSE
High Quality	Original	230	McMaster borehole, geophysics and outcrop data	19.93	16.95
	Declustered	150	McMaster borehole, geophysics and declustered outcrop data	11.52	4.470
Low Quality	Original	4852	Initial extraction of OWD data	8.14	15.02
	Screen1	4651	Removal of obvious errors (duplicates, zero or null values)	7.53	15.34
	Screen2	4184	Removal of points outside 300 m location confidence	7.27	14.49
	Screen3	4036	Removal of points with inaccurate geologic descriptions	6.87	13.77
All	Original	5132	Unscreened low quality and high quality data	8.26	17.29
	Screen3Plus	4086	Addition of intermediate quality data (from aerial photographs, historical consultant reports)	6.81	13.53
	Screened	4236	Screened low quality, intermediate quality data and high quality data	6.9	8.80
	Pushdown	4655	Low quality (screened), intermediate quality and high quality data plus "push down" points not reaching bedrock	7.39	10.39

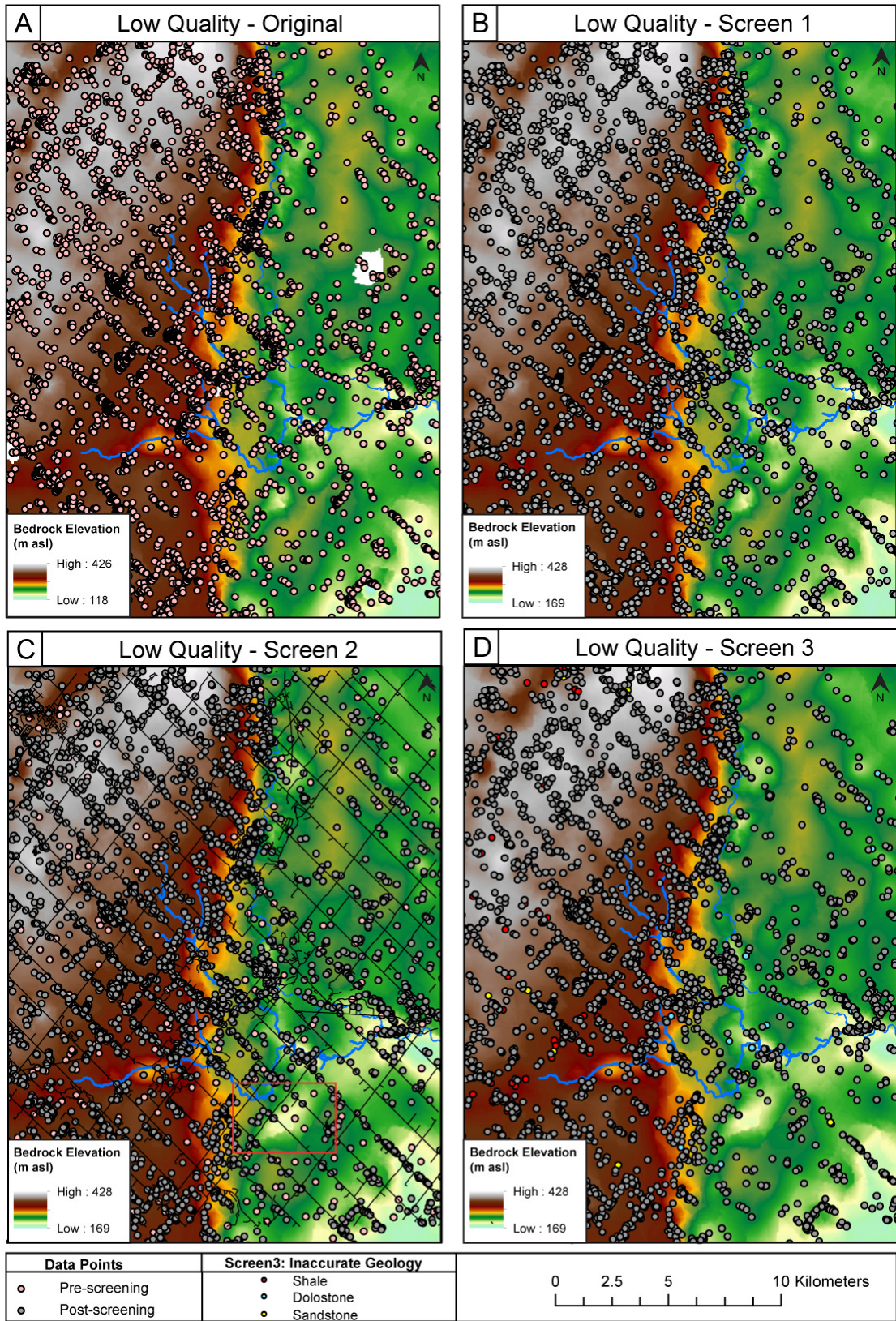
significant error into a model output (Carter & Castillo, 2006; MacCormack & Eyles, 2010) and require identification and removal through a thorough screening process.

3.4.3 Modeling with Extensive Screening of Low Quality Data

A second approach used to model the bedrock topography of the Halton Hills region acknowledges the highly variable quality of data in large digital databases (OWD) and applies an extensive screening mechanism to identify and remove erroneous data points from the low quality dataset. 4852 data points from the ‘Low Quality – Original’ dataset were interpolated using the Ordinary Kriging algorithm in ArcGIS (Fig. 3.7A) to create the ‘Low Quality – Original’ grid (RMSE: 8.14; Table 3.1; Fig. 3.5). Using this model and associated dataset as a starting point, an extensive screening process was conducted involving three stages including; 1. removal of duplicates and null values; 2. removal of potential elevation errors based on reliability codes; and 3. removal of geologic inaccuracies (Appendix A). Visual inspection of the ‘Low Quality – Original’ dataset at a regional scale indicates some apparent clustering of OWD records. Kernel Density Analysis was therefore performed on this dataset with a 90 m search radius but the results showed negligible clustering, with very few points spaced as closely as some points within the high quality dataset.

The first stage of screening involved the removal of duplicate and null values that were identified to be responsible for the gaps in interpolation (displayed as white spaces in Figs, 3.4, 3.6, 3.7A) and anomalous low values identified in the ‘All-Original’ and ‘Low Quality – Original’ grids. At this stage of screening, 201 duplicate or null value

Figure 3.7: Bedrock topography models created at different stages of screening of the low quality (OWD) dataset. For each stage of screening the remaining points after screening are displayed in grey. A) Model created from the ‘Low Quality– Original’ dataset extracted from the OWD prior to screening. Note the white areas where no interpolation could be made. B) Screen 1: model created after removal of obvious erroneous data points (0 or null values, duplicates resulting in “white gaps”). Data points removed from the dataset are displayed in pink. Note the change in minimum bedrock elevation from 118 m asl to 169 m asl due to the removal of a zero value. C) Screen 2: model created after removal of points outside 300 m location confidence, displayed in pink. Many of these correspond to locations in between major roads where water wells are unlikely to be located (see the area outlined in red). Note the change in valley continuity between interpolations at Screen1 and Screen2 within the red square. D) Screen3: removal of points with inaccurate geologic descriptions. Points coloured red (shale), blue (dolostone) and yellow (sandstone) were removed at this stage of screening as they have incorrect geologic descriptions based on their locations. Refer for Fig. 1 for the bedrock geology of the Halton Hills region). Generally, shale underlies the lower, eastern portion of the study area, while dolostone underlies the western, upland region. Sandstone outcrops minimally along the Niagara Escarpment boundary.



records were removed. Removal of these data points also removed the problematic interpolation gaps (see Figs. 3.7A, 3.7B), increased the minimum bedrock elevation from 118 to 169 m asl, and produced an RMSE value of 7.53 (Table 3.1; Fig. 3.5).

The second stage of screening involved the removal of OWD data with potentially significant georeferencing errors (Carter & Castillo, 2006; Gao et al., 2006; MacCormack & Eyles, 2010). Each OWD record contains a location confidence code which provides a confidence level for the accuracy of the record's location in space (Gao et al., 2006; Appendix A). At the second stage of screening, 467 OWD data points were identified to have less than 300 m location accuracy and these points were removed from the dataset. The resulting model 'Low Quality – Screen 2' (Fig. 3.7C; 3.5) has an associated RMSE value of 7.27.

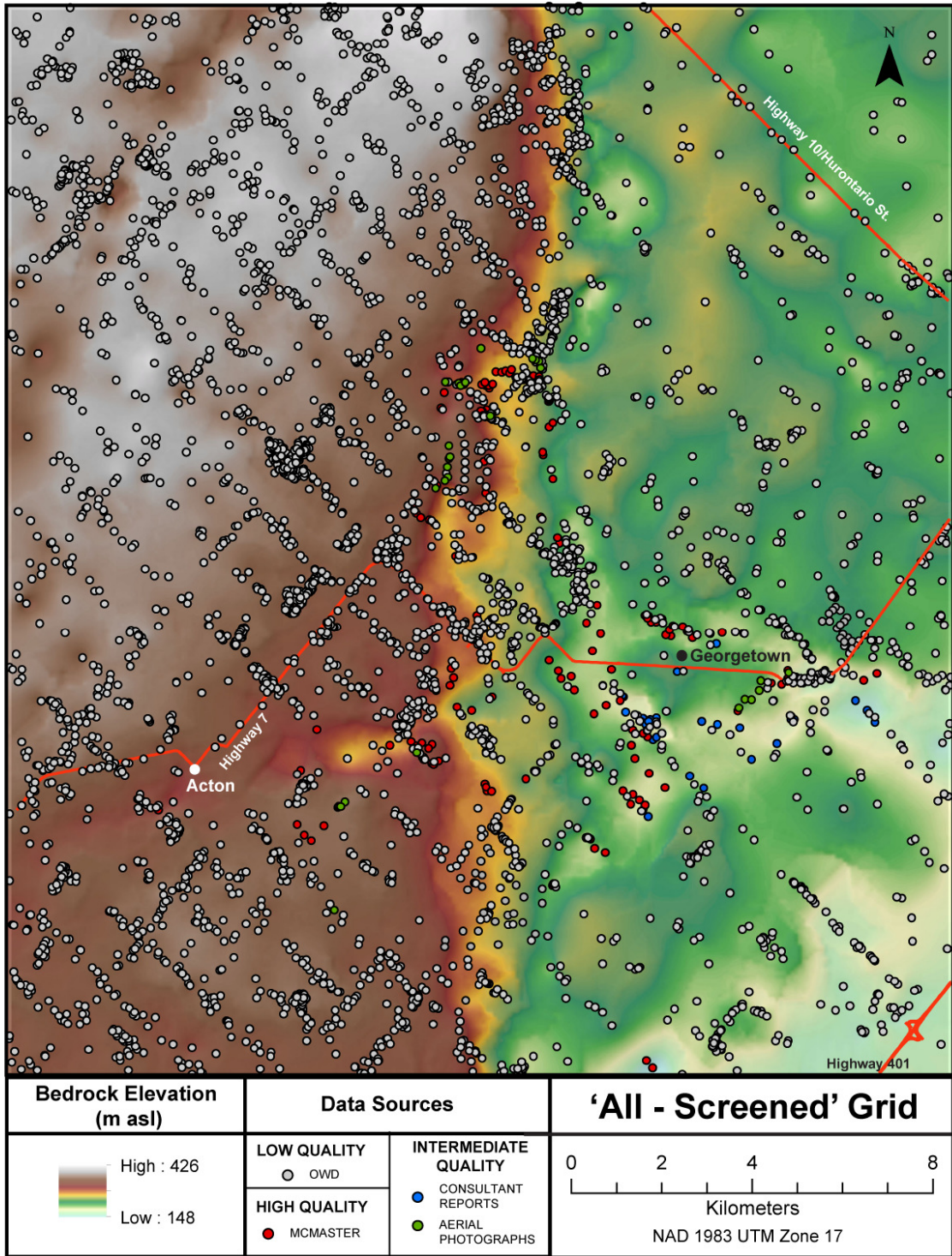
The third stage of screening involved the removal of data points that contained inaccurate geological descriptions. The distribution of reported bedrock types from the OWD were compared with a detailed Paleozoic bedrock geology map (1:50 000; OGS, 2011) of the Halton Hills study area to confirm the accuracy of the geologic data (Appendix A). At this stage of screening an additional 148 data points were removed from the dataset due to geologic inaccuracies, resulting in the 'Low Quality – Screen 3' dataset. The associated grid modeled from these data (Fig. 3.7D) had a reduced RMSE value of 6.87 (Table 3.1; Fig. 3.5).

The continuous reduction of RMSE values associated with modeled grids produced from OWD data at each stage of the screening process validates the removal of potentially problematic data points. After the OWD data were extensively screened, the ‘Low Quality- Screen 3’ dataset was combined with an additional 50 intermediate quality data points obtained from aerial photographs and consultant reports (‘Low Quality – Screen 3 Plus’; Table 3.1; Fig. 3.5), and 150 data high quality data points from the ‘High Quality – Declustered’ dataset to create the ‘All – Screened’ dataset (Figs. 3.5, 3.8; Table 3.1). Interpolation of the bedrock surface from the ‘All – Screened’ dataset has an associated RMSE of 6.90 (Fig. 3.8). While this RMSE value is slightly higher than that obtained from the ‘Low Quality – Screen 3’ dataset (RMSE 6.87), this is likely due to the increased definition of topographic variability in the area where the high quality data points are located (Fig. 3.8). The high degree of confidence associated with these additional high quality data points suggests that the increase in RMSE value is due to actual topographic variability on the bedrock surface at these locations, and not from location or elevation inaccuracies.

3.4.4 Modeling with “Push Down” Points

Some bedrock topography models have incorporated data from boreholes which do not reach bedrock, using the elevation of the base of the borehole as the maximum potential elevation of the bedrock surface (Gao et al., 2006; Logan et al., 2006; Gao, 2011). These data points are considered as ‘push down’ points as they tend to lower the interpolated elevation of the bedrock surface (Gao et al., 2006; Logan et al., 2006, Gao, 2011). The incorporation of ‘push down’ points is explored in this study as a means to

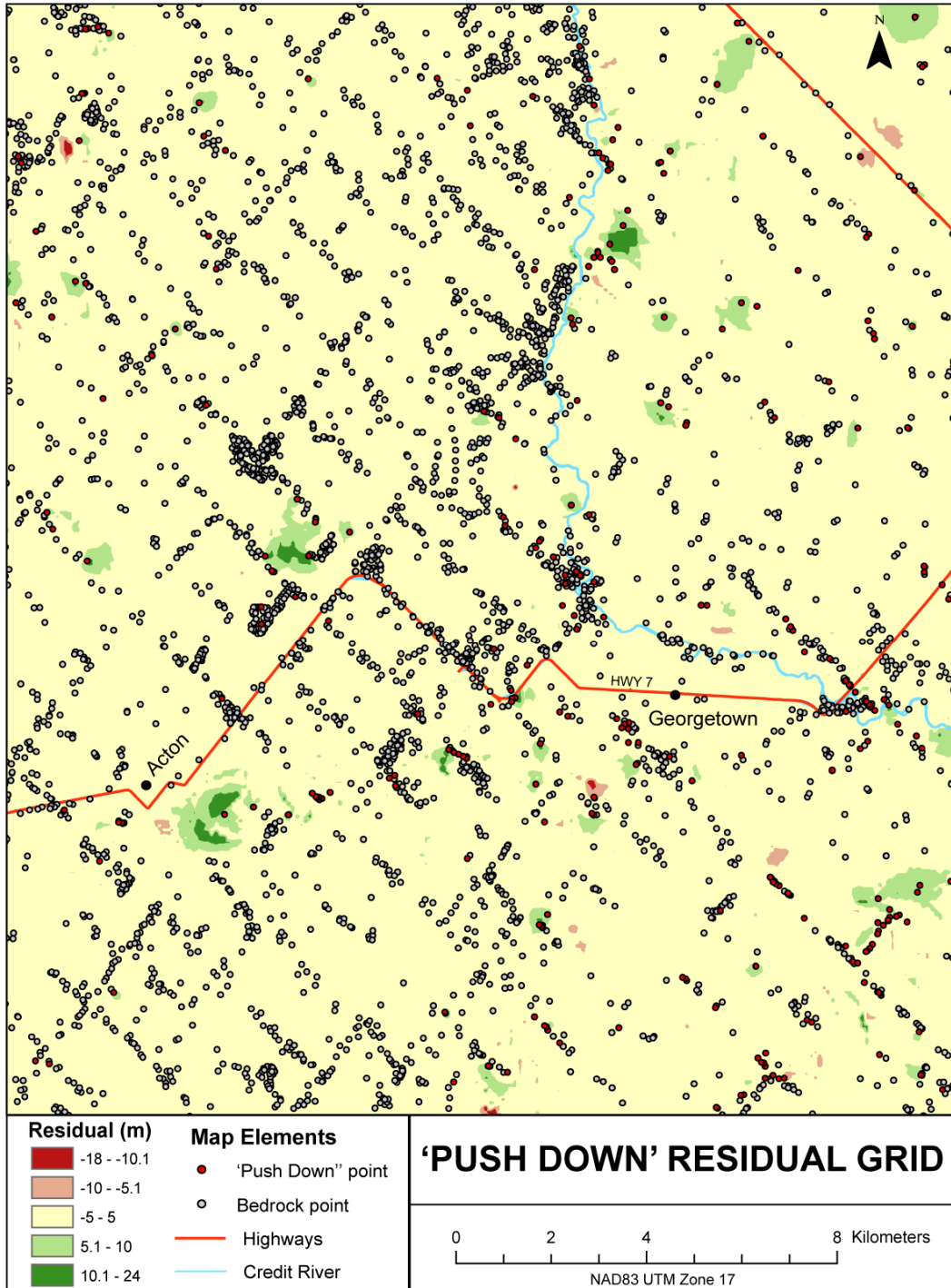
Figure 3.8: "All Data-Screened" bedrock topography model of the Halton Hills region, including high quality primary data (borehole and outcrop) and low quality data from consultant reports and from aerial photography and a DEM of the study area.



enhance the spatial distribution of bedrock elevation data. Data points not reaching bedrock within the Halton Hills study area but with high location confidence (reliability codes less than or equal to 5; see Appendix A) were extracted from the OWD. Using the screening process outlined above, this ‘push-down dataset’ was examined for any problematic data points and records containing unreasonable bedrock elevations and/or duplicate values were identified and eliminated from the dataset. The remaining records were then compared to the previously interpolated bedrock surface (‘All – Screened’ grid), to identify points which terminated below this surface, and could be effectively used as ‘push down’ points. Any points terminating above the ‘All – Screened’ surface were eliminated as they would result in the bedrock surface being unnecessarily ‘pulled up’ in those locations. In total, 419 ‘Push Down’ points were added to the ‘All – Screened’ dataset to create a new ‘Push Down’ dataset. The ‘Push Down’ dataset was then interpolated into a grid, which was visually inspected for errors.

Visual inspection of the ‘Push Down’ grid showed that it differed very slightly from the ‘All – Screened’ grid. A residual map was created to identify areas most affected by the addition of ‘push down’ points (Fig. 3.9) and shows that the elevation of the bedrock surface is only reduced significantly (by greater than 10m) in a very few areas of the Halton Hills region. This may be due to the fact that the ‘All – Screened’ grid was created with 4236 data points, and the incorporation of 419 additional ‘push down’ points (which were generally located in close proximity to existing records reaching bedrock), had little effect on the model. However, it is interesting to note that in some areas the addition of ‘push down’ points increased the modeled elevation of the bedrock surface

Figure 3.9: Residual map to show the difference between the bedrock topography model created from the 'Push Down' and the 'All - Screened' grid. 'Push down' points could only be directly compared to the 'All - Screened' grid at the exact location of the 'push down' to determine if they terminated below the modeled bedrock surface. Negative values (shown in red) represent areas where 'push down' points have actually increased the bedrock elevation value, despite selecting only data points which terminated below the previously interpolated bedrock surface. The elevation of bedrock has been changed by more than 10 m due to the push down process at very few locations.



despite the fact that all of the push-down points terminated below the previously interpolated bedrock surface. This may be due to the fact that the incorporation of additional ‘push down’ points increases the local variability, causing some portions of the model close to the point to increase in value. Over-predicted values (where the ‘Push Down’ grid gave higher than the ‘All – Screened’ Grid) are displayed in red in Fig. 3.9. The RMSE value associated with the ‘Push-Down’ grid (obtained from cross validation) was 7.39 (Table 3.1; Fig. 3.5), which is higher than the ‘All – Screened’ Grid (RMSE 6.90), indicating that variability in the model has increased. Since the level of confidence associated with the ‘push down’ points is relatively low, and the incorporation of these points has minimal (but sometimes negative effects) on the model output, the use of ‘push down’ points was abandoned in this study (Fig. 3.5).

3.4.5 Summary and Comparison of Model Results

Several approaches to modeling the bedrock topography of the Halton Hills region have been explored to identify the model output which most accurately reflects the buried bedrock surface of the region. In order to validate the accuracy of models created from various modeling approaches, a cross-validation technique was applied. Table 3.1 summarizes the RMSE values associated with each model output.

While the RMSE values from this study (ranging between 6.87 and 16.17) are high in comparison to some geostatistical studies (values between 0 and 1; Bourennane et al., 2007; MacCormack & Eyles, 2010), RMSE values in the range of 7 -15 are considered to be acceptable for topographic studies (USGS, 1998). Other studies

investigating areas with high topographic variability have reported similar (if not higher) RMSE values (Bolstad & Stowe, 1994; Hirano et al., 2003). As the range of bedrock elevations observed in the Halton Hills region is high (from 145 to 425 m asl), and the bedrock surface topography is relatively complex due to the presence of the Niagara Escarpment, re-entrant valleys, and potential buried bedrock valleys, RMSE values of this magnitude are deemed acceptable.

The High Quality datasets (clustered and declustered; Fig. 3.4, 3.5) have the highest associated RMSE values and errors (Table 3.1), likely due to the relatively sparse but clustered distribution of high quality data across the Halton Hills study area. Declustering of the 'High Quality – Original' dataset resulted in a significant reduction in the RMSE value (from 19.93 to 11.52; Table 3.1), which clearly indicates that a less clustered dataset, with fewer data points, produces a more accurate model than higher amounts of clustered data. However, the relatively high RMSE values obtained from modeling exclusively with high quality data indicate that these data are insufficient to accurately predict the bedrock surface on a regional scale, and that additional data need to be included to enhance the spatial distribution of the dataset (MacCormack & Eyles, 2010).

The model created from all available data without any screening (All – Original; Fig. 3.5) yielded one of the highest RMSE values of all models that interpolated both high and low quality data (RMSE 8.26; Table 3.1; Fig. 3.5). However, subsequent screening of the Low Quality dataset to remove duplicate and erroneous data points, showed

progressive reduction in RMSE values, and increased the accuracy of the model output at each stage of screening (Table 3.1; Fig. 3.5).

Another modeling approach that included ‘push down’ points in the modeled database was explored but was found to have minimal effect on the overall model, and in some cases caused over-prediction of the elevation of the bedrock surface.

Comparison of all model outputs indicates that the most accurate representation of the bedrock surface can be obtained by using a combination of carefully screened high, intermediate, and low quality data sources (e.g. All – Screened model; Fig. 3.7D, Table 3.1). The All – Screened model is based on 150 high quality data points, 50 intermediate quality data points, and 4036 low quality data points, all of which are given equal value, or weighting, in the creation of the model. However, a new modeling technique has recently been introduced that allows the user to influence the relative weighting of high and low quality data in the interpolation process (MacCormack & Eyles, 2010). This ‘quality weighted’ approach allows the user to give high quality data a greater degree of influence on the model output but uses lower quality data to constrain the model in areas where high quality data are sparse (MacCormack & Eyles, 2010). While this methodology was developed for modeling subsurface stratigraphy in 3D, the technique is applied here to determine if quality weighting of bedrock elevation data enhances the accuracy of models of the bedrock surface of the Halton Hills region.

3.5 Modeling using a Quality Weighted Approach

In order to model the bedrock topography of the Halton Hills region using a quality weighted approach, two screened datasets, from which erroneous points have been removed, the ‘High Quality – Declustered’ (Figs. 3.4B, 3.10) and ‘Low Quality – Screen 3 Plus’ (Fig. 3.10) datasets are used. The ‘intermediate quality’ data described previously in this study was included with the low quality data (‘Low Quality- Screen 3 Plus’) for the purposes of quality weighting. The relatively sparse nature of the high quality data on a regional scale (150 data points over a 550 km² area) is problematic for interpolation in areas where there are few or no high quality data points. For this reason, the study area for the weighted model is reduced to the region surrounding the municipal well fields in the Georgetown area (Princess Anne, Lindsay Court and Cedarvale wellfields; total area of 112 km²) high quality data have more appropriate distribution (Fig. 3.10).

The ‘High Quality – Declustered’ and ‘Low Quality – Screen 3 Plus’ data sets were originally interpolated across the entire study area with a 90 m cell size. These grids were subsequently clipped to the area of interest in the city of Georgetown rather than modeling the reduced study area independently to minimize edge effects along the grid boundaries. These grids were then converted from ‘floating point’ to ‘integer’ grids to permit simple calculations within the Spatial Analyst ‘Raster Calculator’ tool. Within the Raster Calculator, the grids were combined and weighted using the following formula:

Figure 3.10: Quality weighting approach to subsurface modeling. Data were separated into the ‘High Quality – Declustered’ and the ‘Low Quality – Screened’ subsets, which were each allocated a particular ‘weighting’ or degree of influence on the final model. Four model outputs are shown with weightings of 80:20 (high quality: low quality; top right) to 50:50 (bottom right). The weighted data (adding to 100%) were recombined using the Raster Calculator in ArcGIS. High quality data points (orange) and low quality data points (grey) used for these grids are displayed. Note the relatively low amount of topographic detail associated with greater weighting of higher quality data. Numerical results of this procedure are summarized in Table 3.2.

$$(\text{Grid } X_1 * w_1) + (\text{Grid } X_2 * w_2) = \text{GridY}$$

Where Grid X_1 and X_2 are the original unweighted grids, and w_1 and w_2 are the weighting factors associated with each quality weighting scheme.

At this time there is no specific procedure, or quantitative way to determine the specific amounts of weighting to apply to variable quality datasets. The role of expert knowledge is important, as the best models are those that are created by a geoscientist with a thorough understanding of the geological complexity of the study area, their confidence in the data, data distribution, and the purpose of the investigation (Carter & Castillo, 2006; Logan et al., 2006; MacCormack & Eyles, 2010). In this study several quality weighted grids were created, each reflecting different relative weightings of high and low quality data (Fig. 3.10). In these grids, high quality data has a different amounts of influence on the model; for example, 80/20 (Fig. 3.10), indicates that high quality data has an 80% influence on the output model, where low quality data has only 20% influence.

3.5.1 Results of Quality Weighting within the Georgetown Study Area

Visual comparison of the weighted grids shows that when high quality data are weighted heavily (in the 80/20 and 70/30 grids; Fig.3.10) the modeled surfaces appear much ‘smoother’ and have less topographic variability compared to surfaces modeled with unweighted data. Giving the high quality data a slightly lower weighting (a 60/40 or 50/50 ratio; Fig. 3.10), produces a more variable bedrock surface but changes bedrock elevations significantly at the locations of some high quality data points. This indicates

that while topographic trends shown on the weighted bedrock models may be similar to those shown on unweighted models (i.e. relative topographic highs and lows occur in the same general locations), the bedrock values at the locations of high quality data points in the 60/40, 50/50 models (Fig. 3.10) are no longer an accurate reflection of reality.

The various weighted grids were compared with one another and with the ‘All – Screened’ model using a High Quality validation approach (available in ArcGIS Geostatistical Analyst), which compares the predicted values from a dataset with the actual value of high quality data points. This technique generates High Quality Root Mean Square Errors (HQ RMSEs; Table 3.2) in which lower values again indicate a more accurate model (Issaks & Srivastava, 1989; Johnston et al., 2001). The weighted grids that are more heavily influenced by the High Quality dataset (80/20) do appear to show a reduction in RMSE error (HQ RMSE 3.605) compared to those grids in which high quality data are less influential (e.g., 50/50; HQ RMSE 6.279; Table 3.2). However, the predicted values associated with the weighted grids vary substantially from the observed high quality data points, where even the heavily weighted grid (80/20) has a maximum error of 14.2 m, and only 38% of the predicted values are accurate within 1 m of the observed values (Table 3.2). Visual inspection of the grids also indicates another major issue in areas where high quality data points are sparse (e.g., southeast corners of the grids in Fig. 3.10). A significant depression is created on the eastern side of the modeled surface due to the lack of high quality data available to constrain the interpolation in this area. This depression is not apparent on the grid created from the low quality dataset (Fig. 3.10), where data are more abundant. This issue calls the reliability of a quality weighted

Table 3.2: Summary of statistics for various combinations of weighted grids (high quality, low quality) and an unweighted version ('All – Screened') compared to an unweighted version. Note that grids more heavily weighted towards high quality data are better able to predict high quality observations. However, weighting grids no longer honours the high quality data points, as the unweighted grid does.

Grid	Maximum Error (m)	% of predicted points within 1 m of observed points	HQ RMSE (m)
50/50	17.3	18	6.279
60/40	16.04	18	5.309
70/30	15.14	26	4.402
80/20	14.2	38	3.605
All –Screened (unweighted)	0.026	100	0.009

approach in this study into question due to the relatively sparse distribution of high quality data across the study area.

A quality weighted modeling approach was utilized in this study to test its applicability to bedrock topography modeling, and to determine if high quality data could improve the accuracy of the bedrock topography model by being given a greater influence on the modeling process. For the purposes of this study, a quality weighting approach to modeling does not appear to enhance the accuracy of the modeled bedrock surface as it over-smoothes the data, does not maintain the degree of topographic variability required for this study, and creates anomalous features in areas where high quality data are sparse.

As the purpose of this research is to model the bedrock surface to enhance understanding of groundwater movement in the Georgetown region, the ‘best estimation’ of the bedrock surface should be one which truly honours the data points to prevent poor decision making based on an inaccurate model. While exploring a quality weighted approach to optimize the effectiveness of both high and low quality data was worthwhile, a more effective approach may be to simply utilize all carefully screened data with equal weighting and highlight areas of the model in which there is less confidence due to sparse high quality data.

3.6 Bedrock Topography in the Halton Hills Region

The most accurate model (with the lowest RMSE values) of the bedrock surface in the Halton Hills region was created from the ‘All – Screened’ grid (Figs. 3.8, 3.11; Table 3.1). This model honours high quality data points and includes low quality data

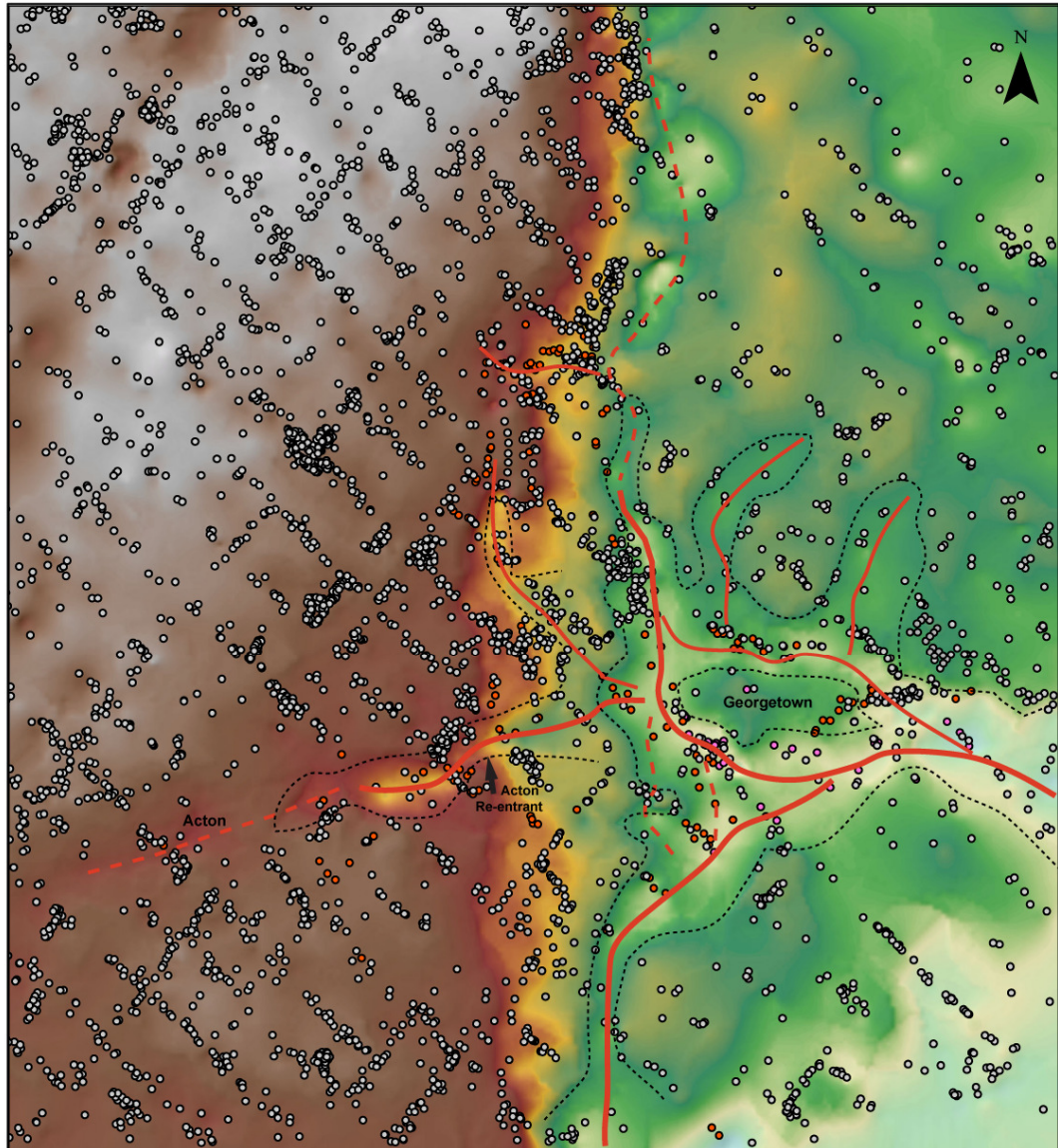
points that have been extensively screened, removing some potential error associated with incorrect location coordinates and geologic descriptions. The model clearly identifies the Niagara Escarpment as a linear feature that trends north to south through the centre of the study area and shows rapid changes in bedrock elevation (Figs. 3.1, 3.11). To the west of the Niagara Escarpment (represented by yellow, brown to grey elevation shading on Fig. 3.11) the bedrock at surface has relatively low relief and consists of the Amabel dolostone that forms the cap rock to the escarpment. Several re-entrant valleys cut through the dolostone cap rock (Straw, 1968), one of which can be clearly seen on the model in the area of Acton (Acton Re-entrant; Fig. 3.11). Below the Niagara Escarpment, to the east (where bedrock elevations are shaded green-blue; Fig. 3.11) the Queenston shale has been deeply incised (up to 40 m) to form a network of buried bedrock valleys. The town of Georgetown appears to lie on a relative bedrock 'high' surrounded by incised valleys which are coincident with the modern Credit River and Silver Creek valleys (Fig. 3.12). It is important to understand the location, form and continuity of these valleys as they host productive aquifer systems that supply potable water to communities in the Halton Hills region.

3.6.1 Defining Buried Bedrock Valleys

Buried bedrock valleys are defined here as continuous, elongate depressions in bedrock which are not (or are minimally) expressed at surface, and which have been

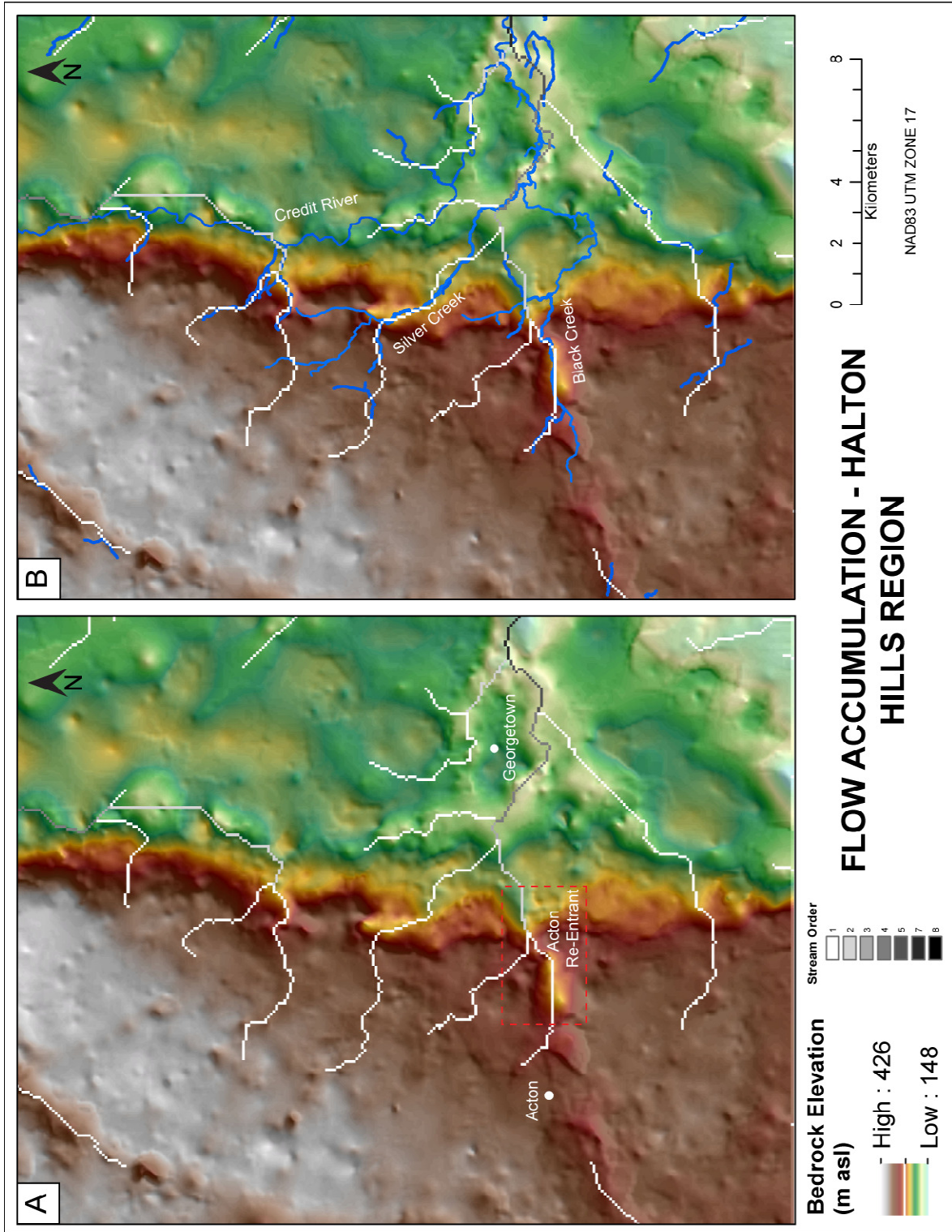
Figure 3.11: Predicted thalwegs of bedrock valleys in the Halton Hills area based on the ‘All – Screened’ grid. Predicted and ‘potential’ valley thalwegs are identified through visual analysis of the bedrock topography model created from the ‘All – Data Screened’ dataset. Note the appearance of the Acton reentrant valley as well as several, potentially interconnected valleys around the town of Georgetown. The continuity of these bedrock valleys is uncertain in some areas due to lack of high and low quality data.

Predicted Buried Valleys Based on 'All Data - Screened' Grid



Bedrock Elevation (m asl)	Data Sources	0 2 4 8 Kilometers
 High : 426 Low : 148	<ul style="list-style-type: none"> ● McMaster data ○ Consultant Reports ○ Ontario Waterwells 	<ul style="list-style-type: none"> ----- Predicted valley extent — Predicted valley thalweg - - - Potential valley thalweg

Figure 3.12: Bedrock topography model (All – Screened, unweighted) comparing buried valley thalwegs and modern fluvial systems using ArcGIS hydrology tools (Flow Accumulation and Stream Order). Progressively darker shades (higher values) of stream order represent the direction down gradient. A) Buried valley thalwegs determined mathematically by determining direction of drainage based on the direction of maximum slope in each grid cell. B) Modern fluvial network (showing major systems; Credit River, Silver and Black Creeks) as well as relevant tributaries and stream reaches coincident with the buried valleys.



covered or buried by younger sediments. Visual inspection of the preferred bedrock topography model ('All-Screened' grid; Figs 3.8, 3.11) clearly identifies a series of buried bedrock valleys within the Queenston Shale lowlands to the east of the Niagara Escarpment (Fig. 3.11).

To validate visual identification of valleys in the area, and to better understand their interconnectivity and possible origin, a computational approach (using ESRI's Hydrology Tool) was utilized to mathematically determine valley gradients, and valley thalwegs. The Hydrology Tool in ESRI's ArcMap was utilized to create a series of rasters based on the 'All – Screened' bedrock topography model (Fig. 3.11). Bedrock valley gradients in the region were determined by computing flow directions from the 'All – Screened' grid, based on the orientation of maximum slope within each grid cell (Fig. 3.12). This allowed identification of the most likely locations of drainage pathways on the bedrock surface (red lines on Fig. 3.11). A Flow Accumulation raster was then created to determine the accumulated 'flow' into each downslope cell and, by identifying areas of drainage focus, to also delineate the thalwegs of buried bedrock channels (ESRI, 2011). This process computationally identifies bedrock valley thalwegs and can be used to validate interpretations made from visual analysis of the 'All – Screened' grid (Fig. 3.11).

A Stream Order raster, which assigns stream order to portions of a raster which represent branches or tributaries of a linear drainage network, was created from the Flow Accumulation raster (ESRI, 2011; Fig. 3.12). The Stream Order raster is used here to provide information about the directionality of flow along the drainage network (Fig. 3.12). An interesting result of the Flow Accumulation and Stream Order interpolation was

the identification of remarkable consistency between the predicted ‘flow network’ on the bedrock surface and the location of modern fluvial systems, particularly the Credit River, Silver Creek and Black Creek systems (Fig. 3.12B). The location of the Silver Creek and Black Creek fluvial systems in particular appear to be strongly influenced by buried bedrock topography.

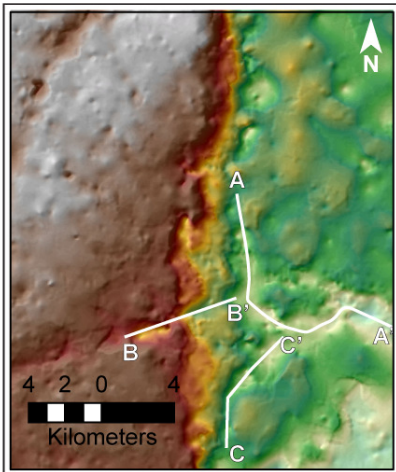
Three significant bedrock channels with relatively clear thalwegs and valley walls can be identified in the Halton Hills region on the basis of visual inspection of the ‘All – Screened’ bedrock topography model (Fig. 3.11) and the Stream Order process with the ArcGIS Hydrology tool (Fig. 3.12). The locations of the Georgetown buried bedrock valley, 16 Mile Creek buried bedrock valley and the Acton buried bedrock (re-entrant) valley are shown in Fig. 3.13. Several smaller valleys can also be identified incising the edge of the Niagara Escarpment, forming ‘tributary’ channels to the main bedrock valley systems (Figs. 3.11, 3.12).

3.6.2 Drift Thickness

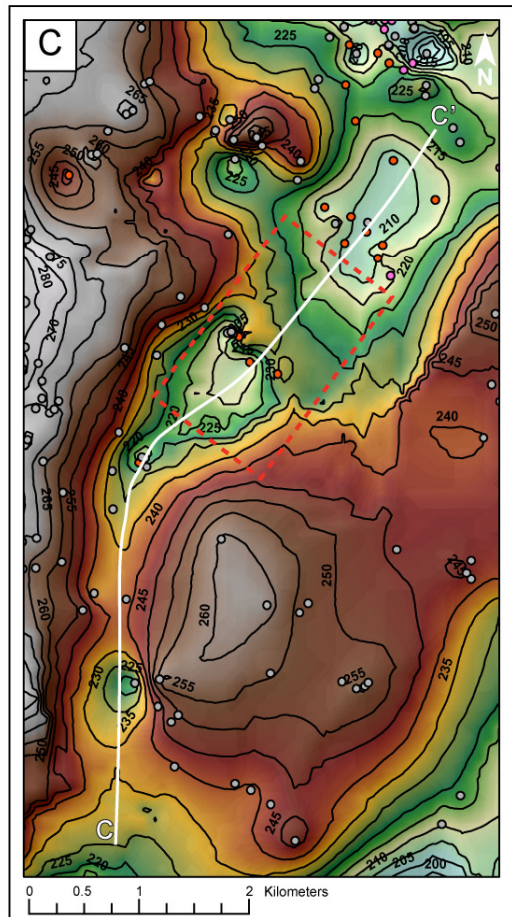
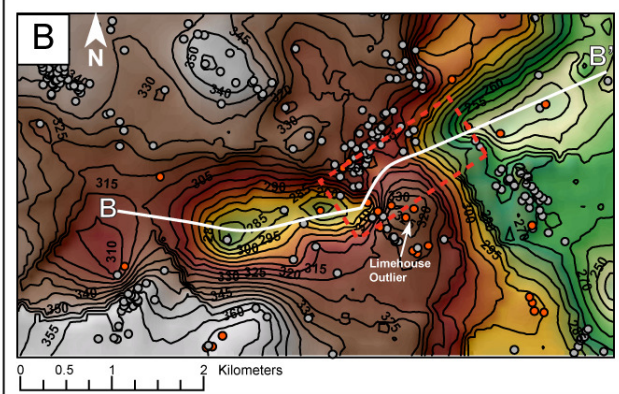
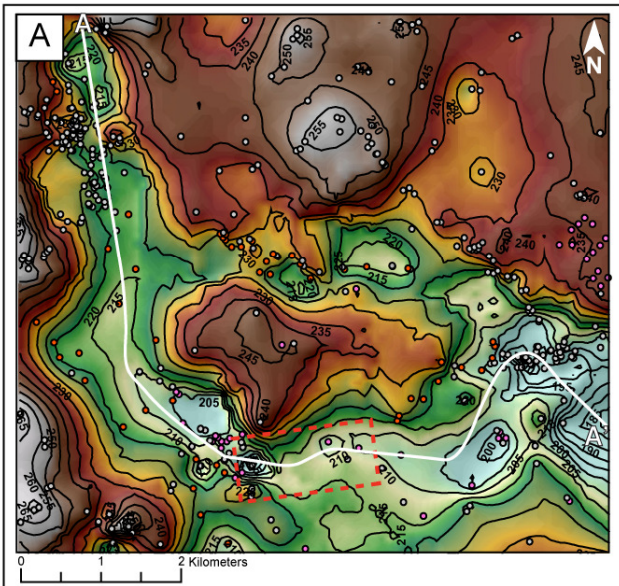
For the purposes of groundwater exploration, it is not only important to understand the location and extent of bedrock valleys, but also the nature and thickness of their sedimentary infill. Most bedrock valleys in the Halton Hills region are filled with Quaternary sediments, which consist of interbedded glaciolacustrine, subglacial and glaciofluvial deposits, the latter of which compose significant aquifers in the area (Meyer & Eyles, 2007). In order to determine the thickness of the sediment covering the bedrock surface and infilling bedrock valleys, a comparison of the bedrock topography and

Figure 3.13: " All – Screened' bedrock topography model displaying three major bedrock valley systems: A) Georgetown buried bedrock valley B) Acton buried bedrock (re-entrant) valley C) 16 Mile Creek buried bedrock valley. Predicted thalwegs of these valleys are shown in red, and problematic areas where valley continuity is uncertain are highlighted in blue dashed boxes that correspond to areas where data (high or low quality) is relatively sparse.

BURIED BEDROCK VALLEYS IN THE HALTON HILLS REGION



Map Elements	Bedrock elevations (m asl)	
Problematic areas	A) High : 267 Low : 178	B) High : 287 Low : 189
Predicted thalweg		
Data Points	C) High : 363 Low : 215	Inset (Regional) High : 426 Low : 148
OWD		
Consultant Reports		
McMaster		



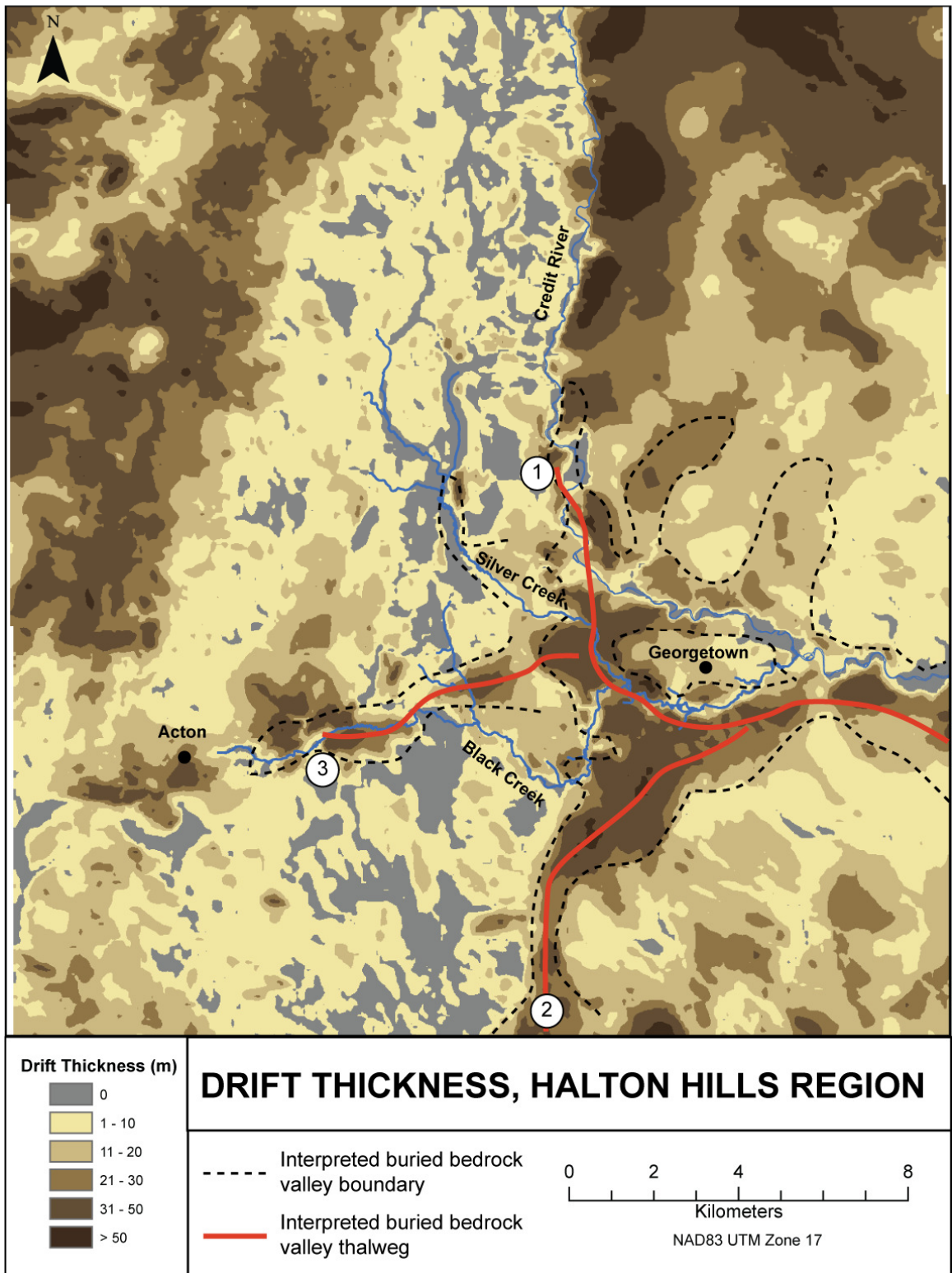
Contour Interval: 5 m
NAD83 UTM Zone 17

modern surface topography is required. A 10 m digital elevation model of the study area (OGDE, 2009) was used to represent the modern surface of the study area and the 'All – Screened' grid (Fig. 3.11) to represent the bedrock surface. The bedrock topography model was then subtracted from the DEM to create a drift thickness map (Fig. 3.14). This drift thickness map was used to confirm the identification of buried bedrock valleys infilled with thick successions of Quaternary sediment, with little to no surface expression in the Halton Hills region. The Georgetown, 16 Mile Creek and Acton buried bedrock valleys are each filled with thick successions of sediment, with the thickest succession (up to 50 m; Fig. 3.14) recorded in the 16 Mile Creek Valley. The Acton buried bedrock (re-entrant) valley also hosts thick successions of sediment (up to 40m; Fig. 3.14) on either side of the Escarpment face. On a regional scale, drift thickness across the study area is highly variable with bedrock exposed at surface (zero drift thickness) along the escarpment and the walls of some modern fluvial systems, and drift cover in excess of 50m thick in bedrock valleys and along the foot of the escarpment (Fig. 3.14).

3.6.3 Buried Bedrock Valleys in Halton Hills, Ontario

Bedrock topography modeling of the Halton Hills, Ontario region has allowed identification of three major buried bedrock valley systems (Georgetown buried bedrock valley, 16 Mile Creek buried bedrock valley and the Acton (Re-entrant) bedrock valley; Figs. 3.8, 3.11, 3.12), all of which have undulating topography, are relatively continuous, kilometres long, hundreds of metres to kilometres wide, up to 40 m deep and are infilled with thick successions of Quaternary sediments. These valleys are not isolated from one

Figure 3.14: Drift thickness of the Halton Hills area and location of interpreted buried bedrock valley boundaries and thalwegs. Drift thickness map is created from subtraction of the “All-Screened” bedrock topography model from the regional digital elevation model. Note the thickness of sediments within the identified buried valleys (1: Georgetown Buried Valley; 2: Sixteen Mile Creek Buried Valley; 3: Limehouse Buried Valley).



another, but interconnect, with the broad ends of the Acton and 16 Mile Creek bedrock valleys extending into the Georgetown buried valley (Fig. 3.12). The characteristics of these three valley systems (maximum and minimum width, depth, associated drift thickness as well as length, orientation and gradient) are summarized in Table 3.3.

3.6.3.1 Georgetown Bedrock Valley

The Georgetown buried bedrock valley is incised by up to 35m into the underlying Queenston shale and is relatively continuous for over 8 km in the Halton Hill study area (Fig. 3.13A). In the northern (upgradient) portions of the valley, the valley is coincident with that of the modern Credit River valley, which trends north to south adjacent to the Niagara Escarpment (Fig. 3.13A). The Georgetown buried bedrock valley appears to be relatively narrow in the north western reaches of the valley, (approximately 800 m wide; Table 3.3), and broadens to approximately 4.5 km wide downgradient towards the east. The thickness of sediment infilling the Georgetown buried bedrock valley varies from 8 m to 50 m (Table 3.3) with lower drift thicknesses occurring in areas where the Georgetown buried valley is coincident with the modern Credit River valley (Fig. 3.13A). The Georgetown buried valley is relatively continuous along its length, but contains an anomalous low point at 190 m asl (Fig. 3.13A), caused by one OWD record. This data point has relatively high reliability and has therefore been incorporated into the model. However, there is some additional uncertainty in the same area (red dashed box in Fig. 3.13A) caused by a lack of data, and further investigation is required to better understand this portion of the system.

Table 3.3: Summary of buried bedrock valley characteristics from the Halton Hills region determined from the ‘All – Screened’ bedrock topography model. Valley depth was determined solely from the change in elevation of the highest observed bedrock point to the lowest observed bedrock point within a valley system. Some valleys contain substantial thicknesses of sediment above bedrock valley walls. *Note that there is some surface expression of the Acton (re-entrant) valley (0 m drift thickness), but large portions of this valley are buried, allowing it to be classified as a partially “buried bedrock valley.”

	Georgetown Buried Bedrock Valley	16 Mile Creek Buried Bedrock Valley	Acton Buried Bedrock (Re-entrant) Valley
Bedrock Substrate	Queenston Shale	Queenston Shale	Amabel dolostone, Clinton- Cataract Group (Cabot Head shale and Whirlpool Sandstone), Queenston Shale
Length	>8km	5 km	5km
Orientation	S, SE, E	NE	NE
Gradient	0.003	0.006	0.016
Minimum Width	800 m	600 m	350 m
Maximum Width	4.5 km	3 km	1.5 km
Minimum Depth	10 m	10 m	15 m
Maximum Depth	35 m	30 m	40 m
Minimum Drift Thickness	8 m	22 m	0 m*
Maximum Drift Thickness	50 m	>50 m	40 m

3.6.3.2 Acton (Re-Entrant) Bedrock Valley

The Acton buried bedrock valley (Fig. 3.13B) is slightly more complex than other major valleys identified in the area as it crosses the Niagara Escarpment, incising the Amabel dolostone and Clinton-Cataract Groups above the Escarpment and the Queenston Shale below the Escarpment (Figs. 3.1, 3.13B). This bedrock valley appears to be deeply incised (up to 40 m) into the Amabel dolostone and underlying Whirlpool sandstone to the southwest of Limehouse, and trends roughly northeast incising through Queenston shale closer to the Niagara Escarpment, approximating the path of the modern Black Creek in this area (Fig. 3.13B). Above the Niagara Escarpment, the Acton buried bedrock valley is quite broad (1.3 km), and becomes narrower (350 m) as it passes through the north-south trending Niagara Escarpment, where the boundaries of the valley are only vaguely expressed at surface (e.g. in the region of the Limehouse outlier; Fig. 3.13B). Drift thickness in the Acton buried bedrock valley ranges from zero (where the valley crosses the Niagara Escarpment), to 40 m (Fig. 3.14). East of the Niagara Escarpment, the Acton buried bedrock valley continues as a broad feature (1.5 km wide), as it extends toward the Georgetown buried bedrock valley (Fig. 3.13B). The bedrock topography model (based on the “All – Screened” dataset; Figs. 3.8, 3.11) shows a 25 m high bedrock ridge along this valley profile (outlined by the red dashed box in Fig. 3.13B), but is poorly constrained due to lack of data in this area.

3.6.3.3 16 Mile Creek Bedrock Valley

The 16 Mile Creek buried bedrock valley is located within the 16 Mile Creek subwatershed (AECOM, 2010). This valley is incised up to 30 m into the underlying Queenston shale bedrock and is relatively continuous for 5 km before it is confluent with

the Georgetown buried bedrock valley system (Fig. 3.13C). The 16 Mile Creek area has been of significant interest for groundwater exploration in recent years, and a number of high quality data points are available to constrain valley depth and extent in this area. This bedrock valley shows a general orientation towards the northeast, and is probably connected with the eastern portion of the Georgetown bedrock valley (Figs. 3.11, 3.13C). The southern (upgradient) portion of the 16 Mile Creek buried bedrock valley is relatively narrow (600 m wide; Fig. 3.11), and broadens down gradient to a width of almost 3 km where it joins the Georgetown buried bedrock valley (Figs. 12B, C). The 16 Mile Creek valley hosts a thick infill of Quaternary sediment (ranging from 22 m to over 50 m; Fig. 3.14; Table 3.3). At one point along the valley a 15 m high 'bedrock ridge' disrupts the valley from its otherwise gradually north east sloping topography (red dashed box in Fig. 3.13C). This ridge is likely an artefact of the interpolation in this area, as only three high quality points define the ridge.

3.6.4 Origin of Buried Bedrock Valleys in Halton Hills

It is extremely difficult to determine the exact origin and age of erosional surfaces on bedrock, particularly those that have been subject to repeated glaciation and deglaciation. The coincident location of some modern fluvial systems in the Halton Hills area (Credit River, Silver Creek, portions of Black Creek; Fig. 3.12), with buried bedrock valleys indicates that the bedrock valleys represent persistent drainage pathways that have been occupied repeatedly over time. The valleys were probably occupied, eroded and modified by a combination of glacial and fluvial processes during the late Quaternary. The Georgetown buried bedrock valley is the longest, and most continuous

buried bedrock valley identified in the Halton Hills region, and may represent the path of a Paleo-Credit River, which drained south east toward Lake Ontario (Meadowvale Valley; Karrow, 2005). The other smaller valleys (16 Mile Creek buried bedrock valley and the Acton buried bedrock valleys) may have served as tributaries to the main Georgetown channel as drainage was directed eastward toward the Lake Ontario basin. The current expression of the Acton buried bedrock (re-entrant) valley is likely more recent (Straw, 1968), also created by both fluvial and glacial processes during the latest Quaternary.

While the orientation and gradient of valleys in the Halton Hills region shows a general south-eastward trend, there is some variability including north, and northeasterly trending valleys. These latter orientations may be related to drainage occurring at various stages of glaciation, perhaps during the Port Huron Stadial (13.2 – 12 Ka) when the Ontario Lobe readvanced out of the Lake Ontario basin toward the northwest, promoting northward flowing drainage (Chapman & Putnam, 1966; Costello & Walker, 1972; Barnett, 1992; Karrow, 2005; Meyer & Eyles, 2007). Fluvial processes operating during glacial as well as interstadial and interglacial periods would have episodically flushed sediments from the valleys and contributed to excavation of the bedrock form.

The Acton bedrock valley is of particular interest due to its classification as a re-entrant valley incised into the relatively resistant carbonate cap rock (Amabel dolostone) of the Niagara Escarpment. Several re-entrant valleys have been identified along the Niagara escarpment, most of which are quite deep, with straight, steep, parallel sides (Straw, 1968) and typically trend north-east to southwest with very few exceptions. This

general trend has been related to the path of regional ice flow during the Quaternary period (Chapman & Putnam, 1966; Straw, 1968), the direction of proposed catastrophic flood pathways (Kor & Cowell, 1998), as well as preferential erosion of pre-existing structural weaknesses, which are generally oriented northeast to southwest across the southern Ontario region (Eyles & Scheidegger, 1995; Eyles et al., 1997). The strong correlations reported between Paleozoic bedrock jointing patterns, buried bedrock valleys, and modern fluvial systems is suggestive that bedrock joints have been exploited by erosive agents (fluvial or glacial processes) as they modified the southern Ontario landscape (Straw, 1968; Eyles et al., 1997).

The form and orientation of the modern (and Paleo) Credit River valley is also interesting in that this valley takes a nearly 90° turn very close to the location of the Acton re-entrant valley (Fig. 3.12). This may indicate a pre-existing structural weakness is controlling valley development in this area, or that the orientation of the valley has been influenced by drainage diversion due to ice blockage. If the Acton re-entrant valley is indeed structurally controlled, this may suggest that the orientation of other valleys in close proximity are also controlled structurally.

3.7 Conclusions

The objective of this study was to delineate, as accurately as possible, the bedrock topography and the geometry and extent of buried bedrock valleys in the Halton Hills region for the purposes of groundwater investigations. Due to the high variability in the quality and reliability of data sources available for this study, several approaches to

bedrock topography modeling have been investigated to determine a ‘best estimation’ of the bedrock surface. The results of this investigation indicate that modeling exclusively with high quality data is insufficient to accurately predict the bedrock surface due to the sparse distribution of high quality data across the study area. The addition of data from large digital databases (such as the OWD) can compensate for this but these data must be extensively screened to remove problematic points such as anomalous outliers, elevation and location inaccuracies, duplicates and null values that can incorporate substantial error into a subsurface model. In this study, a three stage screening approach was applied to data obtained from the OWD, which resulted in the removal of over 20% of the dataset determined to be inaccurate or unreliable. A ‘quality weighting’ approach to modeling (introduced by MacCormack & Eyles, 2010) was also investigated to enhance the influence of ‘high quality’ data points on the model output while utilizing ‘low quality’ data to provide adequate areal coverage. The ‘quality weighted’ approach to modeling did not improve upon the results obtained from non-weighted models and in some instances actually reduced the accuracy of the output model by over-smoothing the surface representation and altering the values of high quality data points.

The ‘best estimation’ of the bedrock surface for the Halton Hills region was created from extensively screened low quality data in conjunction with high quality data points (‘All – Screened’; Fig. 3.8). This combination of data types allowed for an adequate data distribution across the entire study area and high reliability in particular areas of interest where there was a concentration of high quality data.

Three major buried bedrock valley systems, the Georgetown, 16 Mile Creek and Acton buried bedrock valleys have been identified in this study. These valleys are incised primarily into the Queenston shale bedrock, have undulating topography, are relatively continuous for several kilometres, are hundreds of metres to kilometres wide, up to 40 metres deep, and are infilled with thick successions of Quaternary sediment. Analysis of the bedrock topography of the Halton Hills region indicates that the major buried bedrock valleys are relatively continuous, with strong interconnectivity of the Georgetown, Acton and 16 Mile Creek buried bedrock valleys. The three major buried bedrock valleys identified in the Halton Hills region were likely formed by a combination of fluvial and glacial processes active during various stages of glaciation during the late Quaternary period (Straw, 1968; Gao, 2011). The Georgetown buried bedrock valley probably represents the pathway of a Paleo-Credit River, and other buried bedrock valleys in the Halton Hills area may have served as tributaries to this main system. Glacial occupation of the valleys during the Quaternary period likely deepened, and widened these valleys, with fluvial processes periodically evacuating sediment and contributing to bedrock incision (Straw, 1968).

The sedimentary infills of the buried bedrock valleys consist of interbedded glacial, fluvial and lacustrine sediments and record the most recent depositional agents to occupy these topographic lows. The coincident orientation of buried bedrock valleys and bedrock joint systems (Eyles & Scheidegger, 1995; Eyles et al., 1997) in the southern Ontario region, coupled with abrupt changes in directionality of the modern and Paleo Credit River valleys close to the Acton re-entrant valley, suggest that pre-existing

structural weaknesses have controlled the development of some valleys in the Halton Hills Region.

This detailed investigation of the bedrock surface in the Halton Hills region has contributed substantially to the understanding of the buried bedrock topography in southern Ontario. This information also provides insight into some of the factors that control the location and productivity of aquifers within the Halton Hills groundwater system, as the sand and gravel aquifers are, in many locations, hosted in bedrock valleys incised into the Queenston Shale (Meyer & Eyles, 2007). Enhanced understanding of the bedrock surface topography and thickness of overlying Quaternary sediments (drift) also allows for more focussed groundwater exploration programs in the search for additional potable water sources for the rapidly growing Halton Hills region.

While this investigation is focussed on the buried bedrock valleys in the Halton Hills region, similar buried bedrock valleys hosting thick successions of Quaternary sediments have been reported in other regions of North America, including Illinois, Indiana, Michigan, Ohio and Wisconsin (Bleur, 1991; Kempton et al., 1991; Clayton et al., 1999; Greer & Colin, 2009). An improved understanding of the subsurface geometry and interconnectivity of these buried bedrock valley systems will not only allow more detailed late Quaternary paleoenvironmental reconstructions to be made, but will also facilitate the design and implementation of effective groundwater exploration and protection programs in expanding urban centres.

References

- AECOM. 2010. Technical Report-Middle Sixteen Mile Creek Bedrock Valley Investigation. The Regional Municipality of Halton. Project Number 108076.
- Armstrong, D.K & Dodge, J.E.P. 2007. Paleozoic geology of southern Ontario in *Ontario Geology Survey Miscellaneous Release Data* 210.
- Bacj, A.F., Endres, A.L., Hunter, J.A., Pullen, S.E. & Shirota, J. 2004. Three-Dimensional Mapping of Quaternary Deposits in the Waterloo Region, Southwestern Ontario in *Illinois State Geological Survey (IGSG) Open File Series 2004-2008* 12-15.
- Barnett, P.J. 1992. Quaternary Geology of Ontario in *Ontario Geology of Ontario Special Volume* 4, 2, 1011-1088.
- Berger, G.W. & Eyles N. 1994. Thermoluminescence Chronology of Toronto-Area Quaternary Sediments and Implications for the Extent of the Midcontinent Ice Sheet(s) in *Geology* 22, 31-34.
- Boldstad, P.V. & Stowe, T. 1994. An Evaluation of DEM Accuracy: Elevation, Slope, and Aspect. *Photogrammetric Engineering & Remote Sensing* 60, 11, 1327-1332.
- Bourennane, H., King, D., Couturier, A., Bicoullaud, B., Mary, B. and Richard, G. 2007. Uncertainty assessment of soil water content spatial patterns using geostatistical simulations: An empirical comparison of a simulation accounting for single attribute and a simulation accounting for secondary information in *Ecological Modeling* 205, 323-335.
- Brennan, A. 2010. Quaternary stratigraphy of the Georgetown Region Geophysical Interpretation. Halton Hills Geology Workshop, McMaster University 2011.
- Brogly, P.J., Martini, I.P. & Middleton, G.V. 1998. The Queenston Formation: shale-dominated, mixed terrigenous-carbonate deposits of Upper Ordovician, semiarid, muddy shores in Ontario, Canada in *Canadian Journal of Earth Sciences* 35, 702-719.
- Brunton, F.R. 2009. Update of revision to Early Silurian stratigraphy of Niagara Escarpment: integration of sequence stratigraphy/sedimentology/hydrogeology to delineate hydrogeologic units (HGUs). In *Summer of Field Work and Other Activities 2009*, 25-1-25-20. *Ontario Geological survey, Open File Report* 6240.

- Burt, A. 2004. Three-dimensional mapping of Quaternary (superficial) deposits in the Barrie area, central Ontario in *Summary Field Work and Other Activities 2004. Ontario Geological Survey*, 35-1-35-5.
- Carter, T.R. & Castillo, A.C. 2006. Three-dimensional mapping of Paleozoic bedrock formations in the subsurface of southwestern Ontario: A GIS application of the Ontario petroleum well database. In J.R. Harris (Ed.), *GAC Special Paper 44: GIS for the Earth Sciences* (pp.435-450). St. John's: Geological Association of Canada.
- Chang, K. 2006. Introduction to Geographic Information Systems. McGraw-Hill Ryerson, New York, pp. 464.
- Chapman, L.J. and Putnam, D.F. 1966. The Physiography of Southern Ontario, 2nd edition. University of Toronto Press, Toronto.
- Cole, J., Coniglio, M. & Gautrey, S. 2009. The role of buried bedrock valleys on the development of karstic aquifers in flat-lying carbonate bedrock: insights from Guelph, Ontario, Canada in *Hydrogeology Journal* 17, 1411-1425.
- Costello, W.R. and Walker, R.G. 1972. Pleistocene sedimentology, Credit River, Southern Ontario: A new component of the braided river model in *Journal of Sedimentary Research* 42, 389-400.
- Cox, N.J. 2007. Kernel estimation as a basic tool for geomorphological data analysis. *Earth Surface Processes and Landforms* 32, 1902-1912.
- Dey, W.S., Davis, A.M., Abert, C.C., Curry, B.B. & Seiving, J.C. 2005. Three dimensional geologic mapping of groundwater resources in Kane County, Illinois in *Three-Dimensional Geologic Mapping for Groundwater Applications-Workshop Extended Abstracts, Geological Survey of Canada, Open File 5048*, 21-24.
- Easton, J.A. 1988. Buried valleys near Limehouse, Ontario. Unpublished M.Sc. thesis, University of Waterloo, Waterloo, Ontario.
- Environmental Systems Research Institute, Inc. 2011. "An overview of the Hydrology toolset". ArcGIS Resource Center.
http://help.arcgis.com/en/arcgisdesktop/10.0/help/index.html#/An_overview_of_the_Hydrology_tools/009z0000004w000000/.
- Eyles, N. 2002. Ontario Rocks: Three Billion Years of Environmental Change. Fitzhenry & Whiteside, Toronto.

- Eyles, N. & Scheidegger, A.E. 1995. Environmental significance of bedrock jointing in southern Ontario, Canada in *Environmental Geology* 26, 269-277.
- Eyles, N., Arnaud, E., Scheidegger, A.E., and Eyles, C.H. 1997. Bedrock jointing and geomorphology in southwestern Ontario, Canada: an example in tectonic predesign in *Geomorphology* 19, 1-2, 17-34.
- Galve, J.P., Guitierrez, F., Remondo, J., Bonachea, J., Lucha, P., & Cendrero, A. 2009. Evaluating and comparing method of sinkhole susceptibility mapping in the Ebro region Valley eporite karst (NE Spain) in *Geomorphology* 111, 160-172.
- Gao, C. 2011. Buried bedrock valleys and glacial and subglacial meltwater erosion in southern Ontario, Canada in *Canadian Journal of Earth Sciences* 48, 801-818.
- Gao, C., Shiota, J., Kelly, R.I., Brunton, F.R. & van Haaften, J.S. 2006. Bedrock topography and overburden thickness mapping, southern Ontario, in *Ontario Geological Survey, Miscellaneous Release – Data 207*.
- Goodchild, M.F. & Clarke, K.C. 2002. Data Quality in Massive Data sets. In J. Abello, P.M. Pardalos, & M.G.C. Resende (Eds.), *Handbook of Massive Data Sets* (pp. 643-659). Norwell, MA: Kluwer Academic Publishers.
- Hirano et al. 2003 Mapping from Aster stereo image data: DEM Validation and accuracy assessment. *ISPRS Journal of Photogrammetry & Remote Sensing* 57, 356-370.
- Hoke, G.D., Isaacs, B.L., Jordan, T.E. and Yu, J.S. 2004. Groundwater-sapping origin for the giant quebradas of northern Chile in *Geology* 32, 7, 605-608.
- Houlding, S.W. 1994. *3D Geoscience Modeling*. Hong Kong: Springer-Verlag Berlin Heidelberg.
- Howard, K.W.F. 1997. Do tills beneath urban Toronto provide adequate groundwater protection? In J. Chilton (Ed). *Groundwater in the Urban Environment Rotterdam Vol. 1* (pp 433-438). AA Balekma.
- Howard, K.W.F & Livingstone, S.J. 2000. Transport of urban contaminants into Lake Ontario via subsurface flow in *Urban Water* 2, 183-195.
- Isaaks, E.H. & Srivistava, R.M. 1989. *An Introduction to Applied Geostatistics*. New York: Oxford University Press.
- Johnston, K., Ver Hoef, J.M., Krivoruchko, K. & Lucas, N. 2001. *Using ArcGIS Geostatistical Analyst*. USA: ESRI.

- Kauffman, O. & Martin, T. 2008. 3D geological modeling from boreholes, cross-sections and geological maps, application over former natural gas storage in coal mines in *Computers & Geosciences* 34, 278-290.
- Karrow, P.F. 2005. Quaternary geology: Brampton Area in *Ontario Geological Survey Report* 257, 1-59.
- Kor, P.S.G. & Cowell, D.W. 1998. Evidence for catastrophic subglacial meltwater sheetflood events on the Bruce Peninsula, Ontario in *Canadian Journal of Earth Sciences* 35, 1180-1202.
- Logan, C., Russel, H.A.J., Sharpe, D.R. & Kenny, F.M. 2006. The role of GIS and expert knowledge in 3-D modeling, Oak Ridges Moraine, southern Ontario. In J.R.Harris (Ed.), *GAC Special Paper 44: GIS for the Earth Science* (pp. 519-542). St. John's: Geological Association of Canada.
- MacCormack, K.E. 2010. Improving the Accuracy of 3D Geologic Subsurface Models [Ph.D thesis]. McMaster University.
- MacCormack, K.E. and Eyles, C.H., 2010. Enhancing the Reliability of 3-D Subsurface Models through Differential Weighting and Mathematical Recombination of Variable Quality Data. In Delavar, M. and Devillers, R., (eds.) *Spatial Data Quality: From Process to Decisions, Special Issue, Transactions in GIS*, v. 14, p. 401-420. NSERC.
- Meyer, P.A & Eyles, C.H. 2007. Nature and origin of sediments infilling poorly defined buried bedrock valleys adjacent to the Niagara Escarpment, southern Ontario, Canada in *Canadian Journal of Earth Sciences* 4, 1, 89-105.
- Ontario Geospatial Data Exchange (ODGE). 2009. Ontario Fundamental dataset [DEM086]. Peterborough, Ontario. Ontario Ministry of Natural Resources
- Regional Municipality of Halton. 2009. Phase 3 Sustainable Halton Report 3.13
- Sharpe, D.R., Hinton, M.J. & Russel, H.A.J. 2002. The need for basin analysis in regional hydrogeological studies: Oak Ridges Moraine, southern Ontario in *Geoscience Canada* 29, 3-20.
- Spencer, J.W. 1890. Origins of the Basins of the Great Lakes of America in *Quarterly Journal of the Geological Society* 46, 523-533.
- Straw, A. 1968. Late Pleistocene glacial erosion along the Niagara Escarpment of southern Ontario in *Geological Society of America Bulletin* 79,7, 889-910.

- Strong, D.M., Lee, Y.W. & Wang, R.Y. 1997. Data Quality in Context. *Communications of the ACM*, 40,103-110 .
- Thorleifson, L.H. & Berg,R.C. 2002. Introduction-The need for high-quality three-dimensional geological information for groundwater and other environmental application in *Geological Survey of Canada, Open File 1449*.
- United States Geological Survey. 1998. Standards for Digital Elevation Models: Part 25 Specifications.
<http://rockyweb.cr.usgs.gov/nmpstds/acrodcs/dem/2DEM0198.PDF>.
- Venteris, E.R. 2007. 3-D modeling of glacial stratigraphy using public water well data, geological interpretation and geostatistics in *Three-dimensional Geological Mapping for Groundwater Applications: Workshop Extended Abstracts, Minnesota Geological Survey Open-File Report 07-4 81-84*.
- White, K.M. and Sharp, J.M. 2003. Evaluation of groundwater sapping using erosion pin sand field observations of fractures, karst features, streams, and springs. Geological Society of America *Abstracts with Programs* Vol. 35, No.6, September 2003, p. 52
- Zimmerman, D., Pavlik,C., Ruggles, A. & Armstrong, M.P. 1999. An experimental comparison of Ordinary and Universal Kriging and inverse distance weighting in *Mathematical Geology* 31, 375-390.

CHAPTER 4 CONCLUSION

Glaciers are capable of eroding bedrock surfaces through a variety of processes and erosive agents (e.g., abrasion, meltwater, saturated till), and often leave behind extensive assemblages of erosional landforms of highly variable morphology and scale. These erosional landforms provide insight into the former processes operating beneath large ice sheets, contributing toward understanding of ice sheet dynamics, and allowing for advances to be made in past glacial reconstructions and future glacial and climatic predictions (Kleman, 1994; Glasser & Bennett, 2004).

The work reported here, that was conducted at Whitefish Falls, Vineland, Pelee Island, Georgetown (Ontario) and Kelleys Island (Ohio), adds substantially to current knowledge of the subglacial processes responsible for the development of a variety of erosional forms on bedrock. This study presents detailed documentation of a variety of p-form assemblages and buried bedrock valleys as well as maps of former glaciated surfaces which indicate significant spatial and temporal variability in the erosional processes operating on them.

Detailed observations and mapping of assemblages of p-forms at Whitefish Falls, Vineland, Pelee Island and Kelleys Island indicate that:

- P-form development is strongly influenced by bedrock controls, as p-forms develop preferentially, and with higher definition, on substrates that are most susceptible to erosion;

- P-form assemblages are highly variable, and often contain several features which indicate that no single process is responsible for the development of p-forms spatially or temporally, and
- A multi-phase evolution may be responsible for the development of many p-forms in which glacial ice abrades bedrock, leaving behind grooves and streamlined bedrock highs; these are subsequently modified into p-forms by vortices in turbulent subglacial meltwater and abraded by later occupation by ice or saturated till at the base of the ice sheet.

Larger scale erosional features such as buried bedrock valleys are economically significant in several areas of northern North America as they are infilled with thick successions of Quaternary sediments that host productive aquifers (Meyer & Eyles, 2007). As the Regional Municipality of Halton strives to meet the population growth targets of the province of Ontario's "Places to Grow" plan, improved understanding of their groundwater system is required to meet the demand of projected growth (RMH, 2009). As existing municipal aquifers in the Halton region are thought to be hosted within buried bedrock valleys, a detailed model of the bedrock topography of the region was required to aid in the groundwater exploration process.

Several approaches were used to accurately delineate the extent and geometry of buried bedrock valleys in the Halton Hills region. The model that produced the most accurate representation of the bedrock surface (as determined through cross-validation of actual and predicted elevation values) utilized 150 primary 'high quality' data points

obtained from borehole and outcrop, 50 intermediate quality points from consultant reports and remotely sensed data, and over 4000 records from the Ontario Waterwell Database which were subjected to a rigorous three-stage screening process. Results from bedrock topography modeling of the Halton Hills region indicate that:

- Data from large digital databases should be carefully screened prior to modeling, systematically identifying and removing potentially erroneous data points which could substantially reduce the reliability of an output model;
- A ‘Quality Weighted’ approach to subsurface modeling (as introduced by MacCormack & Eyles, 2010) is inappropriate for the Halton Hills study as the models in which high quality data is extremely influential over-smooth actual topographic variability and create unrealistic trends in areas where high quality data are sparse;
- The Halton Hills region contains three major (interconnected?) buried bedrock valley systems, the Georgetown, Acton and 16 Mile Creek buried bedrock valleys, which each contain up to 40 – 50 m of Quaternary sediments and,
- The Georgetown buried bedrock valley may identify the position of a Paleo-Credit river, with other buried bedrock valleys serving as tributaries to this main system. The form of the buried bedrock valleys in the Halton Hills area probably results from repeated erosion and modification by glaciers and fluvial systems during the Quaternary period.

4.1 Future Directions

There are a number of areas that future work on bedrock erosional features could be focussed. First, it is important to enhance understanding of the temporal scale at which subglacial processes operate to create bedrock erosional forms such as p-forms and buried bedrock valleys. Detailed regional mapping of glaciated surfaces in other regions of the Great Lakes basins and elsewhere would provide additional data with which to analyse the spatial and temporal scales at which subglacial processes operate, particularly if geochronological data are available. This may be particularly important for improved understanding of the processes responsible for p-form development.

Second, research on the subsurface stratigraphy and Quaternary depositional history of the Halton Hills region is ongoing, and current understanding of the form and connectivity of the network of buried bedrock valleys in the region will be improved with additional core and outcrop data. The development and application of enhanced modeling techniques that allow more effective utilization of all data types will also allow the creation of more accurate and reliable representations of the buried bedrock surface. In all of these future studies an approach should be taken that utilizes and recognizes the importance of integrating information from many different data sources. Integration of hydrogeological and sedimentological data with the bedrock topography models presented here will substantially expand the database available for groundwater exploration and protection plans in the Halton Hills region.

References

- Glasser, F. N. & Bennett, M.R. 2004. Glacial erosional landforms: origins and significance for paleoglaciology in *Progress in Physical Geography* 28, 1, 43-75.
- Kleman, J. 1994. Preservation of landforms under ice sheets and ice caps in *Geomorphology* 9, 1, 19-32.
- MacCormack, K.E. and Eyles, C.H., 2010. Enhancing the Reliability of 3-D Subsurface Models through Differential Weighting and Mathematical Recombination of Variable Quality Data. In Delavar, M. and Devillers, R., (eds.) *Spatial Data Quality: From Process to Decisions*, Special Issue, Transactions in GIS, v. 14, p. 401-420. NSERC.
- Meyer, P.A & Eyles, C.H. 2007. Nature and origin of sediments infilling poorly defined buried bedrock valleys adjacent to the Niagara Escarpment, southern Ontario, Canada in *Canadian Journal of Earth Sciences* 4, 1, 89-105.
- Regional Municipality of Halton. 2009. Official Plan for the Halton Planning Area, Regional Municipality of Halton *Amendment No. 38 to the Regional Plan (2006)*. December 10, 2009.

APPENDIX A

Screening Stage 2-Georeferencing Errors

The waterwell records in the OWD contain an attribute which identify the coordinate confidence with respect to each record (Table A-1). Higher codes correspond to decreasing accuracy in the position of the record. One of the major issues with the OWD is the variability in location accuracy of the records, as misplaced data points can lead to large errors in interpolation. For example, when manually inspecting the distribution of the OWD data points, most of the points correspond to the road networks, as most of the waterwells are located adjacent to roads (Fig. 3.7C). However, some data points have geographic coordinates that locate them in the middle of farm fields, which is most likely an incorrect representation of the actual well location. On the bedrock topography interpolation of the Southern Ontario region produced by the Ontario Geological Survey (Gao et al., 2006), OWD data with reliability poorer than 500 m were removed from the interpolation. These errors correspond to a greater than 1 cm deviation on 1:50 000 scale maps. Coding of the OWD data utilized in this study allowed the removal of data points with location reliability less than 300 m; many of the data points that were removed from subsequent interpolation were in locations in between major roads.

Surface elevations for most data points within the OWD were assigned values from 1:50 000 topographic maps, which have 10 m surface elevation contours (Gao et al. 2006). Due to the manual assignment of these values some errors may have been

introduced and required further investigation. Surface elevations of the OWD data were therefore compared with the 10 m DEM of the area. Fortunately, all of the OWD data points from the Halton Hills region were within 10 m of the DEM value at each respective location.

At this stage of screening a total of 467 data points with inaccurate location coordinates were removed from the previously screened dataset, leaving behind the ‘Low Quality – Screen 2’ dataset. The RMSE value of the resulting grid (Fig. 7C) interpolated from this dataset was 7.53 (Table 2).

Screening Stage 3-Geologic Inaccuracies

When the OWD data were overlain on the OGS 1:50 000 Paleozoic bedrock geology map (Armstrong and Dodge, 2007), several points were highlighted as having incorrect geologic descriptions (e.g. bedrock was reported as limestone in areas of shale bedrock) despite these points having location confidence within 300 m. The presence of shale in areas where the Amabel Dolostone should be recorded at surface (and vice versa) is problematic because of the relative stratigraphic position of the units (the Cabot Head and Queenston shales are stratigraphically lower than any dolostone in the area).

Table A-1: Table of location confidence codes associated with data from the Ontario Waterwell Database (OWD). For the purposes of this study, data points outside of 300 m location confidence (code > 5), were removed from the interpolation.

Code	Reliability	Description
1	<= 3 m	Within 3 m
2	3 m - 10 m	Within 10 m
3	10 - 30 m	Within 30 m
4	30 m - 100 m	Within 100 m
5	100 m- 300 m	Within 300 m
6	300 m - 1 km	Within 1 km
7	1 km - 3 km	Within 3 km
8	3 km - 10 km	Within 10 km
9	unknown	Unknown

References

- Armstrong, D.K & Dodge, J.E.P. 2007. Paleozoic geology of southern Ontario in *Ontario Geology Survey Miscellaneous Release Data 219*.
- Gao, C., Shirota, J., Kelly, R.I., Brunton, F.R. & van Haaften, J.S. 2006. Bedrock topography and overburden thickness mapping, southern Ontario, in *Ontario Geological Survey, Miscellaneous Release – Data 207*.